BIOCHEMICAL STUDIES

OF

NUCLEOSIDE TRANSPORTERS

FROM

RAT AND GUINEA PIG LUNG

BY

MAGGIE M. SHI

A THESIS SUBMITTED IN PARTIAL FULFILMENT OF

THE REQUIREMENTS FOR THE DEGREE OF

DOCTOR OF PHILOSOPHY

IN

BIOCHEMISTRY

NOVEMBER 1987

THE CHINESE UNIVERSITY OF HONG KONG

Dedicated to my parents

ABSTRACT

This Thesis describes ligand binding, molecular and reconstitution studies of the rat and guinea pig lung nucleoside transporters. Nitrobenzylthioinosine (NBMPR), a potent inhibitor of nucleoside transport, binds tightly (apparent Kd 0.2-0.4 nM) but reversibly to both rat and guinea pig lung membranes, the guinea pig lung membranes possessing a higher density of NBMPR binding sites. Binding was inhibited by nitrobenzylthioguanosine (NBTGR), adenosine and uridine. Dipyridamole, a coronary vasodilator known to be a potent inhibitor of nucleoside transport, was also an effective inhibitor of NBMPR binding to guinea pig membranes (Ki 20 nM). In contrast, NBMPR binding to rat lung membranes were relatively insensitive to dipyridamole (Ki 8.5 nM). Inhibition of NBMPR binding to membranes by dipyridamole was competitive in both species. Species differences in inhibition of NBMPR binding by various other vasodilators such as dilazep, lidoflazine and hexobendine was also observed, with the rat always displaying the lower sensitivity.

Membranes from guinea pig lung exhibited high-affinity binding of [^{3}H]dipyridamole (apparent Kd 2 nM). Binding was inhibited by NBMPR, dilazep and lidoflazine and by the transported nucleosides uridine and adenosine. In contrast, there was no detectable high-affinity binding of [^{3}H]dipyridamole to lung membranes from the rat, a result

consistent with the low sensitivity of rat lung to NBMPR binding to dipyridamole inhibition. Bmax values for high-affinity binding of [^{3}H]dipyridamole and [^{3}H]NBMPR to guinea pig membranes were similar, suggesting that these structurally unrelated ligands bind to the NBMPR-sensitive nucleoside transporter with the same stoichiometry. Parallel kinetic studies on NBMPR binding and dipyridamole binding suggest that the two ligands binding to topographically separate sites.

Data presented in Chapter 4 demonstrate that NBMPR can also be used as a covalent probe of lung nucleoside transporters. Exposure of site-bound [^{3}H]NBMPR to high intensity UV light resulted in the photoaffinity labelling of lung proteins with apparent molecular weights similar to that of the well characterized human erythrocyte nucleoside transporter (Mr 45,000-66,000). Covalent labelling was inhibited by NBTGR and adenosine equally in both species while dipyridamole inhibited covalent labelling in guinea pig lung membranes much more effectively than in the rat. The rat lung nucleoside transport protein had a significantly higher apparent molecular weight than that of the guinea pig (Mr 63,000 vs 55,000). Enzyme digestion experiments with endoglycosidase-F revealed that both the rat and guinea pig lung nucleoside transporters are glycoproteins containing N-linked oligosaccharides. The data provide evidence that the molecular weight difference between the rat and guinea pig lung nucleoside transporters

can be accounted for by different degrees of glycosylation of the two transporters. These experiments and additional trypsin digestion studies provide evidence of molecular similarities between the guinea pig lung and human erythrocyte nucleoside transporters.

The methodology of reconstitution was employed to study the kinetic properties of the lung nucleoside transporter. Uridine transport into vesicles reconstituted with an n-octylglucoside extract from guinea-pig lung plasma membranes was inhibited by NBMPR, dilazep and dipyridamole. The kinetic properties of uridine transport by the reconstituted lung nucleoside transporter were consistent with the simple carrier model (Lieb, 1982) and compared favourably with those of the reconstituted human erythrocyte nucleoside transporter.

PUBLICATIONS

Some of the findings reported here have been published or prepared for publication in the following papers:

Shi, M.M., Wu, J-S. R., Lee, C.M. and Young, J.D. (1984). Nucleoside Transport. Photoaffinity labelling of high-affinity nitrobenzylthioinosine binding sites in rat and guinea pig lung. Biochim. Biophys. Res. Res. Commun., 118: 594-600.

Shi, M.M. and Young, J.D. (1986). Dipyridamole inhibition of nitrobenzylthioinosine binding to nucleoside transporter from guinea pig and rat lung. Biochem. Soc. Trans. 14: 647-648.

Shi, M.M. and Young, J.D. (1986). ^{3}H-Dipyridamole binding to nucleoside transporters from rat and guinea pig lung. Biochem. J. 240: 879-883.

Shi, M.M., Tse, C.M. and Young, J.D. Solubilization and reconstitution of the guinea pig nucleoside transporter. Biochem. J. (submitted).

The work described in this dissertation are the result of my own work. This dissertation is not

substantially the same as any that I have submitted for a degree or diploma or other qualification at any other University.

ACKNOWLEDGEMENTS

The work described in this Thesis was carried out in the Department of Biochemistry, Faculty of Medicine, The Chinese University of Hong Kong, Shatin, Hong Kong, between September 1983 and May 1987. I wish to express my sincere appreciation to my supervisor, Dr. J.D. Young for his guidiance, encouragement and never-ending patience throughout this project.

Thanks are also due to Dr. C.M. Lee for his invaluable advice throughout the study and to Dr. C.M. Tse for his collaboration in the reconstitution studies of the guinea-pig lung nucleoside transporter.

I am also grateful to all my friends, fellow students and colleagues, whose help and advice I have sought over for the last four years.

I wish to thank the staff of the Animal House, The Chinese University of Hong Kong for supplying the animals used in this study.

ABBREVIATIONS

The following abbreviations are used in this Thesis:

ABA : N^6-(p-azidobenzyl) adenosine

ATP : adenosine triphosphate

DTT : dithiothreitol

EDTA : ethylenediaminetetracetic acid

Mr : molecular weight

NBMPR : nitrobenzylthioinosine, (6-((4-nitrobenzyl)thio)-9-β-D-ribofuranosyl purine)

NBTGR : nitrobenzylthioguanosine, (2-amino-6-((4-nitrobenzyl)thio)-9-β-D-ribofuranosyl purine)

PCMBS : p-chloromercuriphenyl sulfonate

PMF : purified plasma membrane fraction

PMSF : phenylmethyl-sulphonyl fluoride

POPOP : 1,4-bis[2-(5-phenyloxazolyl]benzene

PPO : 2,5-diphenyloxazole

SDS : sodium dodecyl sulphate

TABLE OF CONTENTS

CHAPTER 1

GENERAL INTRODUCTION

1.1 PREAMBLE

Nucleoside transport plays a key role in the cellular action of physiological and cytotoxic nucleosides, and inhibition of nucleoside transport is responsible for the pharmacological actions of several drugs, including dipyridamole, a clinically available vasodilator (Young and Jarvis, 1983). In human erythrocytes, nucleoside transport occurs by a rapid, facilitated diffusion process mediated by nucleoside-specific transport elements of the plasma membrane (Canbantchik and Ginsburg, 1977; Koren et al, 1978; Wohlhueter et al, 1979a; Jarvis et al, 1982b). This transport mechanism exhibits a broad substrate specificity, accepting a wide variety of nucleoside derivatives with very diverse nucleobase moieties. A number of potent inhibitors of nucleoside transport are known. The best studied of these is nitrobenzylthioinosine (NBMPR), a member of a family of S-substituted 6-thiopurine nucleosides that interact strongly with the nucleoside transport mechanism in both erythrocytes and a wide variety of other cell types (Paterson et al, 1981; Young and Jarvis, 1983). NBMPR inhibition of nucleoside transport is associated with tight, but reversible, high-affinity binding of inhibitor to the cell membrane. This association represents a specific interaction with components of the nucleoside transport machinery, probably via direct binding to the substrate permeation site (Jarvis and Young, 1980, 1982; Jarvis et al, 1982a,b).

The development of NBMPR and related compounds as specific high-affinity probes of the nucleoside transporter has allowed recent rapid progress in studies of the molecular properties of the carrier mechanism in erythrocytes. In human erythrocytes, the transporter has been partially purified by ion-exchange chromatography using reversible [^{3}H]NBMPR binding activity as an assay of transporter functions (Jarvis and Young, 1981). The purified material consisted largely of band 4.5 polypeptides (nomenclature of Steck (1974); Mr 45,000-66,000 on SDS-polyacrylamide gels). Subsequently it was established that exposure of site-bound [^{3}H]NBMPR to high-intensity UV light results in specific covalent radiolabelling of band 4.5 polypeptides (Wu et al, 1983; Young et al, 1983), providing further evidence to implicate this class of integral membrane proteins in nucleoside permeation. More recently, it has been shown that isolated band 4.5 polypeptides from human and pig erythrocytes catalyse NBMPR-sensitive uridine transport when reconstituted into phospholipid vesicles (Tse et al, 1985; Kwong et al, 1987). Endoglycosidase-F digestion experiments in combination with [^{3}H]NBMPR photolabelling have established that the erythrocyte nucleoside transporter is a glycoprotein (Kwong et al, 1986), while protease studies have been performed to investigate the transmembrane topology of the transporter (Kwong et al, 1987).

At the beginning of the present project in 1983, information concerning the molecular properties of the membrane components responsible for NBMPR-sensitive nucleoside transport was very limited and restricted to erythrocytes. Also, the mechanism by which dipyridamole interacts with the nucleoside transporter was unclear and controversial (Hammond et al, 1981; Jarvis and Young, 1983). In the present project, this latter topic was studied by investigating in detail the effect of dipyridamole on reversible [^{3}H]NBMPR binding and dissociation. These experiments were subsequently extended by parallel kinetic studies of reversible [^{3}H]dipyridamole binding. Another primary objective of the present project was to extend erythrocyte NBMPR photolysis and enzyme digestion studies to a non-erythroid tissue as a first step towards a molecular comparison of NBMPR-sensitive nucleoside transporters in different cell types. The lung was chosen for the series of investigations both because of its high density of high-affinity NBMPR binding sites (Marangos et al, 1982) and because of this tissue's role as a major site for the removal of circulating adenosine, a potent endogenous vasodilator (Kolassa et al, 1971; Bakhle and Vane, 1977). Two species were compared, one with a normal sensitivity to dipyridamole inhibition (guinea pig) and one whose NBMPR-sensitive nucleoside transporters are resistant to inhibition by this vasodilator (rat). In a final series of

experiments, the guinea pig lung nucleoside transporter was reconstituted into liposomes and its kinetic properties studied.

The major section of the present Chapter is a brief review of the literature on molecular and kinetic aspects of nucleoside transport in animal cells. This is followed by a description of the importance of the lung's physiological role as a major site for removal of circulating adenosine. The experimental strategy adopted in the present investigation and its objectives are then detailed. Finally, the organisation of the remainder of the Thesis is outlined.

1.2 PHYSIOLOGICAL AND PHARMACOLOGICAL IMPORTANCE OF NUCLEOSIDES

1.2.1 Biological Effects of Physiological Nucleosides

Nucleosides have a multitude of biochemical and physiological effects. For example, adenosine is believed to participate in processes such as modulation of immune responses, regulation of blood flow, platelet aggregation, renal function, neuromodulation in the central nervous system, neurotransmission, muscle contraction and numerous other biological processes (Harmon et al, 1978, Walker et al, 1979; Stone, 1981; Daly, 1982; Berne et al, 1983). Its unique mechanism of formation has led to the suggestion that adenosine functions as a novel form of cellular regulator for which the term "retaliatory metabolite" has been proposed (Newby, 1984). In addition, adenosine is also a physiological precursor of erythrocyte ATP in man (Valentine et al, 1977). Adenosine appears to produce most of its effects through specific extracellular adenosine receptors (Stone, 1981) and it is removed from the extracellular medium by transport into cells followed by metabolism (Fox and Kelly, 1978). Inhibition of the nucleoside transport system would, therefore, be expected to potentiate the biological effects of adenosine. Many structurally unrelated, pharmacologically active compounds such as NBMPR and the coronary vasodilators dipyridamole, dilazep, hexobendine and lidoflazine share an ability to

inhibit cellular accumulation of adenosine and potentiate adenosine effects.

Inosine has been shown to be an *in vivo* energy source for adult pig erythrocytes, cells unable to metabolise glucose (Young *et al*, 1985; 1986; Zeidler *et al*, 1985). In these cells, NBMPR functions as an *in vivo* inhibitor of energy metabolism (Young *et al*, 1986).

1.2.2 Nucleoside Analogues

Nucleoside analogues are widely used as therapeutic agents for the treatment of human neoplastic and viral diseases (Walker *et al*, 1979; De Clercq *et al*, 1980; Gauri, 1981; Tattersall and Fox, 1981; De Clercq, 1984). Of various cytotoxic nucleosides with clinical application as antineoplastic agents, the best known is cytosine arabinoside (ara C) which is an essential part of the current treatment of acute myeloid leukaemia (Wiemik, 1980; Hess and Zirkle, 1980). As well, 5-aracytidine has established clinical applications. Several nucleoside derivatives, notably acyclovir, are effective inhibitors of the proliferation of DNA viruses (De Clercq *et al*, 1980; De Clercq, 1984) and 3′-azido-3′deoxythymidine has potential therapeutic application in the treatment of acquired immunodeficiency syndrome (AIDS) (see Nature(1987), vol. 325, p564). Nucleoside analogues may also have application in the chemotherapy of parasitic infections (el Kouni *et al*, 1983; 1986;).

As seen from the foregoing account, nucleosides exhibit a multitude of biochemical, physiological and pharmacological effects. Each of these actions of nucleosides and nucleoside analogues require their transport into or out of cells. The nucleoside transport capacity of target cells and the 'transportability' of a nucleoside analogue, that is, its acceptability as a substrate for the nucleoside transporter, are important determinants of cytotoxicity. For example, measurements of NBMPR binding capacity (Section 1.3.2a) are likely to prove useful in assessing the therapeutic potential of ara C in human acute leukaemias (Wiley et al, 1983; 1985).

1.3 TRANSPORT OF NUCLEOSIDES BY ANIMAL CELLS

The entry of nucleosides and nucleoside analogues into mammalian cells occurs mainly by way of facilitated diffusion nucleoside-specific transport elements in the plasma membrane. The substrate specificity of the nucleoside transport machinery in mammalian cells is very broad in that a single type of transport mechanism mediates entry of (i) the physiological nucleosides (purine or pyrimidine ribosides and deoxyribonucleosides), and (ii) a variety of nucleoside derivatives with very diverse nucleobase moieties. Transporter function is typically inhibited by low concentrations (0.1-10 nM) of NBMPR (Section 1.3.2a), NBMPR-insensitive facilitated diffusion nucleoside transport systems that are inhibited only by micromolar (>1 uM) concentrations of NBMPR and also sodium-dependent nucleoside transport systems are present in some cell types.

1.3.1 Kinetic Studies

Nucleoside transport is a rapid, reversible, non-concentrative "facilitated-diffusion" process. in erythrocytes and in cultured cells of various types (Cabantchik and Ginsburg, 1977; Wohlhueter et al, 1979a; Harley et al, 1982; Jarvis et al, 1983a). The kinetics of nucleoside transport have been most extensively studied in mammalian erythrocytes using radioactively-labelled uridine, a nucleoside that is not metabolized by red blood

cells (Cabantchik and Ginsburg, 1977; Jarvis et al, 1983a; 1983b). The results of these studies indicate that the kinetic properties of the human erythrocyte system are consistent with a simple carrier model (Cabantchik and Ginsburg, 1977; Jarvis et al, 1983a; Lieb et al, 1982; Young and Jarvis, 1983). Using erythrocytes from human fresh blood, the Km and Vmax values for zero-trans uridine influx are identical to those determined for zero-trans uridine efflux, demonstrating that the carrier is symmetrical (Jarvis et al, 1983a; Jarvis and Martin, 1986). However, the kinetics of uridine transport in erythrocytes from outdated blood are asymmetrical, with efflux having a three- to four-fold higher Km and Vmax than influx (Jarvis et al, 1983a; Plagemann and Wohlhueter, 1984a). Molecular rate constants, estimated using the procedures described by Lieb (1982) (see also Stein, 1986) and interpreted in terms of a two-complex formulation of the simple carrier model (Fig. 1.1) can be used to explain for the above observations. The carrier is symmetrical in erythrocytes from fresh blood, k1 being equal to k2, but is asymmetrical in cells from out-dated blood, k2 being approximately 4-fold larger than k1. This kinetic difference between nucleoside transport in fresh and outdated erythrocytes is attributed to differences in the "mobility" that is, conformational change, of the unloaded carrier and is accentuated at low temperature (Plagemann and Wohlhueter, 1984b; Jarvis and Martin,

Figure 1.1 Two-complex formulation of the simple carrier model

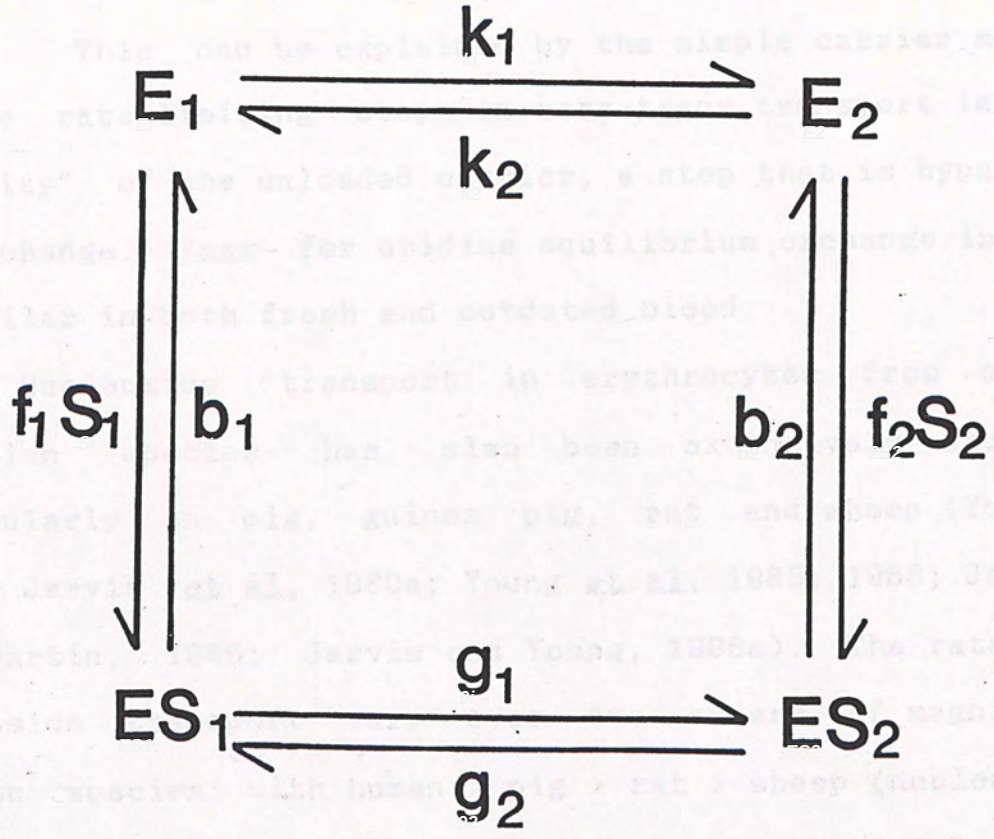

E represents the substrate-free form of the carrier, ES represents the carrier-substrate complex. Rate constants as indicated next to the appropiate reaction steps. Subscripts represent carrier forms available at, or steps originating in, sides 1 or 2 of the membrane, respectively.

1986). Interestingly, uridine equilibrium exchange, that is, the unidirectional flux of radioactively-labelled nucleoside at equal concentrations of uridine on the two sides of the membrane, has higher Km and Vmax values than net flux (Jarvis et al, 1983a; 1983b; Jarvis and Martin, 1986). This can be explained by the simple carrier model if the rate-limiting step in zero-trans transport is the "mobility" of the unloaded carrier, a step that is bypassed in exchange. Vmax for uridine equilibrium exchange influx is similar in both fresh and outdated blood.

Nucleoside transport in erythrocytes from other mammalian species has also been extensively studied particularly in pig, guinea pig, rat and sheep (Young, 1978; Jarvis et al, 1980a; Young et al, 1985; 1986; Jarvis and Martin, 1986; Jarvis and Young, 1986a). The rates of nucleoside transport vary over two orders of magnitude between species with human > pig > rat > sheep (nucleoside permeable type) > guinea-pig > sheep (nucleoside impermeable type) (Duhm, 1974; Jarvis et al, 1982b; Young and Jarvis, 1983). These differences in transport capacity are largely due to species differences in the cellular density of nucleoside transporters as determined by measurements of NBMPR binding (Jarvis and Young, 1982; Young and Jarvis, 1983) (see also Section 1.3.2a and Table 1.1).

Kinetic studies with cultured cells indicate that the facilitated diffusion nucleoside transporters in these

cells also exhibit directional symmetry (Wohlhueter and Plagemann, 1982). Transport of nucleosides in HeLa and Novikoff rat hepatoma cells are consistent with a simple carrier model (Wohlhueter et al, 1979a; Wohlhueter and Plagemann, 1982). However, in contrast to human erythrocytes, uridine transport parameters in Novikoff rat hepatoma cells for zero-trans and equilibrium exchange influx are similar, demonstrating equal mobility of the substrate-loaded and empty (i.e substrate-unloaded) carrier (Wohlhueter and Plagemann, 1982). However, nucleoside transporters in erythrocytes and cultured animal cells differ significantly in their translocation capacities, the calculated translocation capacities for uridine zero-trans influx of cultured cell lines are generally 10-fold lower than for erythrocytes (Young and Jarvis, 1983) (Table 1.1). Another difference in nucleoside transporter properties between cultured cells and erythrocytes is that nucleoside transporters from some cell types may, in addition, exhibit a significant affinity for free nucleosbases (Wohlhueter et al, 1979a; Slaughter et al, 1981; Plagemann and Wohlhueter, 1984a).

1.3.2 Inhibitor Studies

Specific inhibitors of carrier-mediated membrane transport of nucleosides have proved invaluable in attempts to isolate and identify nucleoside transport components.

Table 1.1 Comparison of Vmax for zero-trans uridine influx with Bmax for the binding of nitrobenzylthioinosine (NBMPR) in erythrocytes and cultured cells

Cell type	Uridine Vmax (10^{19} xmol/cell per s)	NBMPR Bmax (10^{21} xmol/cell)	Translocation capacity (molecules/site/s)
Human erythrocytes	26	18.3	142
Guinea-pig erythrocytes	0.07	0.045	155
Nucleoside-permeable-type sheep erythrocytes	0.053	0.029	181
HeLa S3 monolayer	110	1100	10
S49 mouse lymphoma	30	110	27
Chinese-hamster ovary	46	550	8.3

Vmax values at 22-25 °C for uridine influx and maximum high-affinity NBMPR-binding activities for cells were taken from Young and Jarvis (1983). Translocation capacities are calculated from the ratio uridine Vmax : NBMPR Bmax.

Figure 1.2 Chemical Structures

a) 6-Thiopurine nucleoside derivatives

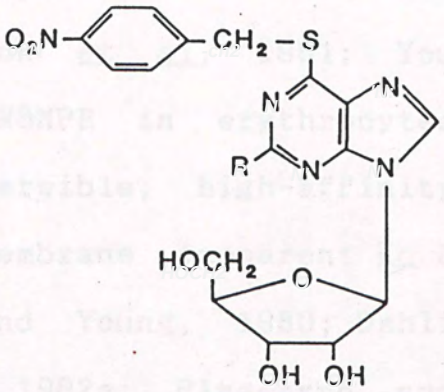

Nitrobenzylthioinosine R = H

Nitrobenzylthioguanosine R = NH_2

b) Nucleosides

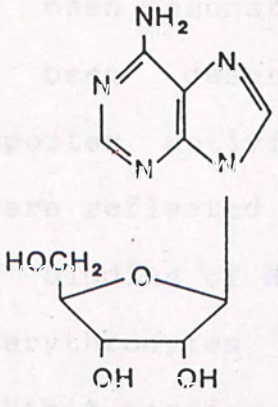

Adenosine

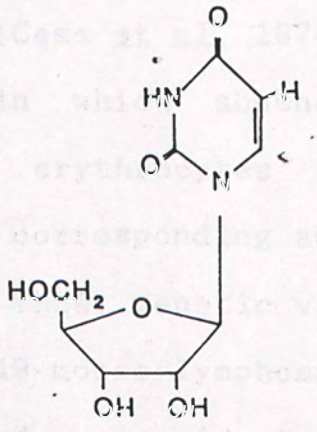

Uridine

1.3.2a Nitrobenzylthioinosine (NBMPR)

The best characterised and most useful inhibitor in the study of nucleoside transport is NBMPR (Fig. 1.2). NBMPR and certain related S -derivatives of 6-thiopurine nucleosides are very potent, reversible inhibitors of nucleoside transport in a wide variety of cell types and tissues (Paterson et al, 1981; Young and Jarvis, 1983). Inhibition by NBMPR in erythrocytes is associated with tight, but reversible, high-affinity binding of inhibitor to the cell membrane (apparent Kd 0.1-1 nM) (Cass et al, 1974; Jarvis and Young, 1980; Dahlig-Harley et al, 1981; Jarvis et al, 1982a; Plagemann and Wohlhueter, 1984a). Transported nucleosides such as uridine and adenosine (Fig. 1.2) are competitive inhibitors of high-affinity NBMPR binding (Jarvis et al, 1982; 1983). A direct proportionality between binding site occupancy by NBMPR and fractional inhibition of uridine transport in human erythrocytes has been demonstrated (Cass et al, 1974), and instances have been described in which absences of nucleoside transporter activity in erythrocytes and in cultured cells were reflected in the corresponding absences of site-specific binding of NBMPR. Thus, genetic variants of both sheep erythrocytes and S49 mouse lymphoma cells that do not exhibit carrier-mediated nucleoside transport also do not possess high-affinity NBMPR sites (Jarvis and Young, 1980, Cass et al, 1981). As well, in erythrocytes from various species, the maximum cellular transport

capacity (Vmax) for uridine was found to be directly related to the number of membrane transporter elements (NBMPR binding sites) present in each of the cell types studied (Jarvis and Young, 1980, 1982; Jarvis et al, 1982b).

Kinetically, NBMPR is a simple competitive inhibitor of zero-trans uridine influx and equilibrium exchange in human, nucleoside-permeable sheep and guinea pig erythrocytes, but a non-competitve inhibitor of uridine zero-trans efflux (Eilam and Cabantchik, 1977; Jarvis et al, 1982a; 1983b). Conversely, transported nucleosides are competitive inhibitors of high-affinity NBMPR binding (Jarvis et al, 1982a, b). Together, these findings are consistent with a model proposed by Jarvis and Young (1982) in which the erythrocyte NBMPR binding site is located partially or totally within the outward facing conformation of the transporter nucleoside permeation site, this binding being stabilized by the interaction of the nitrobenzene ring with an adjacent hydrophobic domain on the transporter (Jarvis and Young, 1982; Jarvis et al, 1982a; 1983b; see Fig. 1.3). It is considered that high-affinity NBMPR binding activity represents a specific quantitative assay of nucleoside transport protein in those cells where NBMPR has been shown to totally inhibit transport activity.

Although there is strong evidence that NBMPR binds directly to the nucleoside permeation site on the nucleoside transporter, the possibility that NBMPR binds to

Figure 1.3 A possible molecular model for the erythrocyte nucleoside transporter

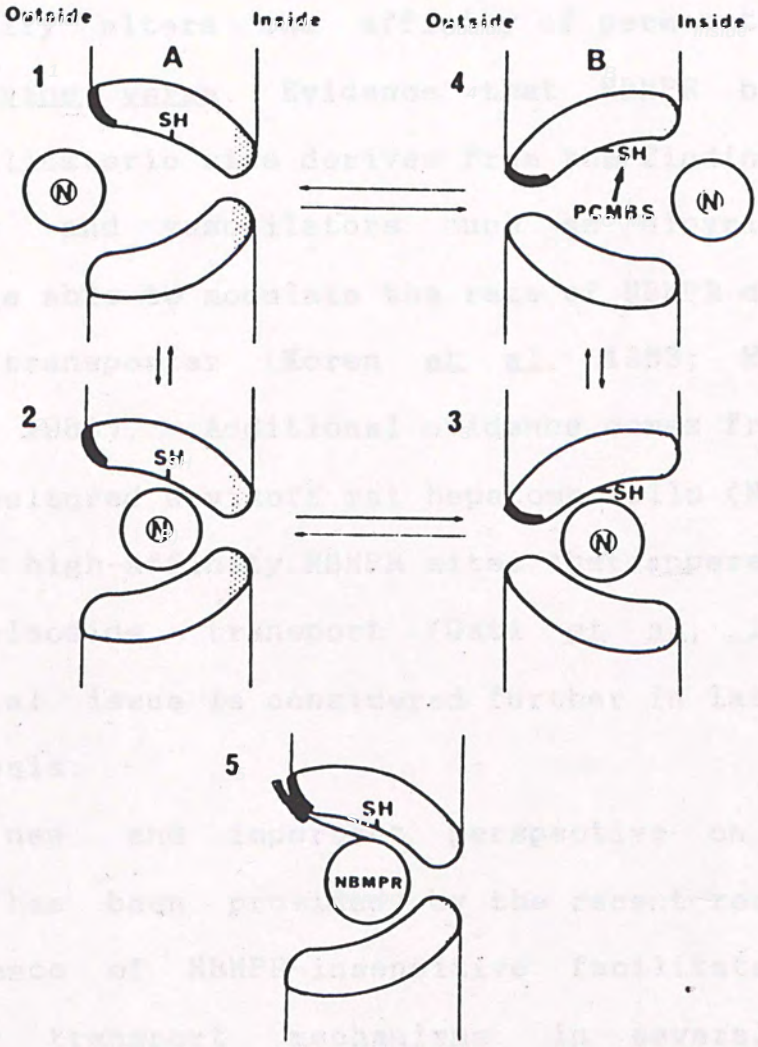

When the transport site is in the outward-facing conformation (A) (panel 1), it can bind nucleoside (2) and then undergo a re-orientation to the inward-facing form (3) after which the nucleoside is released (4) (conformation B). The conformational change can occur both in the presence and absence of bound nucleoside. NBMPR occupies the transport site in the outward-facing form (5).

a separate allosteric inhibitor site cannot be ruled out. In this separate site model of the NBMPR-sensitive nucleoside transporter, binding of NBMPR at one site allosterically alters the affinity of permeant at another site and vice versa. Evidence that NBMPR binds to a separate allosteric site derives from the finding that both nucleosides and vasodilators such as dipyridamole and dilazep are able to modulate the rate of NBMPR dissociation from the transporter (Koren et al, 1983; Hammond and Clanachan, 1985). Additional evidence comes from a cloned line of cultured Novikoff rat hepatoma cells (Novikoff-UA) possessing high-affinity NBMPR sites that apparently do not block nucleoside transport (Gati et al, 1986). This controversial issue is considered further in later Chapters of this Thesis.

A new and important perspective on nucleoside transport has been provided by the recent recognition of the existence of NBMPR-insensitive facilitated-diffusion nucleoside transport mechanisms in several lines of neoplastic cells. Studies with Novikoff rat hepatoma cells and Walker 256 carcinosarcoma cells have shown that these cells transport nucleosides by a non-concentrative (sodium-independent) system that is not inhibited by nanomolar concentrations of NBMPR (Wohlhueter et al, 1978; Belt, 1983a; 1983b). These cells also lack high-affinity NBMPR binding sites. Other cultured neoplastic cells such as L1210, L5178Y and P388 murine leukaemia cells,

transformed hamster fibroblasts and HeLa cells exhibit mixed NBMPR-sensitive and NBMPR-insensitive transport (Dahlig-Harley et al, 1981; Belt, 1983; Eilam and Cabantchik, 1977, Plagemann and Wohlhueter, 1985). These two transporters are indistinguishable with respect to substrate specificity, affinity for nucleosides and dipyridamole sensitivity (Belt, 1983; Plagemann and Wohlhueter, 1984a). The low sensitivity of some facilitated diffusion nucleoside transporters to NBMPR inhibition may reflect small structural or conformational changes in the transporter protein, resulting in a decrease in affinity of NBMPR binding and hence transport inhibition. Indeed, NBMPR-sensitive and NBMPR-insensitive, facilitated-diffusion nucleoside transport may reflect different functional states of the same transporter polypeptide. However, the molecular properties of NBMPR-insensitive nucleoside transport systems remain to be elucidated.

1.3.2b Sodium-dependent nucleoside transport

Recent studies of nucleoside uptake by rat renal brush border vesicles (Le Hir and Dubach, 1984; 1985), in intestinal enterocytes from guinea pigs (Schwenk et al, 1984) and rabbit intestinal brush border membranes vesicles (Jarvis, 1985) have shown the existence of a separate sodium-dependent, concentrative, NBMPR-insensitive nucleoside transport system. This sodium-dependent nucleoside transporter also exhibits a broad specificity

for both purine and pyrimidine nucleosides and displays a high-affinity (Km < 10uM) for physiological nucleoside permeants (Le Hir and Dubach, 1984). A joint presence of the sodium-dependent, concentrative (NBMPR-insensitive) nucleoside transporter and the NBMPR-sensitive, apparently equilibrative nucleoside transport system has been reported in cultured rat intestinal epithelial cells (Jakobs and Paterson, 1986). The detailed properties of the sodium-dependent nucleoside transport system remain to be investigated. It seems likely that this transporter will be found to be more widely distributed than renal and intestinal brush border membranes.

1.3.2c Coronary vasodilators

Dipyridamole and several other vasoactive drugs such as dilazep, hexobendine and lidoflazine were introduced as coronary vasodilators (Kinsella et al, 1962) and have subsequently had their pharmacological effects attributed to an inhibition of nucleoside transport (Kolassa et al, 1970; Sano, 1974). These coronary vasodialtors are potent inhibitors of nucleoside transport in many cell types and tissues. They inhibit adenosine transport, thus potentiating the actions of adenosine on coronary blood flow.

Dipyridamole, the most extensively studied coronary vasodilator, potentiates adenosine-induced increases in coronary blood flow in man (Kinsella et al, 1962, Feldman

et al, 1981). Other pharmacological responses to adenosine which are potentiated by dipyridamole include relaxation of the smooth muscle of trachea (Davies et al, 1982), depression of nerve cell firing rates (Phillis et al, 1979) and adenosine-elicited accumulation of cyclic AMP in brain slices (Nimit et al, 1981;). All these effects of dipyridamole can be abolished by adenosine receptor antagonists which supports the theory that dipyridamole may be producing an increase in the extracellular concentration of adenosine available to interact with adenosine receptors.

Dipyridamole is a poor inhibitor (Ki > 100 uM) of adenosine deaminase (Kubler et al, 1970; Schrader et al, 1972) and adenosine kinase (Schrader et al, 1972), enzymes involved in the inactivation of adenosine. Therefore, the adenosine-potentiating action of dipyridamole was attributed to an inhibition of the cellular uptake of adenosine (Hopkins, 1973; Coleman, 1976; Huang and Drummond, 1976). Inhibition of nucleoside uptake by dipyridamole has been described in a variety of cell types including erythrocytes (Turnheim et al, 1978; Rogler-Brown and Parks, 1980; Jarvis et al, 1982), platelets (Lips et al, 1980), lymphocytes (Pazdur et al, 1980), cardiac tissue (Kolassa et al, 1970; Mustafa, 1979), Novikoff rat hepatoma cells (Plagemann, 1971), guinea pig smooth muscle (Kolassa et al, 1978b) and guinea pig and rat cortical synaptosomes (Bender et al, 1980; Barberis et al, 1981).

The mechanism by which dipyridamole produces its inhibition of nucleoside transport is still a matter of some dispute (see for example Jarvis and Young, 1983). Competitive, non-competitive and mixed type inhibition by dipyridamole has been reported in different cell types. Nucleoside transporter heterogeneity is also apparent with respect to inhibition by dipyridamole. For example, several studies suggest that there may be significant species variation in the potency of dipyridamole as an inhibitor of nucleoside transport. Thus, in all instances so far studied, rat tissues have been found to be resistant to dipyridamole inhibition (Kolassa et al, 1971; Hopkins and Goldie, 1971; Sakai et al, 1981; Wu et al, 1981; Barker and Clanachan, 1982). Furthermore, nucleoside transport in JPA4 cells (a mutagenized clone derived form S49 murine T-lymphoma cells, cells exhibiting pure NBMPR-sensitive nucleoside trasnport) is partially insensitive to dipyridamole inhibition. It should be noted that dipyridamole appears to be a relatively non-specific inhibitor of membrane transport processes because it also inhibits the transport of anions, purine bases, 2-deoxy-D-glucose and D-glucosamine (Plagemann and Richey, 1974). NBMPR-insensitive facilitated nucleoside transport is generally sensitive to dipyridamole inhibition (Belt, 1983; Belt and Noel, 1986) while the sodium-dependent nucleoside transporter is not (Jarvis, personal communication).

Dilazep and the structurally related compound hexobendine have been shown to increase coronary and cerebral blood flow in dogs (Sano, 1974; Fujii et al, 1981). These coronary vasodilators are also potent inhibitors of adenosine uptake (Ki < 0.1 uM) in human erythrocytes (Turnheim et al, 1978), cardiac cells (Mustafa, 1979), guinea pig epithelium (Kolassa et al, 1978b), and rat brain capillaries (Wu and Phillis, 1982).

Lidoflazine is a long-acting coronary vasodilator which acts both directly on the smooth muscle of coronary vessels (VanNeuten and Vanhoutte, 1980) and indirectly via a potentiation of adenosine-induced vasodilation (Van Belle, 1970). The direct effect of lidoflazine appears to be due to an inhibition of calcium influx, thereby inhibiting smooth muscle contraction. Lidoflazine has been shown to decrease the rate of disappearance of adenosine from whole blood of various species (Van Belle, 1970) and these effects were attributed to an inhibition of adenosine uptake. Lidoflazine has also been shown to inhibit the uptake of adenosine by guinea pig epithelial cells (Kolassa et al, 1978b) and cardiac cells (Mustafa, 1979). Lidoflazine is generally 10-fold less potent than dipyridamole as an inhibitor of adenosine uptake (Mustafa, 1979).

Fig. 1.4 compares the chemical structures of the various coronary vasodilators.

Figure 1.4 Chemical structures of coronary vasodilators

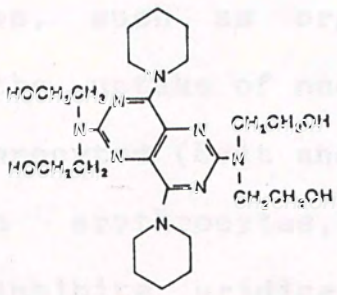

Dipyridamole

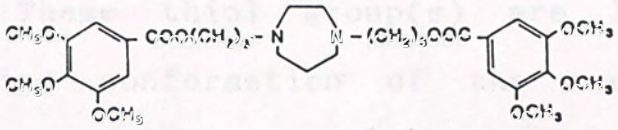

Dilazep

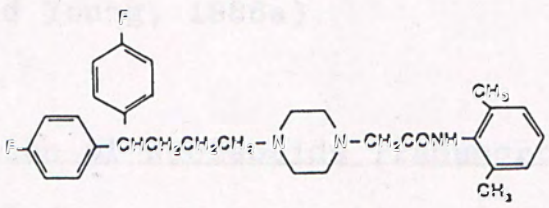

Lidoflazine

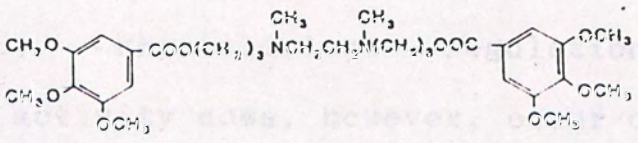

Hexobendine

1.3.2d Other inhibitors

A number of other substances chemically unrelated to nucleosides, such as organomercurials, have been found to inhibit the uptake of nucleosides by cultured animal cells and erythrocytes (Belt and Noel, 1985; Jarvis et al, 1986). In human erythrocytes, p-chloromecuriphenyl sulphonate (PCMBS) inhibits uridine transport and NBMPR binding by interacting with nucleoside transporter thiol group(s) exposed to the cytoplasmic membrane surface (Tse et al, 1985). These thiol group(s) are located within the inward-facing conformation of the nucleoside transporter permeation site. In contrast, the PCMBS-reactive thiol(s) in NBMPR-insensitive transporters are accessible from the external membrane surface (Belt, 1983a; Belt and Noel, 1985; Jarvis and Young, 1986a).

1.3.3 Regulation of Nucleoside Transport

Early studies demonstrating that nucleoside uptake by cultured cells could be modified by a variety of factors including hormones and cyclic nucleotides (Plagemann and Richey, 1974) can be attributed to effects on intracellular nucleoside phosphorylation rather than transport per se (Koren et al, 1978; Rozengurt et al, 1978; Wohlhueter et al, 1979b). Physiological regulation of nucleoside transport activity does, however, occur during reticulocyte maturation (Tucker and Young, 1980; Jarvis and Young, 1982). Maturation of sheep reticulocytes during in vitro

culture results in the parallel loss of transport activity and NBMPR binding (Jarvis and Young, 1982). This loss of transport activity and NBMPR binding during reticulocyte maturation is restricted to certain species (e.g. sheep but not pig or human) and may involve release from the cell of transporter polypeptides in vesicular form (Johnstone et al, 1985).

1.3.4 Molecular Properties of the NBMPR-sensitive Nucleoside Transporter

The protein nature of the erythrocyte nucleoside transporter was formally demonstrated by studies of the effects of proteases and organomercurials on NBMPR binding and nucleoside transport (Paterson et al, 1980; Jarvis and Young, 1982). The transporter has been shown to exhibit chemical asymmetry, with trypsin and PCMBS-sensitive sites located on the inner surface of the cell membrane (Jarvis and Young, 1982; Tse et al, 1985).

The first successful approach towards transporter isolation used high-affinity NBMPR-binding as an assay for the carrier and resulted in a 13-fold purification of the transporter from human erythrocyte 'ghosts' by a combination of detergent extraction and fractionation on a DEAE-cellulose ion-exchange column. The partially-purified preparation consisted largely of band 4.5 polypeptides (nomenclature of Steck (1974)) as detected on SDS-polyacrylamide electropherograms. Band 4.5 polypeptides

have also been implicated in glucose transport (see e.g. Wheeler and Hinkle, 1985). As a result, partially-purified band 4.5 preparations from human erythrocytes consist largely of glucose transporter, with the nucleoside transporter present as a minor component. In human erythrocytes the nucleoside carrier represents at most 0.2% of the total membrane protein.

The use of NBMPR as a probe for exploring the molecular properties of the NBMPR-sensitive nucleoside transport system is complicated by the reversible nature of its binding to the carrier protein and by the finding that some detergents, such as Triton X-100, are potent inhibitors of NBMPR binding (Cass et al, 1974; Jarvis and Young, 1980, 1981; Koren et al,1983). To overcome these limitations, a photoaffinity analogue of NBMPR, [^{3}H]^{6}N -(p-azidobenzyl) adenosine (ABA), was synthesized and tested for its ability to photoaffinity label the nucleoside transporter in human erythrocytes (Young et al, 1983). At the same time, NBMPR itself was shown to be cross-linked to its binding site simply by exposure to high-intensity UV light (Young et al, 1983). Since NBMPR has a higher affinity for the NBMPR-sensitive nucleoside transport system (apparent Kd 0.1-1.0 nM) than ABA (apparent Kd 15 nM), and because it is readily available in radioactive form with a high specific activity, [^{3}H]NBMPR has become the preferred radioligand in photoaffinity labelling studies. Photoactivation of

site-bound [^{3}H]NBMPR or [^{3}H]ABA of human erythrocyte 'ghosts' in the presence of dithiothreitol as free radical scavenger results in selective incorporation of radioactivity into band 4.5 polypeptides (apparent Mr 45,000-66,000). This radiolabelling is blocked by transported nucleosides, and by nucleoside inhibitors such as nitrobenzylthioguanosine (NBTGR) and dipyridamole (Wu et al, 1983). Also, [^{3}H]NBMPR selectively labels band 4.5 polypeptides in membranes from pig erythrocytes (Wu et al, 1983a; Young et al, 1985), cells which transport nucleosides rapidly, but which lack a functional glucose transporter (Kim and McManus, 1971; Jarvis et al, 1980a; Young et al, 1985). The pig erythrocyte nucleoside transporter migrates with a significantly higher apparent molecular weight on SDS-polyacrylamide gels than the human transporter (Mr (average) 64,000 c.f. 55,000) (Kwong et al, 1985). The specificity of covalent labelling by [^{3}H]NBMPR was further demonstrated by the absence of ^{3}H incorporation into membranes prepared from nucleoside transport-deficient sheep erythrocytes, cells which lack functional nucleoside transporters (Wu et al, 1983a). Partially-purified band 4.5 polypeptides isolated from human erythrocyte membranes were also found to be covalently labelled by NBMPR (Wu et al, 1983b). These results provide strong evidence that the erythrocyte nucleoside transporter is a band 4.5 polypeptide. Radiation-inactivation analysis of both reversible

NBMPR-binding and uridine transport estimate that the erythrocyte transporter has an *in situ* molecular weight of 120,000, suggesting that the carrier may exist in the membrane as a dimer (Jarvis, 1980b; 1984).

To explore the transmembrane topology of the erythrocyte nucleoside transporter, [^{3}H]NBMPR covalently-labelled intact cells and unsealed membrane 'ghosts' have been subjected to controlled proteolysis. Low concentrations of trypsin under iso-osmotic saline conditions were found to have no effect on [^{3}H]NBMPR-photolabelled band 4.5 in intact human erythrocytes (Janmohamed *et al*, 1985). In contrast, two radioactive fragments of apparent Mr 38,000 and 23,000 were produced when unsealed erythrocyte membranes are treated with trypsin (Janmohamed *et al*, 1985). The Mr 38,000 fragment migrates as a braod peak, suggesting that carbohydrate is attached to this fragment. These results suggest that the trypsin-sensitive regions of the transporter are exposed on the inner surface of the human erythrocyte membrane. Subsequent studies of trypsin treatment of the pig nucleoside transporter established that the transport polypeptide in this species is also not susceptible to proteolysis from the extracellular surface of the membrane but is again cleaved by trypsin at the cytoplasmic surface.

Enzyme digestion studies have also been performed with endoglycosidase-F, an enzyme that cleaves glycans of

both the high-mannose and the complex types. Following endoglycosidase-F treatment, the [^{3}H]NBMPR-labelled peak and the Coomassie blue staining profile on SDS-polyacrylamide gels of partially-purified human erythrocyte band 4.5 polypeptides shifts from the broad band of Mr 55,000 to a sharp Mr 46,000 band, providing evidence that the nucleoside transporter of human erythrocytes is a glycoprotein (Kwong et al, 1986). The pig erythrocyte nucleoside transporter has also been shown to be a glycoprotein but the carbohydrate structures in the two species are different; endo-β-galactosidase cleaves only the human transporter and not the pig, while endoglycosidase F cleaves both (Kwong et al, 1985). The polypeptide structures of the two transporters also differ, the deglycosylated pig protein migrating on SDS-polyacrylamide gels with an apparent Mr of 57,000 compared with 44,000 for the deglycosylated human erythrocyte nucleoside transporter (Kwong et al, 1985).

A partially-purified preparation of human erythrocyte NBMPR-binding protein (consisting >95% of band 4.5 polypeptides) was reconstituted into soybean phospholipid vesicles by a freeze-thaw-sonication procedure (Tse et al, 1985). The reconstituted proteoliposomes exhibited NBTGR-sensitive [^{14}C]uridine influx that was inhibited by adensoine, inosine, dipyridamole and dilazep. Uridine transport by the reconstituted band 4.5 preparation was saturable (apparent Km for influx 0.21 mM with a Vmax

value of 1.8 nmol/mg protein per s at 15°C) (Tse et al, 1985). Similarly, partially-purified pig erythrocyte band 4.5 polypeptides exhibit NBTGR-sensitive uridine transport when reconstituted into phospholipid vesicles, but, unlike human band 4.5 polypeptides, are incapable of stereospecific glucose transport (Kwong et al, 1986).

Specific antibodies to the glucose transporter (Boyle et al, 1985) have been used to 'negatively' purify the nucleoside transporter from human erythrocyte band 4.5 polypeptides. Preliminary experiments have demonstrated a 76-fold enrichment of human erythrocyte nucleoside transporter by this method (Kwong et al, 1986), a value which is 6-fold greater than that achieved by ion-exchange chromatography (Jarvis and Young, 1981).

1.4 LUNG'S RELEVANCE TO NUCLEOSIDE TRANSPORT

The lung is thought of primarily as an organ for gas exchange and the biochemical properties of the pulmonary circulation are often neglected. The importance of the metabolic functions of the lung and the effect of the pulmonary circulation on blood-borne substances should be emphasized since it may have important physiological and clinical implications (Bakhle and Vane, 1974; Bakhle and Vane, 1977). The biochemical processes occuring within the pulmonary circulation result in the removal or release of many biologically active substances. Both endogenous and exogenous substances are removed during passage through the pulmonary circulation (see e.g. Fishman and Pietra, 1963; Bakhle and Vane, 1977). Three unique properties of the pulmonary circulation are relevant to this role:

(i) It is the only vascular system in the body which receives the entire cardiac output.

(ii) It contains the largest capillary bed in the body.

(iii) It occupies a unique position between the venous and arterial circulations.

For these reasons, venous blood will come into contact with an enormous area of pulmonary endothelium, known to be biochemically active, before it reaches the systemic circulation. Thus, the blood levels of physiologically important substances are likely to be modified before they reach the heart and systemic circulation. Compounds for which this is known to occur

include 5-hydroxytryptamine, noradrenaline, prostaglandins, bradykinin, adenine nucleotides, endogenous hormones e.g. steroids, insulin and a number of circulating vasoactive agents (e.g. adenosine), and this process is believed to be important in maintaining vascular homeostasis (Gillis and Roth, 1976). In the context of this Thesis, only the lung's role in the removal of nucleosides, in particular, adenosine will be discussed.

Binet and Burnstein (1950) first described the disappearance of ATP on passage through the lung, and in subsequent studies in which radiolabelled nucleotides were infused (Ryan and Smith, 1971; Cooper et al, 1979), it was shown that the pulmonary bed degrades ATP to adenosine via specific enzymes on the surface of the capillary endothelium. The possiblity of cellular uptake and metabolism of the adenosine thus formed was not, however, investigated. It was not until 1971 that the removal of adenosine from the pulmonary circulation was first reported. These early in vivo experiments (Kolassa et al, 1971) demonstrated that, in the rat and guinea pig, the majority of radioactivity following intravenous injection of labelled adenosine was retained by the lungs. In addition, it was observed that there was a significant difference in the ability of lungs from the two animals to dispose of adenosine. Thus, Kolassa et al (1971) observed that guinea pig lung was able to remove 50% more adenosine than rat lung. These authors also reported a marked

difference between the two species with respect to the ability of dipyridamole to inhibit adenosine uptake. In subsequent isolated lung perfusion studies (Bakhle and Chelliah, 1983), it was shown that both rat and guinea pig perfused lung were capable of removing adenosine from the vascular space by a combined process of uptake and subsequent intracellular metabolism. Similar dipyridamole sensitivity differences between guinea pig and rat lung were also reported, dipyridamole being more potent in decreasing uptake in guinea pig lung than in rat lung.

Therefore, at least in guinea pig and rat, the pulmonary endothelium appears to play a major role in the removal of circulating adenosine. Support for this view comes from work by Pearson et al (1978) who found that pig aortic endothelial cells in culture rapidly transported adenosine in a manner which was inhibited by dipyridamole. The high uptake capacity of these cells led the authors to conclude that pulmonary endothelial cells are the major route for the removal of circulating adenosine in the pig. Subsequent studies in isolated piglet perfused lung also demonstrated that adenosine was efficiently taken up from the pulmonary vascular bed, and that the process was potently inhibited by dipyridamole (Hellewell and Pearson, 1983).

1.5 EXPERIMENTAL APPROACH AND OBJECTIVES

Physiologically, lung is important for adenosine removal as detailed in the previous Section. Hence there is a need to characterize nucleoside transport in this tissue, both with respect to kinetic behaviour and also with respect to pharmacology. However, transport experiments using perfused whole lung suffer certain inherent limitations. For example, kinetic values for tissue nucleoside uptake based on such studies do not report initial rates of permeation across the endothelial cell membrane and are likely to reflect net effects of several metabolic processes, in addition to that of membrane transport. Also, the isolation of pulmonary endothelial cells is inherently difficult. Therfore, in this present study, I have attempted to study functional aspects of nucleoside transport in lung by alternative approaches. Lung tissues possesses a very high density of NBMPR binding sites (Marangos *et al*, 1982). Hence, my initial series of experiments developed the use of reversible NBMPR binding to study nucleoside transporter function in plasma membranes of rat and guinea pig lung. In the course of these experiments, I found that the rat and guinea pig lung nucleoside transporters differed significantly in dipyridamole sensitivity. [^{3}H]dipyridamole binding studies and kinetic experiments on [^{3}H]NBMPR binding were subsequently carried out in an attempt to obtain a better understanding of the mechanism by which dipyridamole

interacts with the transporter and in particular relationship between NBMPR and dipyridamole binding sites in the two species.

In a complementary series of experiments, nucleoside transport in lung was studied directly, making use of reconstitution methodology. These studies were necessary to ensure that the NBMPR binding protein characterized in other experiments did in fact represent the NBMPR-sensitive nucleoside transporter. To do this, the NBMPR binding protein from guinea pig lung plasma membranes was solubilised in detergent and reconstituted into proteoliposomes. A major advantage of this technique is that it was possible to perform detailed kinetic experiments, permitting an in depth comparison of transport parameters in lung and erythrocytes.

Another major objective of my study was to investigate the molecular properties of the NBMPR-sensitive nucleoside transporter in the lung as a first step towards a molecular comparison of nucleoside transporters in non-erythroid tissues with those well characterized systems present in human and pig erythrocytes. For these investigations, radiolabelled NBMPR was used as a covalent probe to photoaffinity label the NBMPR binding sites in lung plasma membranes, the labelled proteins being characterized by SDS-polyacrylamide gel electrophoresis. Labelling patterns were compared with that given by red blood cells. It was observed that rat and guinea pig lung

nucleoside transporters have significantly different apparent molecular weights on SDS-polyacrylamide gels. The origin of this molecular weight difference in the two species was explored by limited proteolysis and endoglycosidase-F digestion experiments.

1.6 ORGANIZATION OF THESIS

The remainder of the thesis is divided into six Chapters. In Chapter Two, a detailed investigation of NBMPR binding to rat and guinea pig lung crude membranes is presented. The kinetics of NBMPR binding and dissociation are also described. A parallel chracterization of [^{3}H]dipyridamole binding to guinea pig and rat lung crude membranes is described in Chapter Three.

In Chapter Four, an in depth study of the photoaffinity labelling of lung crude plasma membranes by [^{3}H]NBMPR is presented. Conditions for photoincorporation of [^{3}H]NBMPR into lung membranes are described and the identity of the membrane polypeptides radiolabelled by [^{3}H]NBMPR is investigated. This Chapter also presents evidence that the rat and guinea pig lung nucleoside transporters are glycoproteins and explores the origin of a molecular weight difference between the nucleoside transporters from these two species.

Chapter Five describes conditions for the preparation of a more enriched lung plasma membrane preparation possessing a higher specific activity of NBMPR binding. This Chapter also describes the characterisation of reversible and covalent NBMPR binding in this enriched plasma membrane preparation.

In Chapter Six, the NBMPR binding protein extracted from the enriched guinea pig lung membranes is shown to catalyse NBTGR-sensitive uridine transport when

reconstituted into proteoliposomes. The system's kinetic properties are characterized in detail and compared with those of the reconstituted human erythrocyte nucleoside transporter.

Finally, Chapter Seven presents a general discussion of the results presented in preceding Chapters.

CHAPTER 2

NITROBENZYLTHIOINOSINE BINDING TO RAT AND GUINEA PIG LUNG CRUDE PLASMA MEMBRANES

2.1 INTRODUCTION

In recent years, functions other than respiration have been attributed to the lung. One such nonrespiratory function is a pharmacokinetic role in the disposition of endogenous and exogenous compounds in the blood. Of particular interest is the physiological role of the lung in the removal of adenosine, a potent vasodilator and endogenous regulator of the microcirculation (Drury and Szent-Gyorgi, 1929; Baer and Drummond, 1979). *In vivo* perfusion studies by Kolassa *et al* (1971) suggest that, at least in the guinea pig and the rat, the pulmonary endothelium plays a major role in the removal of circulating adenosine. Kolassa *et al* (1971) observed that guinea pig lung was able to remove 50% more adenosine than rat lung, and reported significant differences between the two species in the ability of dipyridamole to inhibit uptake of adenosine. Similar differences between guinea pig and rat lung were also reported more recently by Bakhle and Chelliah (1983).

As detailed in the General Introduction, it is well established that high-affinity binding of [^{3}H]NBMPR to human erythrocyte 'ghosts' represents a specific interaction with functional elements of the erythrocyte nucleoside transporter (Cass *et al*, 1974; Jarvis and Young, 1980, 1982; Young and Jarvis, 1983). Preliminary experiments by Marangos *et al* (1982) have also revealed a high density of high-affinity NBMPR binding sites in rat

lung. The aim of the experiments described in this Chapter was to investigate NBMPR binding to membrane preparations from lung tissue as a first step towards a molecular and functional characterization of NBMPR-sensitive nucleoside transporters in this tissue. A detailed characterization of reversible NBMPR binding to rat and guinea pig lung crude plasma membranes is presented. Kinetic studies of NBMPR binding in the presence and in the absence of dipyridamole were used to explore the origin of the species difference in dipyridamole sensitivity.

2.2 METHODS

2.2.1 Tissue and Membrane Preparation

Male Sprague-Dawley rats (400-450g) and Dunkin-Hartley guinea pigs (700-800 g) were anaesthetised with ether and the lungs perfused *in situ* with heparinized saline to remove trapped erythrocytes. Lung tissue was then removed from the animals, washed twice in ice-cold saline and homogenized in 25 volumes (w/v) of ice-cold 50 mM Tris-HCl (pH 7.4 at 22°C) using a Brinkmann Polytron PT-10 (setting 5, 6 s). Samples were centrifuged at 3000g for 10 min and the pellet discarded. The supernatant was then centrifuged at 45,000 g for 10 min, and the pellets washed 3 times in 25 volumes of Tris-HCl before resuspension in the same volume of buffer. This crude membrane preparation was used without further purification.

Protein was determined by the method of Lowry *et al* (1951).

2.2.2 Equilibrium High Affinity NBMPR Binding

Rat and guinea-pig lung membranes in 50 mM Tris-HCl (0.05 - 0.08 mg protein) were incubated with graded concentrations of [^{3}H]NBMPR (final equilibrium concentrations 0.05 - 10 nM) in a total volume of 1 ml for 30 min at 22°C in the presence or in the absence of 20 uM NBTGR as competing non-radioactive ligand. Incubations were terminated by filtration on glass fibre filters

(Whatman GF/B, which were washed with ice-cold buffer before sample filtration) under suction. The filters were washed four times with 3 ml aliquots of ice-cold buffer, the entire procedure being completed within 15 s. The filters were dried and added to 10 ml of scintillation fluid. Vials were shaken at room temperature overnight before counting. [^{3}H]NBMPR binding to membranes was expressed per mg protein. Nonspecific binding was defined as binding in the presence of 20 uM NBTGR (corrected for absorption of radioactive ligand by the filters). Specific binding was calculated as the difference in binding in the presence and in the absence of NBTGR. Equilibrium concentrations of unbound [^{3}H]NBMPR were calculated from the differences between the starting [^{3}H]NBMPR concentrations and the amounts of ligand bound to membranes and filters.

2.2.3 Kinetic Studies of NBMPR-binding

2.2.3a Dissociation kinetics of NBMPR binding

Rat and guinea pig lung membranes were incubated with [^{3}H]NBMPR (final equilibrium concentration 2 nM) for 30 min at 22`C. Incubations were terminated by centrifugation at 40,000 g for 15 min. The membrane pellets were washed once with 10 ml of ice-cold 50 mM Tris-HCl buffer (pH 7.4 at 22`C) and resuspended at a protein concentration of 2 mg/ml. The [^{3}H]NBMPR-labelled

membranes were kept on ice for up to 3 h. Control experiments demonstrated that the amount of [^{3}H]NBMPR bound to the lung crude membranes of both species remained constant during this period. Dissociation was initiated by adding 250 ul of ice-cold [^{3}H]NBMPR-labelled membrane to 60 ml of 50 mM Tris buffer, pH7.4 at 22^{0}C containing no addition or graded concentrations of dipyridamole (100 nM - 100 uM) either in the presence or in the absence of 20 nM NBTGR. The medium was continuously stirred and at various time intervals (0.5-20 min) after the addition of the membranes, 5 ml portions were removed and filtered immediately through glass-fibre filters under suction. The filters were washed four times with 3 ml aliquots of ice-cold buffer, the entire procedure being completed within 15 s. The filters were dried and counted for radioactivity as described above. Dissociation of radioligand from non-specific binding sites was determined by labelling the lung membranes with [^{3}H]NBMPR in the presence of 5 uM NBTGR and then measuring the rate of dissociation by the above procedure. Dissociation of non-specific [^{3}H]NBMPR binding was limited to the first 1 min of incubation. Thereafter, no further dissociation of radioligand occured. Non-specific binding was typically less than 5% of the total binding. Specific [^{3}H]NBMPR binding was calculated as the difference between total binding and non-specific binding measured in the presence of excess nonradioactive NBTGR.

The suspension medium used in the majority of dissociation experiments contained 20 nM nonradioactive NBTGR so as to prevent re-binding of dissociated [^{3}H]NBMPR (Jarvis et al, 1983). Results obtained were evaluated by using the following equation derived for a simple bimolecular reaction:

$$\ln (Bt / Beq) = - Koff \times t \quad \text{equation (1)}$$

where Beq is the specific binding at time zero, Bt is the specific binding at time t, and Koff is the dissociation rate constant.

2.2.3b Association kinetics of NBMPR binding

The experimental conditions for measuring the association kinetics of [^{3}H]NBMPR binding were designed to be pseudo-first order, that is, the concentration of free radioactive ligand, [L] in equation (2) below is constant throughout the reaction (Bennett, 1978). A low protein concentration in a relatively large volume of [^{3}H]NBMPR was used so as to achieve the above condition. Binding was started by adding 50 ug of lung membrane to 60 ml of 0.5 nM [^{3}H]NBMPR ($\pm$ 10^{-8} - 10^{-4} M dipyridamole) at 22^{o}C. After various time intervals (0-40 min), 5 ml aliquots of the reaction mixture were removed and filtered as described above (Section 2.2.2) and the bound radioactivity was determined. Non-specific binding was measured in the presence of 5 uM NBTGR, and specific binding was obtained as the difference in binding in the absence and in

the presence of 5uM NBTGR.

To analyse the data, values obtained were plotted according to the rate equation:

$$\ln [(B_{eq} - B_t) / B_{eq}] = - (K_{on} [L] + K_{off}) \times t$$

equation (2)

where B_{eq} and B_t are the concentrations of bound receptor at equilibrium and at time t, K_{on} and K_{off} are the association and dissociation rate constants, respectively and [L] is the free radiolabelled-ligand concentration at steady state. The percentage of total ligand bound at the 0.5nM [^{3}H]NBMPR used was less than 10% , hence, [L] in equation (2) can be considered to be constant throughout the experiment.

2.3 RESULTS

2.3.1 Characterisation of NBMPR Binding to Lung Membranes

Fig. 2.1 shows representative data for the concentration-dependence of [^{3}H]NBMPR binding to rat and guinea-pig lung membranes, demonstrating the presence of both high-affinity saturable (NBTGR-sensitive) and nonsaturable (NBTGR-insensitive) binding components in the two species. Specific binding saturated at about 2.5 nM [^{3}H]NBMPR, Scatchard analyses of the data indicating a single population of binding sites with a similar dissociation constant (Kd) in the two species (0.2-0.4 nM), but a 2-fold difference in the number of binding sites (Bmax), guinea pig being higher than rat (Table 2.1 and Fig. 2.2). Calculated Hill coefficients for specific high affinity NBMPR binding were 1.03 and 0.98 for rat and guinea pig lung membranes, respectively (Fig. 2.2 and Table 2.1). Both species exhibited the same amount of non-specific (NBTGR-insensitive) [^{3}H]NBMPR binding (1.5 pmol/mg protein at 10 nM NBMPR). Dissociation experiments confirmed that high-affinity NBMPR binding to lung membranes was reversible (see Section 2.3.2a).

The effects of two physiological nucleosides, adenosine and uridine, on NBTGR-sensitive NBMPR binding to rat and guinea pig lung crude membranes are shown in Fig. 2.3. The concentrations of nucleosides required to induce 50% inhibition (IC_{50}) of high-affinity NBMPR

Figure 2.1 Concentration dependence of NBMPR binding to rat and guinea-pig lung crude membranes

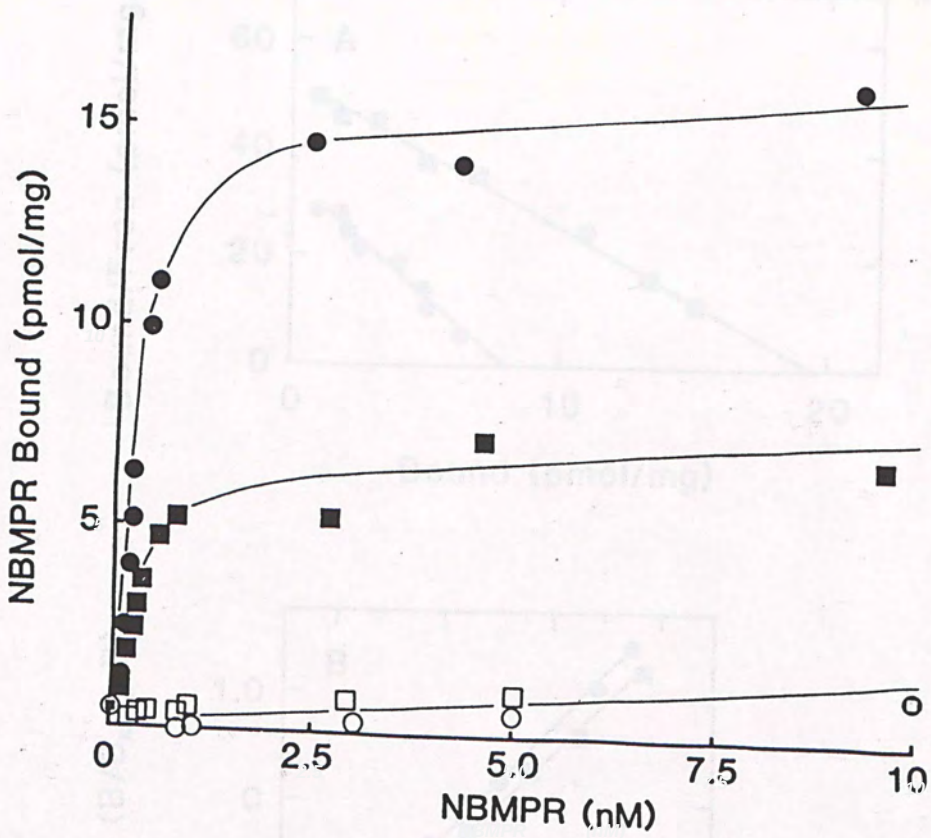

[^{3}H]NBMPR binding to rat (■ , □) and guinea-pig (● , ○) lung membranes was measured in the absence (■ , ●) and in the presence (□ , ○) of 20 uM NBTGR as competing ligand. Values are means of duplicate estimates.

Figure 2.2 Scatchard and Hill plots of site-specific NBMPR binding to rat and guinea pig lung crude membranes

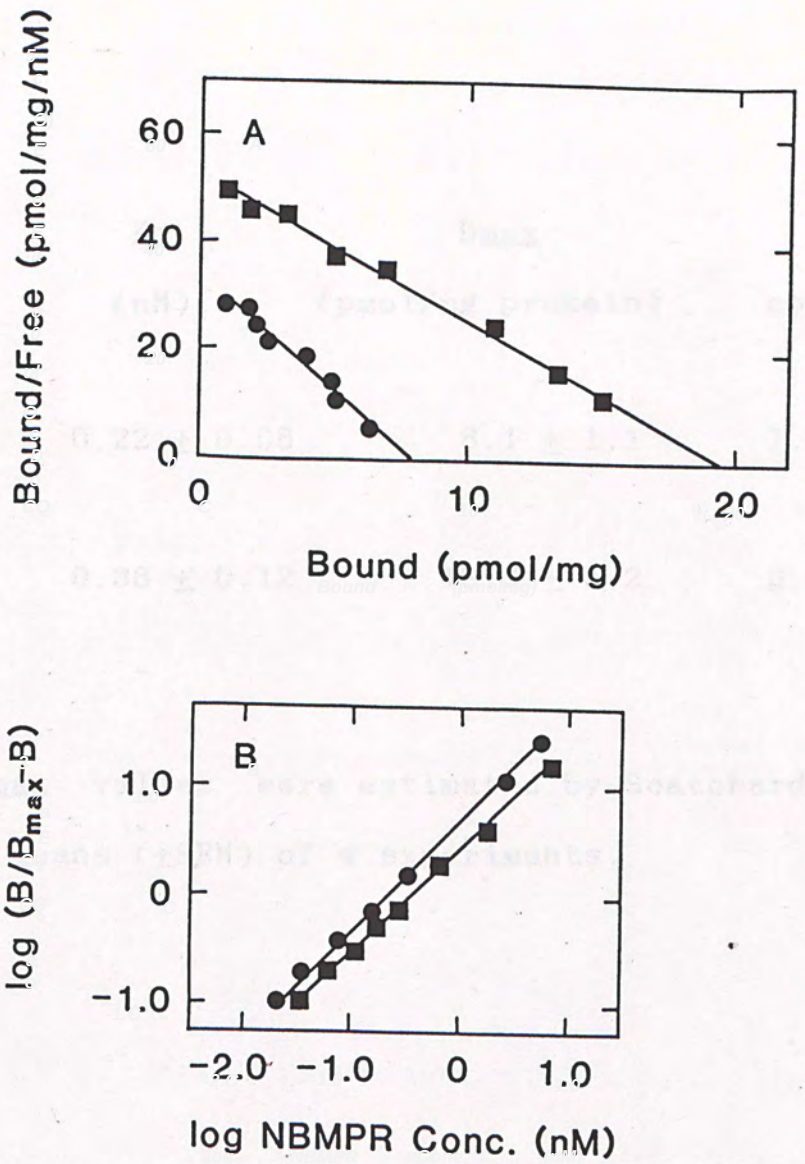

Scatchard (A) and Hill (B) plots of site specific binding of NBMPR to rat and guinea-pig lung PMF. These plots were obtained using data for guinea pig (■) and rat (●) lung crude membranes presented in Fig. 2.1.

Table 2.1 Binding parameters for NBMPR binding to lung crude membranes

	Kd (nM)	Bmax (pmol/mg protein)	Hill coefficient
Rat	0.22 ± 0.08	8.1 ± 1.1	1.03 ± 0.18
Guinea pig	0.38 ± 0.12	19.3 ± 5.2	0.98 ± 0.13

Kd and Bmax values were estimated by Scatchard analysis. Values are means (±SEM) of 4 experiments.

Figure 2.3 Dipyridamole, adenosine and uridine inhibition of NBMPR binding to rat and guinea-pig lung crude membranes

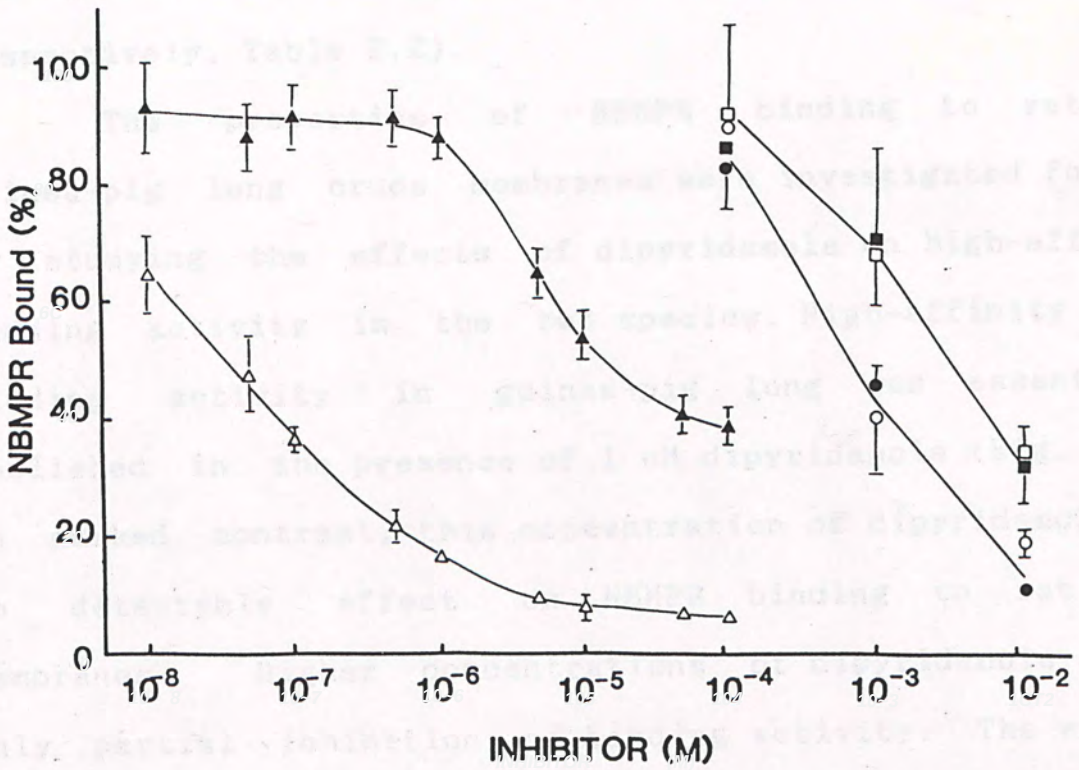

The effects of varying concentrations of dipyridamole (△ , ▲), adenosine (○ , ●) and uridine (□ , ■) on equilibrium NBTGR-sensitive [^{3}H]NBMPR binding (NBMPR concentration 0.5 nM) to rat (closed symbols) and guinea-pig (open symbols) lung membrane preparations were determined as described in the text. Data are expressed as percentages of control values and are means (±SEM) of triplicate estimates.

binding (0.5 nM) were similar in the two species: 7 mM and 0.8 mM for uridine and adenosine, respectively. High concentrations of adenosine, a more effective inhibitor of NBMPR binding than uridine, induced essentially complete inhibition of NBMPR binding activity (estimated Ki of 0.28 mM and 2 mM for adenosine and uridine in both species, respectively, Table 2.2).

The properties of NBMPR binding to rat and guinea-pig lung crude membranes were investigated further by studying the effects of dipyridamole on high-affinity binding activity in the two species. High-affinity NBMPR binding activity in guinea-pig lung was essentially abolished in the presence of 1 uM dipyridamole (Fig. 2.3). In marked contrast, this concentration of dipyridamole had no detectable effect on NBMPR binding to rat lung membranes. Higher concentrations of dipyridamole caused only partial inhibition of binding activity. The effects of other vasodilators, dilazep, lidoflazine and hexobendine, on NBMPR binding to lung crude membranes were also investigated. Table 2.3 presents the IC_{50} values of various vasodilators on equilibrium NBTGR-sensitive [^{3}H]NBMPR binding. IC_{50} values were 10-300 fold lower in guinea-pig than in rat. However, the order of potency of these compounds as inhibitors of NBMPR binding were similar in the two species (dilazep > dipyridamole, hexobendine > lidoflazine). This order of potency correlates with the relative abilities of these compounds

Table 2.2 Estimated Ki values for adenosine and uridine inhibition of NBMPR binding to rat and guinea-pig lung crude membranes

Nucleoside	Ki (mM)
Adenosine	0.28
Uridine	2.0

Ki calculated according to $Ki = IC_{50}/(1+[L]/Kd)$. IC_{50} values extracted from Fig. 2.3.

Table 2.3 IC_{50} values for various vasodilators as inhibitors of NBMPR binding to rat and guinea-pig lung crude membranes

	IC_{50} (nM)		Ratio
	Guinea-pig	Rat	(Rat/Guinea pig)
Dipyridamole	45.0±3.2	13400±1410	297
Dilazep	4.8±0.28	83±7.4	17.3
Lidoflazine	300.0±19	>10,000	>33
Hexobendine	43.0±3.9	1400±110	13.7

IC_{50} values were determined by testing eight to ten drug concentrations for inhibition of [^{3}H]NBMPR binding (0.5 nM). Each compound was tested at least three times. Values are means (±SEM). See Table 2.4 for estimated Ki values.

Table 2.4 Estimated Ki values for various vasodilators as inhibitors of NBMPR binding to guinea pig and rat lung crude membranes

	Ki (nM)	
	Guinea pig	Rat
Dipyridamole	20	5600
Dilazep	2	35
Lidoflazine	110	>4200
Hexobendine	18	590

Ki values estimated by $Ki = IC_{50}/(1+[L]/Kd)$.

IC_{50} values are from data presented in Table 2.3.

to inhibit adenosine uptake in other tissues (Kolassa et al, 1978; Mustafa, 1979).

In order to assess the nature of dipyridamole inhibiton of NBMPR binding to guinea pig and rat lung crude membranes, measurements of equilibrium NBMPR binding (0.05-5 nM [^{3}H]NBMPR) were made in both species in the presence and in the absence of graded concentrations of dipyridamole (10^{-8} - 10^{-4} M). Figs. 2.4(a) and (b) are Lineweaver-Burke plots of representative inhibition experiments in the two species. In both cases, dipyridamole functioned as a competitive inhibitor of [^{3}H]NBMPR binding. Mean apparent Ki values from several experiments were 1.8 ± 0.46 (x 10^{-8})M and 8.53 ± 2.00 (x 10^{-6})M for guinea pig and rat membranes, respectively, a difference of 470-fold.

Kinetic studies of [^{3}H]NBMPR dissociation and association were subsequently undertaken to investigate the mechanism of action of dipyridamole in the two species in more detail (see Section 2.3.2).

2.3.2 Kinetic Studies of NBMPR Binding to Lung Membranes

2.3.2a Dissociation kinetics of NBMPR binding

In initial experiments, the dissociation of bound [^{3}H]NBMPR was measured by resuspending [^{3}H]NBMPR-labelled membranes in a large volume of ligand-free 50 mM Tris-HCl buffer, pH 7.4 at 22^{o}C. When these data were

Figure 2.4 Inhibition of equilibrium NBMPR binding to rat (A) and guinea-pig lung (B) membranes by dipyridamole

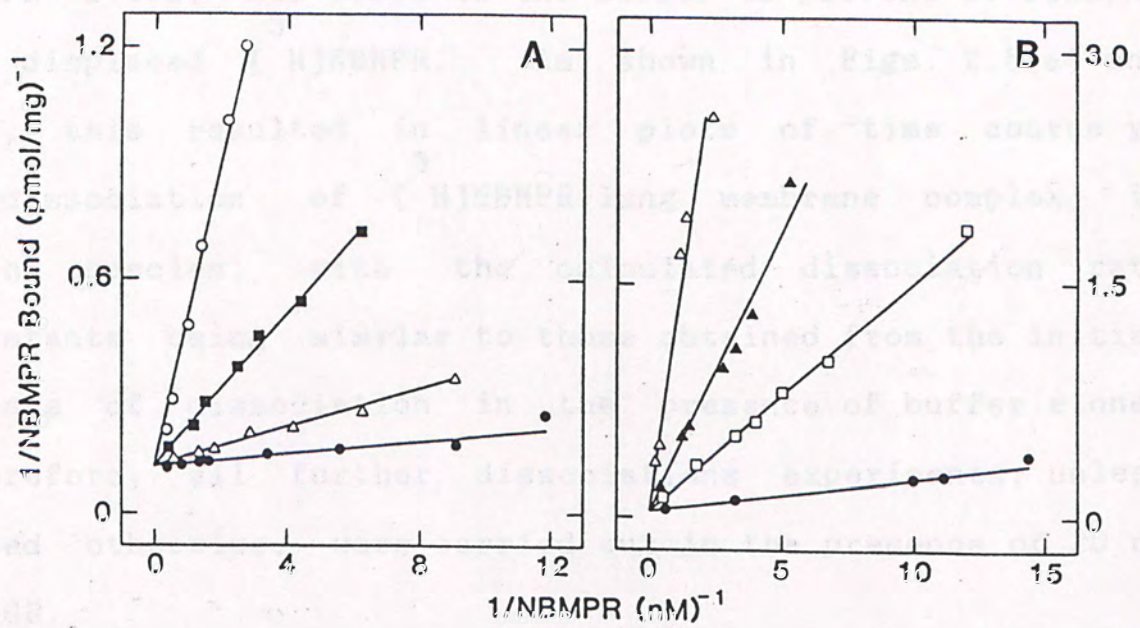

Equilibrium [^{3}H]NBMPR binding to lung membranes was determined as described in the text. Dipyridamole concentrations (rat): ● ,control; △ ,10-6M; ■ ,10-5M; ○ ,10-4 M. Dipyridamole concentrations (guinea-pig): ● ,control; □ ,10-8 M; ▲ ,10-7 M; △ ,10-6 M.

plotted in accordance with equation (1), curvilinear plots of time course *vs* ln(dissociation of [^{3}H]NBMPR-lung membrane complex) was observed (Figs. 2.5(a) and (b)), suggestive of either the presence of two or more components of dissociation or the re-binding of free [^{3}H]NBMPR. Inorder to eliminate the latter possibility, nonradioactive NBTGR (20nM), sufficient to saturate the high-affinity NBMPR sites, was added to the buffer to prevent re-binding by displaced [^{3}H]NBMPR. As shown in Figs. 2.5(a) and (b), this resulted in linear plots of time course *vs* ln(dissociation of [^{3}H]NBMPR-lung membrane complex) in both species, with the calculated dissociation rate constants being similar to those obtained from the initial phases of dissociation in the presence of buffer alone. Therefore, all further dissociations experiments, unless noted otherwise, were carried out in the presence of 20 nM NBTGR.

Representative dissociation curves for [^{3}H]NBMPR in the presence and in the absence of dipyridamole (0-50 uM) are shown in Figs. 2.6(a) and (b). For both the rat and the guinea pig, dipyridamole decreased the rate of [^{3}H]NBMPR dissociation. Figs. 2.7(a) and (b) demonstrate the concentration dependence of this effect. In contrast to the equilibrium binding experiments (Figs. 2.4(a) and (b)), dipyridamole was equally effective as inhibitor of [^{3}H]NBMPR dissociation in the two species. The apparent rates of dissociation of [^{3}H]NBMPR (app. *Koff*) in the

Figure 2.5 Time course of dissociation of NBMPR-lung membrane complex in the rat (A) and guinea-pig (B)

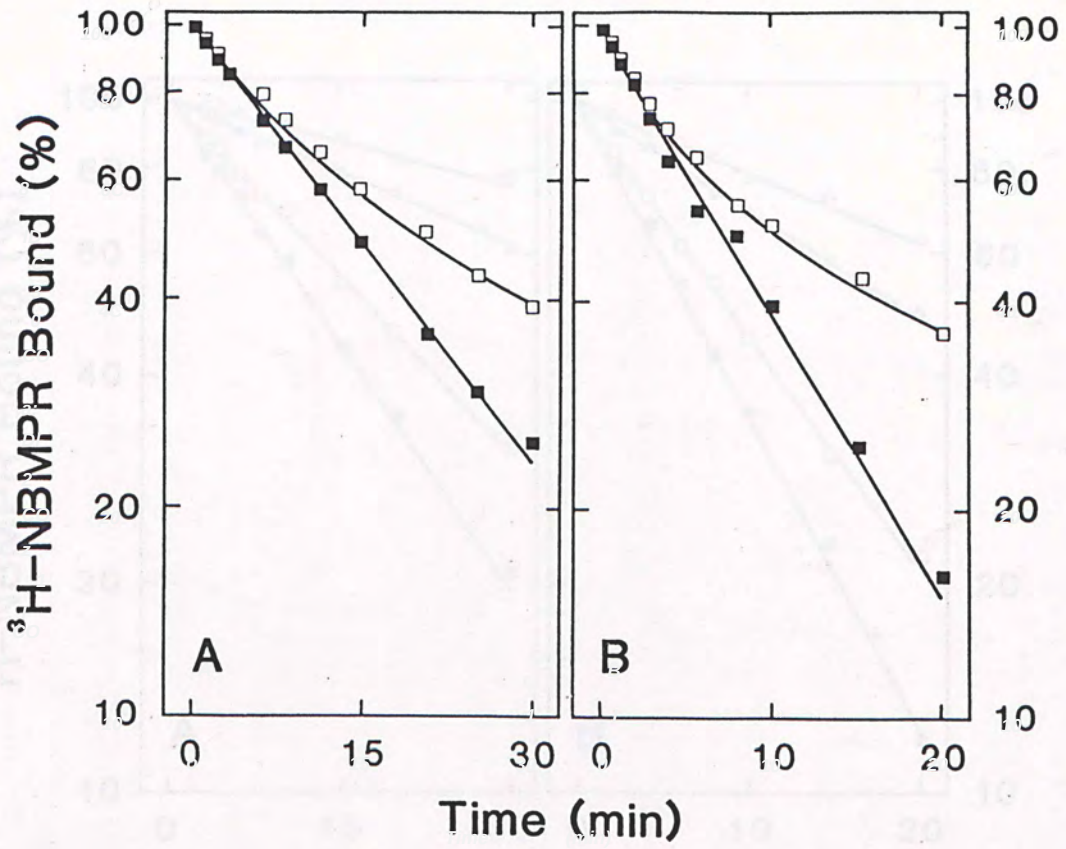

Lung crude membranes were pre-equilibrated with 2 nM [^{3}H]NBMPR at 22°C for 30 min, washed free of unbound ligand and dissociation (also at 22°C) initiated by the addition of 50 ul of labelled membranes to 60 ml of 50 mM Tris-HCl, pH 7.4, containing no addition (□) or 20 nM NBMPR (■). The percentage of the remaining specifically-bound [^{3}H]NBMPR at various times was plotted as described in the text (equation 1). At time zero there was 7.2 pmol and 17.3 pmol of [^{3}H]NBMPR bound per mg of protein for rat and guinea pig lung crude membranes, respectively.

Figure 2.6 Effect of dipyridamole on the dissociation of NBMPR-lung membrane complex in the rat (A) and guinea pig (B)

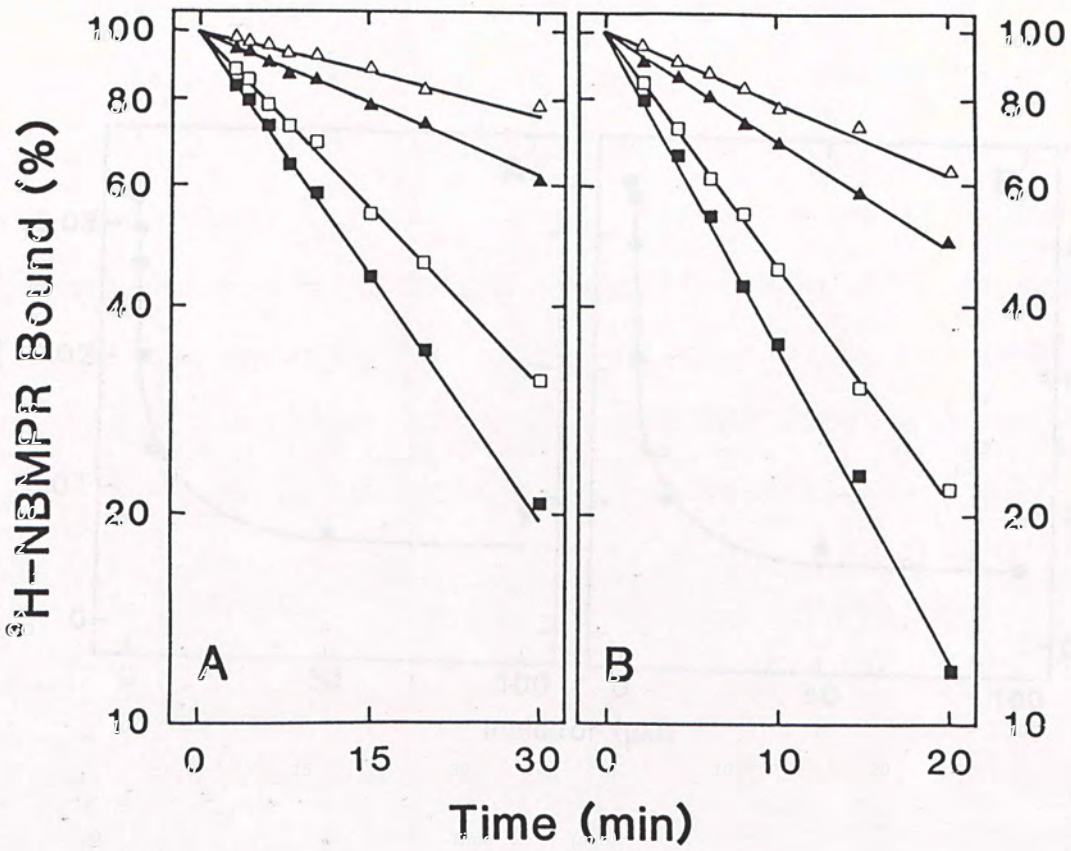

Lung crude membranes were pre-equilibrated with [^{3}H]NBMPR and washed free of excess unbound ligand as described in the legend to Fig. 2.5. Dissociation at 22°C was initiated by the addition of 50 ul of labelled membranes to 60 ml of 50 mM Tris-HCl buffer containing 20 nM NBTGR, with no addition (■), 2.5 uM-dipyridamole (□), 10 uM-dipyridamole (▲), or 50 uM-dipyridamole (△). The percentage of remaining specifically-bound [^{3}H]NBMPR at various times was plotted as described in the text (equation 1).

Figure 2.7 Dissociation of bound NBMPR from rat (A) and guinea-pig lung membranes (B) in the presence of dipyridamole

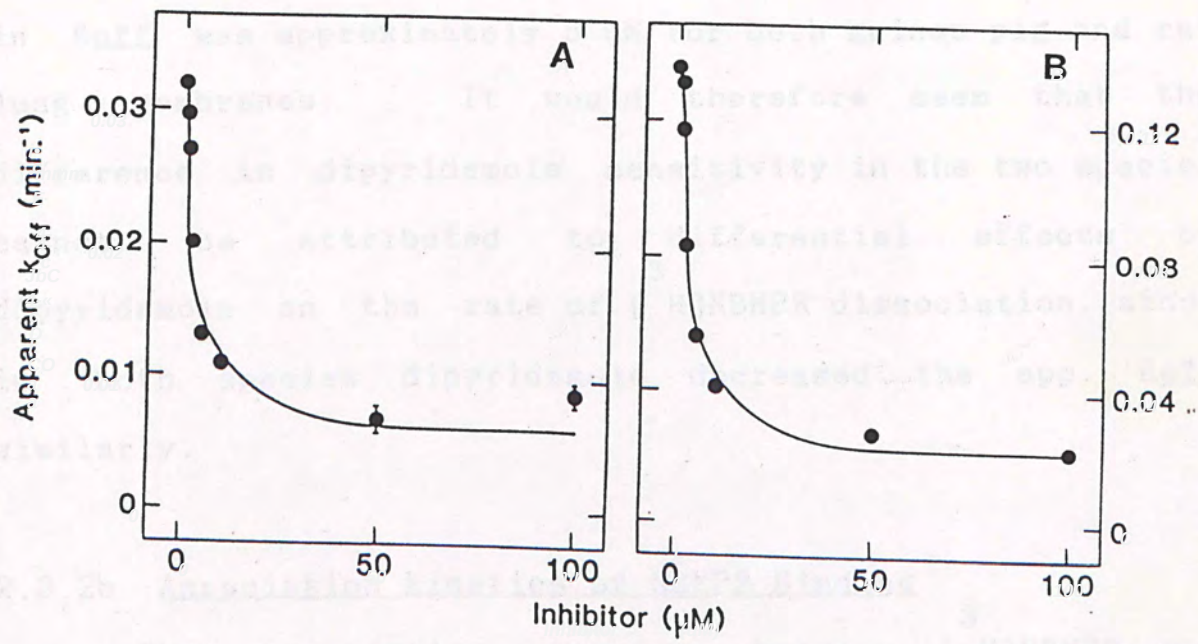

Apparent dissociation rate constants (apparent Koff) were determined from experiments similar to those presented in Fig. 2.6. and plotted as a function of dipyridamole concentration. Results are the means(±SEM) of four independent experiments. For most of the values, error bars fell within the data points.

absence of inhibitor were 0.123 ± 0.010 min^{-1} and 0.034 ± 0.006 min^{-1} for guinea pig and rat lung crude membranes, respectively. The decrease in app. Koff by dipyridamole in both species appeared to plateau off at a dipyridamole concentration of 50 uM and the concentration of dipyridamole required to induce half-maximal reduction in Koff was approximately 5 uM for both guinea pig and rat lung membranes. It would therefore seem that the difference in dipyridamole sensitivity in the two species cannot be attributed to differential effects of dipyridamole on the rate of [^{3}H]NBMPR dissociation, since in both species dipyridamole decreased the app. Koff similarly.

2.3.2b Association Kinetics of NBMPR Binding

The association reaction between [^{3}H]NBMPR and lung crude membranes was studied under pseudo-first-order conditions (see Section 2.2.3b). Association was initiated by incubating lung membrane with 0.5 nM [^{3}H]NBMPR at 22°C in the presence and in the absence of dipyridamole. The rate of complex-formation was measured as a function of time and representative plots are shown in Figs. 2.8(a) and (b). In the absence of any inhibitor, binding of [^{3}H]NBMPR to lung membranes in both species reached a steady state within 10 min after the reaction was initiated, and the time required to reach 50% saturation was approximately 1.5 min. In the presence of dipyridamole,

Figure 2.8 Time course of NBMPR binding to rat (A) and guinea-pig lung crude membranes (B) in the presence of dipyridamole

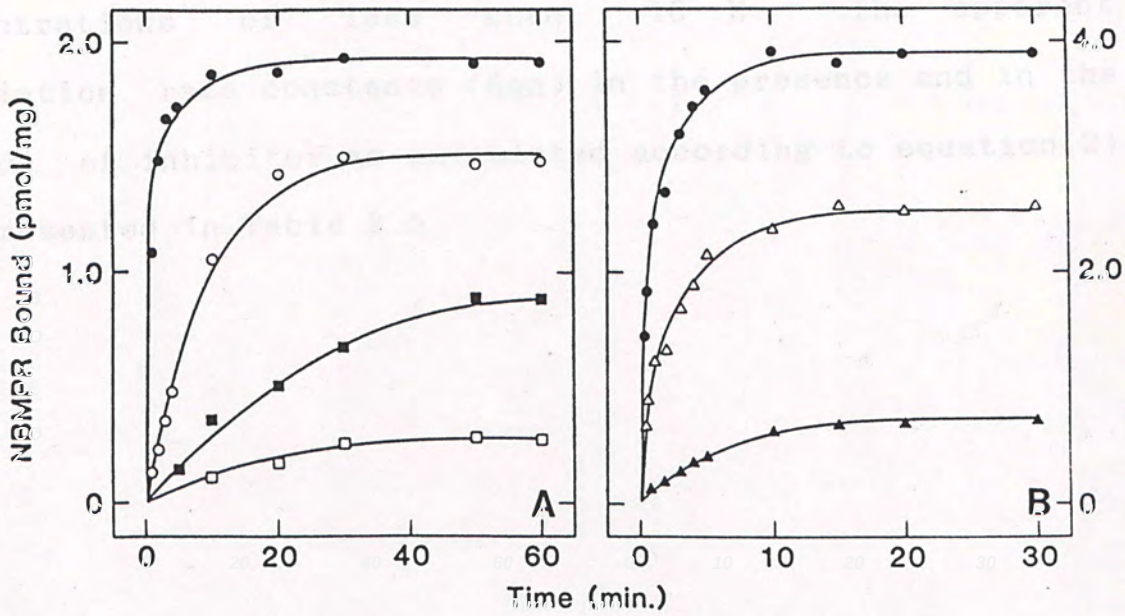

Rat and guinea pig lung membranes were incubated with 0.5 nM [^{3}H]NBMPR in the presence and in the absence of various concentrations of dipyridamole. Dipyridamole concentrations (rat): ● ,control; ○ ,10-6 M; ■ ,10-5 M; □ ,10-4 M. Dipyridamole concentrations (guinea-pig): ● ,control; △ ,10-8 M; ▲ ,10-7 M. Values are the means of duplicate estimates.

binding of [^{3}H]NBMPR to lung membranes in the two species behaved differently. Association of [^{3}H]NBMPR to guinea-pig lung membranes was slowed down even in the presence of 10^{-8} M dipyridamole, and association was totally abolished in the presence of 10^{-6} M dipyridamole. In the rat, association was not affected by dipyridamole concentrations of less than 10^{-7} M. The apparent association rate constants (Kon) in the presence and in the absence of inhibitor as calculated according to equation(2) are presented in Table 2.5.

Table 2.5 Apparent association rate constants for NBMPR binding to lung crude membranes

Dipyridamole Concentration (M)	Kon ($\times 10^{9}$ M^{-1} min^{-1})	
	Guinea pig	Rat
0	0.68±0.15	0.53±0.068
10^{-8}	0.18±0.02	0.52±0.062
10^{-7}	0.085±0.013	0.50±0.073
10^{-6}	---	0.30±0.041
10^{-5}	---	0.04±0.006
10^{-4}	---	0.01±0.002

Apparent association rate constants (Kon) were determined as described in text. Values are means (±SEM) of 3 experiments.

2.4 DISCUSSION

Kinetic studies of nucleoside transport in a variety of cell types have established that physiological and cytotoxic nucleoside molecules cross the plasma membrane of animal cells mainly by an NBMPR-sensitive nucleoside-specific facilitated diffusion process which is independent of subsequent intracellular nucleoside metabolism (Plagemann and Wohlheuter, 1980; Paterson *et al*, 1981; Young and Jarvis, 1983). In this Chapter, I have been able to demonstrate the presence of saturable, high-affinity binding sites for NBMPR in crude membrane preparations from both rat and guinea-pig lung. Kd values for NBMPR binding to these sites were very similar in the two species (0.22 and 0.38 nM in rat and guinea pig, respectively). However, Bmax values for high-affinity NBMPR binding to rat and guinea-pig lung crude membranes differed significantly, guinea pig membranes having the higher density of NBMPR binding sites (approximately 19 pmol/mg protein compared with 8 pmol/mg protein for rat lung membranes).

As predicted from studies of nucleoside transporters in other cell types, high-affinity NBMPR binding to lung plasma membranes was inhibited by adenosine, uridine, dipyridamole, dilazep and other vasodilators. Adenosine was a more effective inhibitor of NBMPR binding than uridine, a result consistent with the known relative affinities of these two nucleosides for the transporter in other systems, adenosine usually having the lower apparent

Km. For example, human erythrocytes exhibit apparent Km values of 61 uM and 0.8 mM for adenosine and uridine equilibrium exchange influx at 25°C, respectively (Jarvis et al, 1983; Plagemann et al, 1985).

As shown in Fig. 2.2, NBMPR binding to rat and guinea pig lung crude membranes were equally susceptible to nucleoside inhibition. In contrast, there was a large species difference in dipyridamole sensitivity, Ki values in the two preparations differed by more than two orders of magnitude (20 nM and 5.6 uM for guinea pig and rat lung membranes, respectively, Table 2.4). It has previously been shown that adenosine uptake by intact rat lung is approximatedly 100 times less sensitive to dipyridamole than guinea pig lung (Kolassa et al, 1971). Lung NBMPR binding sites in the two species therefore have the properties expected of nucleoside transport proteins in this tissue.

Like dipyridamole, dilazep, another vasodilator, was also found to be a less potent inhibitor of equilibrium [^{3}H]NBMPR binding to rat lung membranes (Ki values of 2 and 35 nM for guinea pig and rat membranes, respectively. See Table 2.4). Lidoflazine and hexobendine were also less effective in rat lung membranes (Ki values of 110 and 18 nM, >4.2 uM and 0.59 uM for lidoflazine and hexobendine in guinea pig and rat lung membranes, respectively, see Table 2.4).

The mechanism by which dipyridamole (and other

vasodilators) inhibits nucleoside transport has been a matter of dispute. Competitive (Lips et al, 1980; Jarvis et al, 1982), mixed (Turnheim et al, 1978) and non-competitive (Meunier and Morel, 1978; Rogler-Brown and Parks, 1980) inhibition kinetics have been reported in different systems. A more recent study, published after the experiments reported in this Chapter were completed, has shown that dipyridamole being a competitive inhibitor of uridine equilibrium exchange influx into guinea pig erythrocytes (apparent Ki 1 nM) (Jarvis, 1986). In the present series of experiments, dipyridamole was found to be a competitive inhibitor of equilibrium [^{3}H]NBMPR binding to guinea-pig lung membranes with an apparent Ki value of 1.8×10^{-8} M. Dipyridamole was considerably less effective at inhibiting [^{3}H]NBMPR binding to rat lung membranes, but again, inhibition of equilibrium [^{3}H]NBMPR binding was competitive, with an apparent Ki value of 8.5×10^{-6} M.

As shown in Fig. 2.8, low concentrations of dipyridamole (10^{-8} - 10^{-7} M) had a marked effect on the association of [^{3}H]NBMPR with its binding site on guinea-pig lung membranes. In contrast, much higher concentrations (10^{-6} - 10^{-4} M) were required to produce comparable effects in rat lung membranes. The effects of various concentrations of dipyridamole on NBMPR dissociation from rat and guinea-pig lung membranes was also compared. As presented in Fig. 2.7, concentrations of dipyridamole < 1 uM had no significant effect on NBMPR

dissociation in either species, while higher concentrations of vasodilator were equally effective at slowing down the rate of NBMPR dissociation in the two species (half-maximal inhibition of dissociation at 5 uM dipyridamole). In the guinea pig, dipyridamole concentrations of 10^{-8} -10^{-7} M exert their effects on NBMPR binding affinity (Kd) by only decreasing Kon (Table 2.6). In the rat, dipyridamole concentrations of 10^{-6} -10^{-4} M decreased both Koff and Kon, but decreasing Kon to a larger extent and therefore producing an increase in Kd for NBMPR binding with increasing concentrations of dipyridamole (Table 2.7). The determined kinetic constants for NBMPR association and dissociation (Section 2.3.2) are in close agreement with the equilibrium binding measurements in Section 2.3.1, that is, Koff / Kon = Kd., as summarized in Tables 2.6 and 2.7. In human erythrocytes, dipyridamole (>200 nM) has also been shown to decrease the rate of dissociation of [^{3}H]NBMPR from its binding sites (Jarvis et al, 1983). Similarly, dilazep has also been reported to decrease the rate of dissociation of NBMPR from the binding-site complex of cultured hamster cell (Nil SV) membrane preparations (Koren et al, 1983).

In conclusion, I have demonstrated the presence of high-affinity NBMPR sites in guinea pig and rat lung crude membranes which display similar characteristics to those found in erythrocyte membranes. As expected from previous studies, there was a marked species difference in the

ability of dipyridamole to inhibit NBMPR binding, the guinea pig association rate constant being considerably more sensitive to dipyridamole inhibition than the corresponding rate constant for the association of NBMPR with rat lung membranes. Possible mechanisms by which dipyridamole interacts with NBMPR-sensitive nucleoside transporters in these two species are discussed in detail in the General Discussion.

Table 2.6 Summary of kinetics parameters of NBMPR binding to guinea pig lung crude membranes

Dipyridamole Concentration (M)	Koff (min^{-1})	Kon ($x10^{9} M^{-1} min^{-1}$)	Koff/Kon (nM)
0	0.123	0.68	0.18
10^{-8}	0.121	0.18	0.67
10^{-7}	0.118	0.085	1.39

Values of Koff and Kon are taken from Section 2.3.2a and Table 2.5, respectively.

Table 2.7 Summary of kinetics parameters of NBMPR binding to rat lung crude membranes

Dipyridamole Concentration (M)	Koff (min^{-1})	Kon ($x10^{9} M^{-1} min^{-1}$)	Koff/Kon (nM)
0	0.034	0.53	0.06
10^{-6}	0.028	0.30	0.09
10^{-5}	0.010	0.04	0.25
10^{-4}	0.009	0.01	0.9

Values of Koff and Kon are taken from Section 2.3.2a and Table 2.5, respectively.

CHAPTER 3

DIPYRIDAMOLE BINDING TO RAT AND GUINEA PIG LUNG CRUDE PLASMA MEMBRANES

3.1 INTRODUCTION

The results presented in Chapter 2, established that guinea-pig and rat lung membranes possess a high density of nucleoside transporters, as judged by assays of high-affinity [^{3}H]NBMPR binding activity. Species differences in inhibition of NBMPR binding by dipyridamole and various other vasodilators were observed. Other investigators have also reported significant species variation in the potency of dipyridamole as an inhibitor of nucleoside transport, with rat tissues exhibiting a low sensitivity to this vasodilator (Hopkins and Goldie, 1971; Kolassa and Pfleger, 1975; Wu and Young, 1984; Williams et al, 1984; Jarvis and Young, 1986). In the rat, the uptake of adenosine into intact perfused lung is about 100 times less sensitive to dipyridamole inhibition than in guinea pig (Kolassa et al, 1971; Kolassa and Pfleger, 1974; Bakhle and Chelliah, 1983).

During the course of the present project, high-specific activity [^{3}H]dipyridamole became commercially available. In the present Chapter, the characteristics of equilibrium [^{3}H]dipyridamole binding to guinea-pig and rat lung crude membranes are described and results compared with the NBMPR-binding experiments presented in Chapter 2. Dipyridamole dissociation experiments using guinea pig lung membranes were also performed in an attempt to explore the topographical relationship between NBMPR and dipyridamole nucleoside

transporter binding sites. Results from these experiments suggest that NBMPR and dipyridamole bind to the NBMPR-sensitive nucleoside transporter with the same stoichiometry, but at separate sites.

3.2 METHODS

3.2.1 Tissue and Membrane Preparation

Rat and guinea pig lung crude membranes were prepared as described in Chapter 2 (Section 2.2.1).

3.2.2 Dipyridamole and NBMPR Binding

Rat and guinea-pig lung crude membranes in 50 mM-Tris/HCl (0.05-0.08 mg of protein) were incubated with [^{3}H]dipyridamole (final equilibrium concentrations 0.05-30 nM) in a total volume of 1 ml at 22^{o}C in the absence and in the presence of 20 uM NBMPR or 50 uM-dipyridamole as competing non-radioactive ligands. Incubations (typically 30 min) were terminated on glass-fibre filters (Whatman GF/B, which were washed with ice-cold buffer before sample filtration). The filters were processed and radioactivity counted as described previously for equilibrium NBMPR binding (Chapter 2, Section 2.2.2). [^{3}H]Dipyridamole binding to membranes was expressed per mg of protein. Equilibrium concentrations of unbound [^{3}H]ligand were estimated from the differences between total [^{3}H]dipyridamole concentrations and the amounts of ligand bound to membranes and filters. Control time-course experiments confirmed that equilibrium was reached for all radioligand concentrations during the 30 min incubation period. Bmax values for [^{3}H]NBMPR binding were determined at 5 nM-radioactive ligand (±20 uM non-radioactive NBMPR) as

described previously (Chapter 2, section 2.2).

It was noticed in the course of this series of experiments that [^{3}H]dipyridamole, in contrast with NBMPR, had a tendency to stick to the disposable polypropylene tubes and pipette tips used in the binding experiments. For this reason, [^{3}H]dipyridamole concentrations in the concentration-dependence experiments were determined directly by counting for radioactivity aliquots (0.1 ml) from each incubation immediately before filtration. ^{3}H radioactivity present in these aliquots (including that adsorbed by the pipette tips used in the transfer) was converted first to d.p.m. by using n-[^{3}H]hexadecane as internal standard and then to ligand concentration (nM) by using the [^{3}H]dipyridamole specific radioactivity value supplied by the manufacturer (see Appendix). A similar procedure was used to convert membrane-bound c.p.m. into pmol. For the sake of consistency, values for membrane-bound [^{3}H]NBMPR quoted in the present Chapter were determined in the same way.

3.2.3 Dissociation Kinetics of Dipyridamole Binding

Guinea-pig lung crude membranes were incubated with [^{3}H]dipyridamole (20 nM) for 30 min at 22^{o}C. Incubations were terminated by centrifugation at 40,000g for 15 min. The membrane pellets were washed once with 10 ml of ice-cold 50 mM Tris-HCl buffer, pH 7.4 at 22^{o}C and resuspended at a protein concentration of 2 mg/ml. The

[^{3}H]dipyridamole-labelled membranes were kept on ice for up to 2 h. Control experiments demonstrated that the amount of [^{3}H]dipyridamole bound to the lung crude membranes remained constant during this period. Dissociation (22^{o}C) was initiated by adding 250 ul of ice-cold [^{3}H]dipyridamole-labelled membrane to 60 ml of 50 mM Tris buffer, containing no addition, graded concentrations of NBMPR in the presence of dipyridamole (20 nM or 20 uM) or dipyridamole alone (20nM or 20 uM). The medium was continuously stirred and at various time intervals (0.5-2.5 min) after the addition of membrane, 5 ml portions were removed and filtered through glass-fibre filters under suction. The filters were washed four times with 3 ml aliquots of ice-cold buffer, the entire procedure being completed within 15 s. The filters were dried and added to 10 ml of scintillation fluid and counted for radioactivity. Dissociation of radioligand from non-specific binding sites was determined by labelling the membranes with [^{3}H]dipyridamole in the presence of 20 uM NBMPR and then measuring the rate of dissociation by the above procedures. Non-specific binding was typically less than 10% of the total binding. Specific binding was calculated as the difference between total binding and non-specific binding. Results obtained were evaluated according to equation (1) as described in Chapter 2 (Section 2.2.3a).

3.3 RESULTS

3.3.1 Time-course of Dipyridamole Binding to Rat and Guinea-pig Lung Crude Membranes

A representative time course for [^{3}H]dipyridamole binding (initial concentration 5 nM) to guinea-pig lung membranes, measured both in the absence and in the presence of 20 uM-NBMPR as competing non-radioactive ligand is shown in Fig. 3.1 (a). The results demonstrate the presence of a large component of NBMPR-sensitive binding (12.8 pmol/mg of protein). The half-time for [^{3}H]dipyridamole binding to these sites at 22^{0}C was approximately 2 min, full equilibration occuring within 15 min. [^{3}H]dipyridamole binding in the presence of NBMPR, which includes adsorption of radioactive ligand by the filters as well as non-specific (NBMPR-insensitive) binding to membranes, was not time-dependent and accounted for 19.8% of the total binding at equilibrium. In control experiments, [^{3}H]ligand binding to glass-fibre filters was unaffected by NBMPR.

In marked contrast with guinea-pig membranes, there was no detectable NBMPR-sensitive binding of [^{3}H]-dipyridamole to membranes from rat lung (Fig. 3.1 (b)). This result is in accord with the species difference in dipyridamole inhibition of NBMPR binding in lung crude membranes described in Chapter 2 (Ki 5.6 uM and 20 nM in rat and guinea pig lung crude membranes, respectively).

Figure 3.1 Time-course of dipyridamole binding to guinea-pig (A) and rat lung membranes (B)

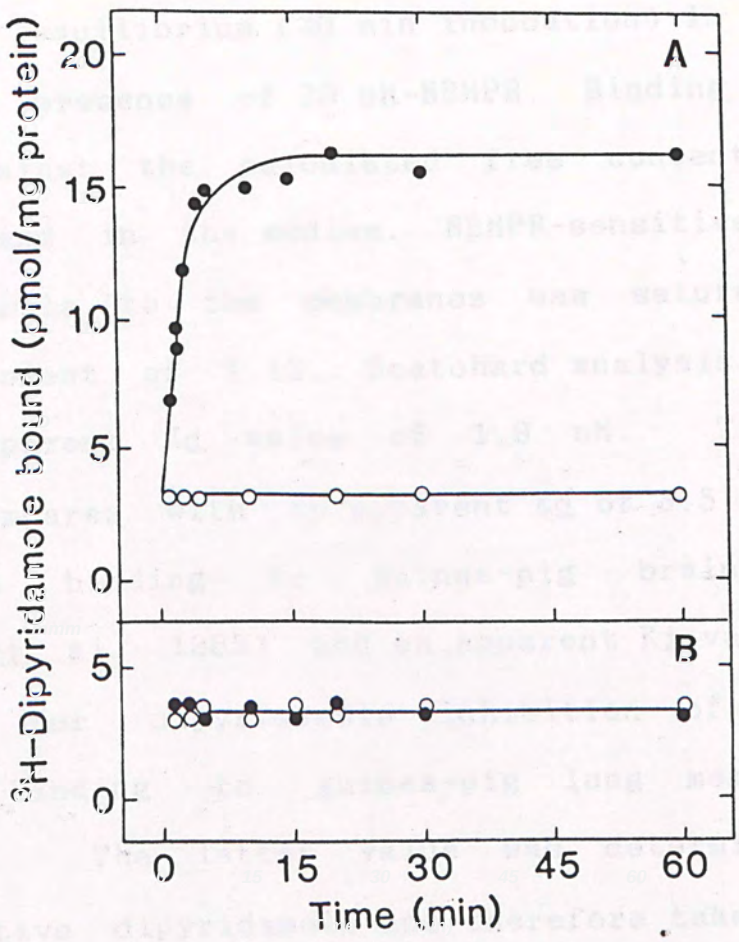

Binding of 5 nM-[^{3}H]dipyridamole was measured at 22°C in the absence (●) and in the presence (○) of 20 uM-NBMPR as competing non-radioactive ligand. Values are means of duplicate determinations.

3.3.2 Concentration-dependence of Dipyridamole Binding to Lung Membranes

Fig. 3.2(a) presents the concentration-dependence of [^{3}H]dipyridamole binding to guinea-pig lung membranes, measured at equilibrium (30 min incubation) in the absence and in the presence of 20 uM-NBMPR. Binding activity is plotted against the calculated free concentrations of unbound ligand in the medium. NBMPR-sensitive binding of [^{3}H]dipyridamole to the membranes was saturable, with a Hill coefficient of 1.12. Scatchard analysis of the data gave an apparent Kd value of 1.9 nM. This affinity constant compares with an apparent Kd of 3.5 nM for [^{3}H]-dipyridamole binding to guinea-pig brain membranes (Marangos *et al*, 1985) and an apparent Ki value of 18 nM determined for dipyridamole inhibition of equilibrium [^{3}H]NBMPR binding to guinea-pig lung membranes (see Chapter 2). The latter value was determined by using non-radioactive dipyridamole and therefore takes no account of ligand depletion by membranes or adsorption of ligand by incubation tubes *etc*. The Bmax value for NBMPR-sensitive [^{3}H]dipyridamole binding in the experiment shown in Fig. 3.2(a) was 25.5 pmol/mg of protein, compared with a Bmax of 17.1 pmol/mg of protein for [^{3}H]NBMPR binding to the same membrane preparation. Mean Bmax values for four different guinea pig lung membrane preparations were 24.8 and 19.9 pmol/mg of protein for [^{3}H]dipyridamole and [^{3}H]NBMPR respectively (Table 3.1). As also shown in

Figure 3.2 Concentration-dependence of dipyridamole binding to guinea-pig (A) and rat lung membranes (B)

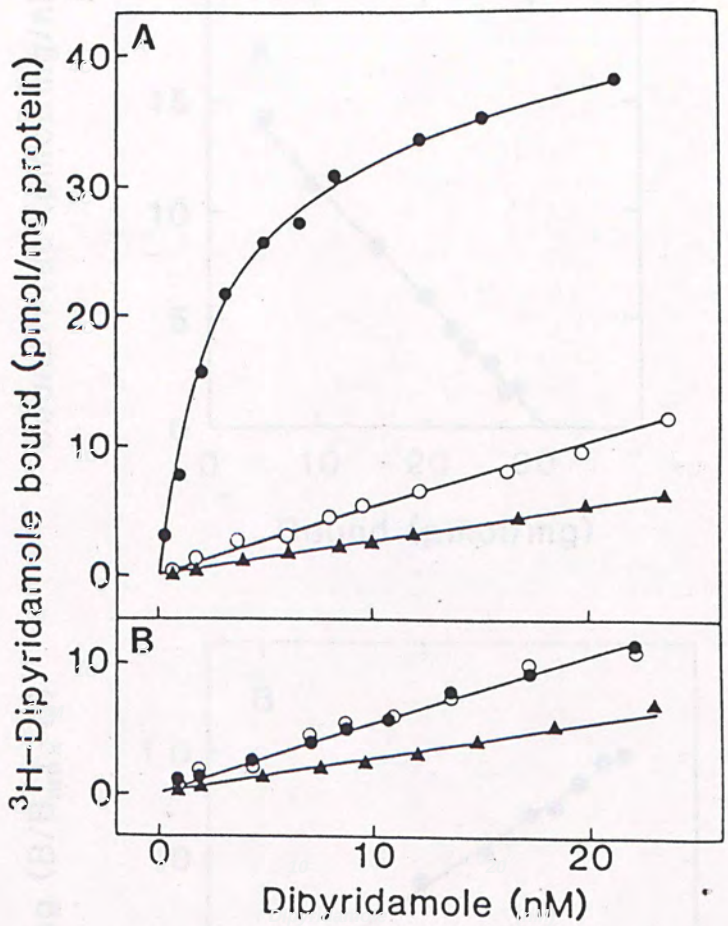

Binding of [^{3}H]dipyridamole was measured at 22°C (30 min incubation) in the absence (●) and in the presence of 20 uM-NBMPR (○) or 50 uM-nonradioactive dipyridamole (▲). Values are means of triplicate determinations. Standard errors (not shown) were typically less than 10% of mean values.

Figure 3.3 Scatchard and Hill plots of site-specific dipyridamole binding to guinea pig lung crude membranes

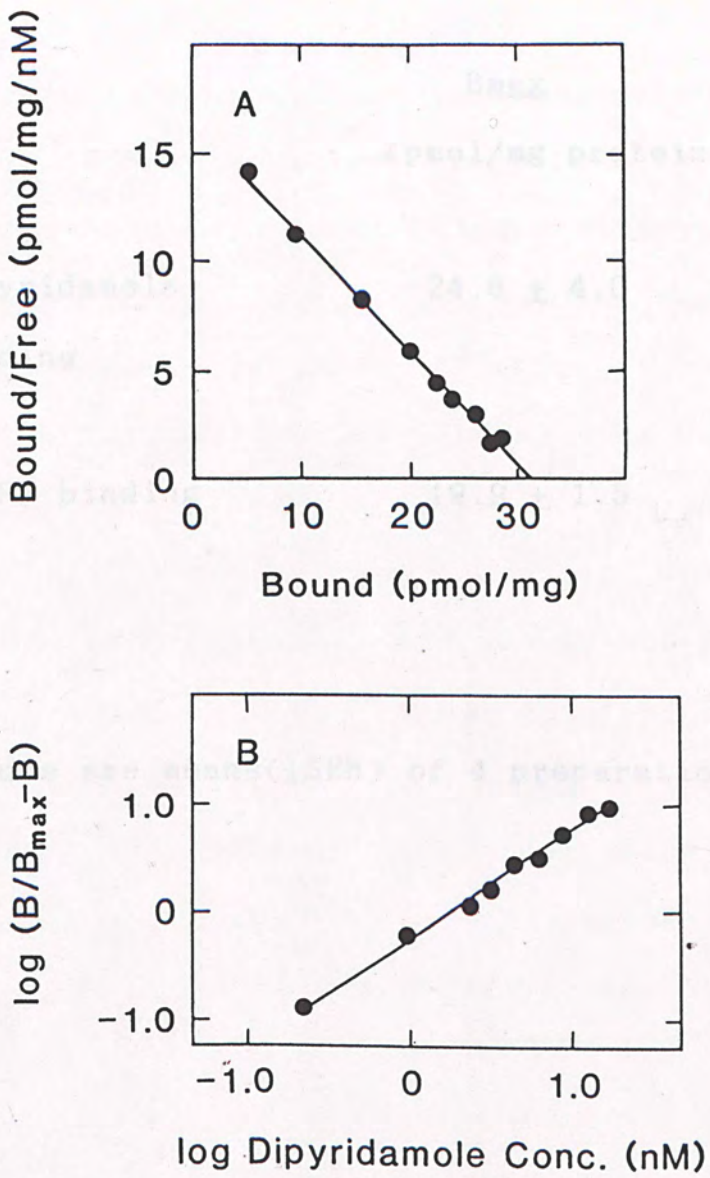

Scatchard (A) and Hill (B) plots of site specific binding of dipyridamole to guinea pig lung crude membranes. These plots were obtained using data from Fig. 3.2.

Table 3.1 Bmax for dipyridamole and NBMPR binding to guinea pig lung crude membranes

	Bmax (pmol/mg protein)
Dipyridamole binding	24.8 ± 4.0
NBMPR binding	19.9 ± 1.5

Values are means(±SEM) of 4 preparations.

Fig. 3.2(a), high-affinity binding of [^{3}H]dipyridamole to guinea-pig lung membranes was abolished in the presence of excess non-radioactive dipyridamole (50 uM). Non-saturable [^{3}H]ligand binding in the presence of dipyridamole was less than with NBMPR, indicating the occurrence of low affinity radioligand binding (to membranes or filters) unrelated to NBMPR-sensitive nucleoside transport. Data from a comparable experiment using membranes prepared from rat lung are shown in Fig. 3.2(b). As expected from the results presented in Fig. 3.1(b), no NBMPR-sensitive binding of [^{3}H]dipyridamole binding was detected. Thus, [^{3}H]-dipyridamole binding was non-saturable and co-plotted with radioligand binding measured in the presence of 20uM-NBMPR. As in guinea-pig membranes, [^{3}H]ligand binding in the presence of 50 uM-dipyridamole was lower, the difference amounting to the equivalent of 2.5 pmol/mg of protein (10 nM-[^{3}H]ligand) in both species. The [^{3}H]NBMPR binding capacity of the rat membranes used in this experiment was 8.2 pmol/mg of protein.

3.3.3 Inhibitor Studies

The transported nucleosides adenosine and uridine and the vasodilators dilazep and lidoflazine were tested for their ability to inhibit high-affinity (NBMPR-sensitive) binding of [^{3}H]-dipyridamole to guinea-pig lung membranes. As shown in Table 3.2, both nucleosides

Table 3.2 Effects of nucleosides on high-affinity binding of dipyridamole to guinea-pig lung membranes

Nucleoside	Concentration (mM)	Binding (% of control)
Adenosine	0.1	73.5±5.2
	1.0	53.0±5.6
	10.0	24.7±1.4
Uridine	0.1	83.7±4.4
	1.0	65.8±6.3
	10.0	48.6±4.5

Binding of [^{3}H]dipyridamole (5 nM) was measured at 22°C (30 min incubation) in the absence and in the presence of various concentrations of competing nucleoside and corrected for non-specific radioligand binding measured in the presence of 20 uM-NBMPR (see Fig. 3.2). Values are means(±SEM) of triplicate determinations.

competed with the [^{3}H]ligand for binding to the high-affinity sites. Adenosine was more effective than uridine (IC_{50} 0.95 and 7.2 mM respectively at 5 nM-[^{3}H]dipyridamole), in agreement with their relative potency as inhibitors of NBMPR binding to guinea pig lung crude membranes (IC_{50} 0.8 mM and 7 mM for adenosine and uridine, respectively, at 0.5 nM NBMPR). Similarly, dilazep and lidoflazine inhibited high-affinity (NBMPR-sensitive) binding of [^{3}H]dipyridamole to guinea-pig membranes (Fig. 3.4). IC_{50} values for this inhibition were 16 and 140 nM respectively (5 nM-[^{3}H]dipyridamole). These results again correlate well with IC_{50} values for these drugs as inhibitors of NBMPR binding to guinea pig lung crude membranes (IC_{50} 4 and 300 nM for dilazep and lidoflazine, respectively, 0.5 nM [^{3}H]NBMPR). For comparison, the estimated IC_{50} value for NBMPR inhibition of [^{3}H]dipyridamole binding was 3.2 nM (see also Fig. 3.4). Within experimental error, dilazep, lidoflazine and NBMPR displaced maximally the same amount of radioligand. Pseudo-Hill coefficients for this inhibition were 0.82, 0.86 and 0.88 respectively. None of these compounds had significant effects on NBMPR-insensitive [^{3}H]dipyridamole binding (Table 3.3.), additional evidence that this component of radioligand binding is not related to nucleoside transport.

Figure 3.4 Effects of dilazep, lidoflazine and NBMPR on high-affinity binding of dipyridamole to guinea-pig lung membranes

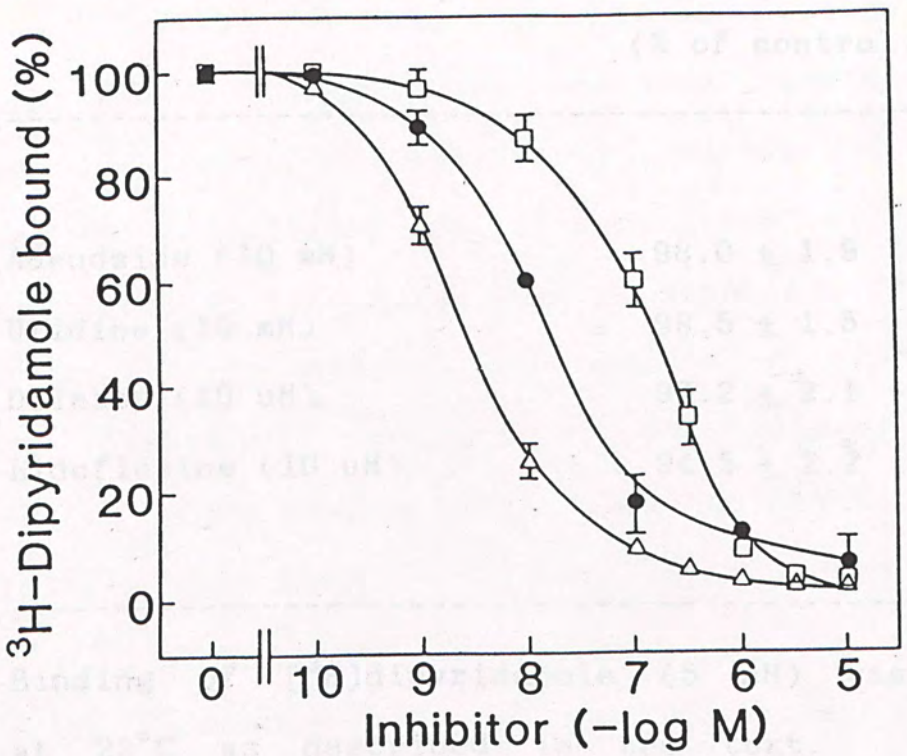

Binding of [^{3}H]dipyridamole (5 nM) was measured at 22°C (30 min incubation) in the absence and in the presence of various concentrations of dilazep (●), lidoflazine (□) and NBMPR (△) and corrected for non-specific radioligand binding measured in the presence of 20 uM NBMPR. Values are means(±SEM) of triplicate determinations.

Table 3.3 Effects of nucleosides and vasodilators on NBMPR-insensitive dipyridamole binding to guinea pig lung membranes

Inhibitor	NBMPR-insensitive binding (% of control)
Adenosine (10 mM)	98.0 ± 1.9
Uridine (10 mM)	99.5 ± 1.5
Dilazep (10 uM)	97.2 ± 2.1
Lidoflazine (10 uM)	94.5 ± 2.2

Binding of [^{3}H]dipyridamole (5 nM) was measured at 22°C as described in the text. Values are means(±SEM) of triplicate determinations.

3.3.4 Dissociation Kinetics of Dipyridamole Binding

In the representative dissociation experiments shown in Fig. 3.5, dissociation of bound [^{3}H]dipyridamole (0-20 min) was first measured by resuspending [^{3}H]dipyridamole-labelled membranes in a large volume of ligand-free 50 mM Tris-HCl buffer, pH 7.4 at 22°C. When these data were plotted in accordance with equation (1) (Chapter 2, Section 2.2.3a), a curvilinear plot of time *vs* ln([^{3}H]dipyridamole bound) was observed, suggestive of re-binding of free [^{3}H]dipyridamole and also nonspecific absorption of radioligand by filters (see also Section 3.2.2 for problems associated with non-specific binding of [^{3}H]dipyridamole to glass and plastic). Inorder to eliminate membrane rebinding of [^{3}H]dipyridamole, nonradioactive dipyridamole (20 nM), sufficient to saturate high-affinity dipyridamole sites, was added to the dissociation buffer. As also shown in Fig. 3.5, this substantially extended the linear phase of [^{3}H]dipyridamole dissociation, with the dissociation rate being similar to that observed for the initial phase of dissociation in the presence of buffer alone (see also Fig. 3.6 and Table 3.6). Under this experimental condition (*i.e.* in the presence of 20 nM dipyridamole), it was found that NBMPR at a concentration of 20 nM had no significant effect on [^{3}H]dipyridamole dissociation. However, at the higher concentration of 20 uM, NBMPR substantially increased the rate of dissociation of dipyridamole from the

guinea pig lung crude membranes (Fig. 3.5). In the same experiment, it was also observed that inclusion of 20 uM nonradioactive dipyridamole in the dissociation buffer also induced an apparent increase in the rate of [^{3}H]dipyridamole dissociation, but this was attributed to competition between cold dipyridamole and the [^{3}H]ligand for low-affinity binding sites on the glass-fibre filters. As detailed previously (Section 3.3.1), NBMPR had no significant effect on retention of [^{3}H]dipyridamole by filters.

A representative dissociation experiment for a shorter period of time (up to 2 min) is presented in Fig. 3.6. The dissociation of [^{3}H]dipyridamole from its binding sites in guinea-pig lung membranes was much faster than the corresponding dissociation rate for [^{3}H]NBMPR. Dissociation of [^{3}H]dipyridamole from its binding sites into buffer alone plotted according to equation (1) was again curvilinear, the app. Koff for the initial phase of dissociation being 0.528 min^{-1}. Dissociation of [^{3}H]dipyridamole in the presence of 20 nM non-radioactive dipyridamole was linear for the 2 min incubation period with an apparent Koff of 0.60 min^{-1}, a value very similar to that obtained for the initial phase of [^{3}H]dipyridamole dissociation into buffer alone. In contrast, the inclusion of 20 uM non-radioactive dipyridamole in the dissociation buffer again induced a substantial increase in the apparent rate of [^{3}H]dipyridamole dissociation (see

Figure 3.5 Time-course (20 min) of dissociation of dipyridamole from guinea pig lung membranes

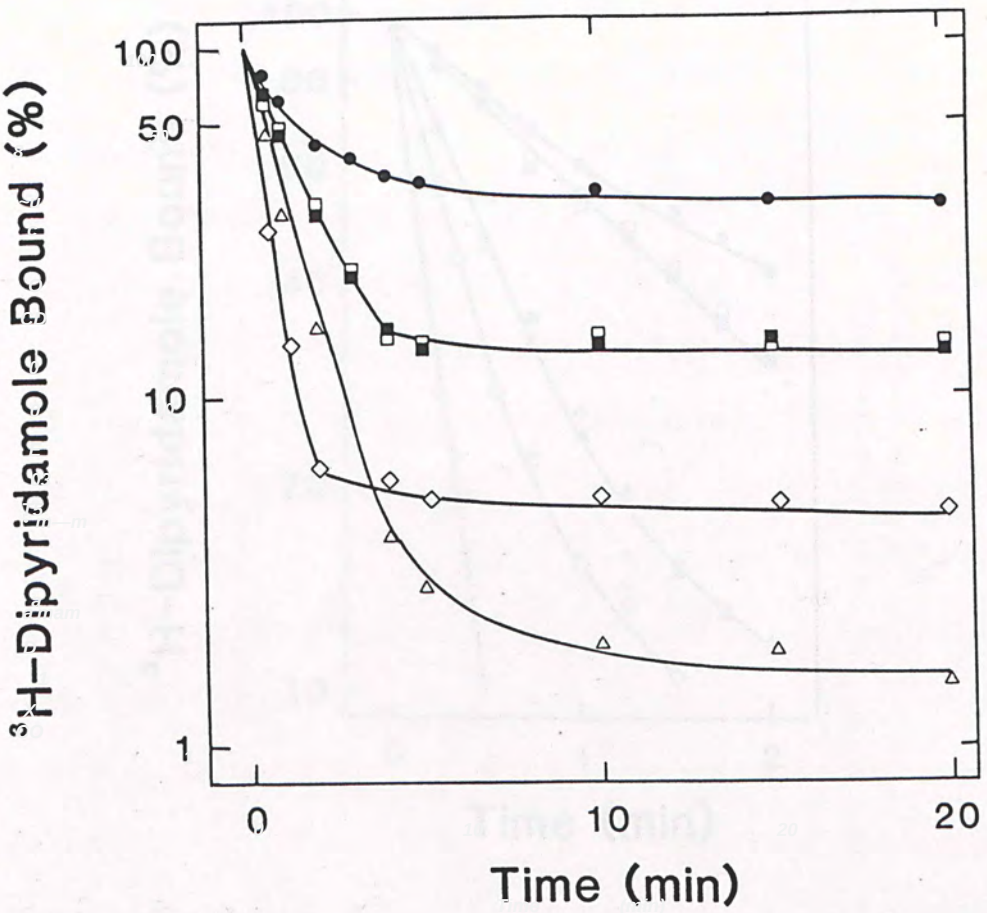

Guinea pig lung crude membranes were incubated with [^{3}H]dipyridamole (20 nM) at 22 °C for 30 min. [^{3}H]dipyridamole-labelled membranes were washed free of excess ^{3}H-ligand and dissociation (22 °C) was initiated by the addition of 50 ul of labelled membranes to 60 ml of pre-warmed 50 mM Tris-HCl buffer containing no addition (●), 20nM-dipyridamole (□), 20nM-dipyridamole+20nM-NBMPR (■), 20nM-dipyridamole+20uM-NBMPR (◇) or 20uM-dipyridamole (△).

Figure 3.6 Time-course (2 min) of dissociation of dipyridamole from guinea-pig lung membranes

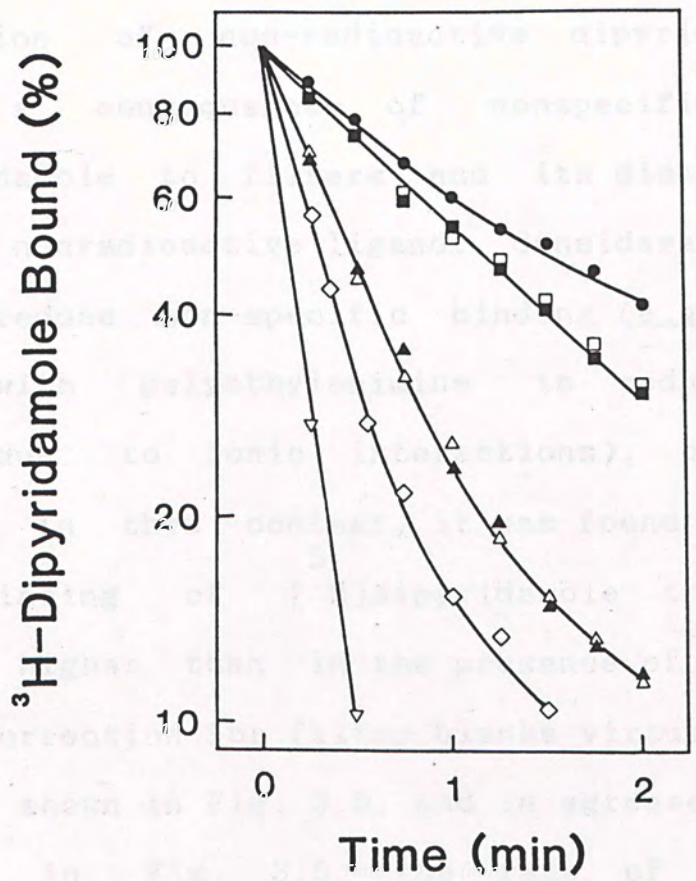

Guinea-pig membranes were incubated with [^{3}H]dipyridamole (20 nM) at 22 ^{0}C for 30 min. [^{3}H]dipyridamole-labelled membranes were washed free of excess ^{3}H-ligand and dissociation (22 ^{0}C) was initiated by the addition of 50 ul of labelled membranes to 60 ml of prewarmed 50 mM Tris-HCl buffer, containing no addition (●), 20 nM-dipyridamole (□), 20nM-dipyridamole+20nM-NBMPR (■), 20nM-dipyridamole +20uM-NBMPR (◇), 20uM-dipyridamole (△), 20uM-dipyridamole +20nM-NBMPR (▲), 20uM-dipyridamole+20uM-NBMPR (▽).

also Table 3.4).

As mentioned in the previous paragraph, this 2.5-fold increase in app. Koff in the presence of a high concentration of non-radioactive dipyridamole is most probably a consequence of nonspecific binding of [^{3}H]dipyridamole to filters and its displacement by high levels of nonradioactive ligand. Considerable efforts were made to reduce non-specific binding (e.g. by pretreating filters with polyethylenimine to reduce non-specific binding due to ionic interactions), but with little success. In this context, it was found that nonspecific filter binding of [^{3}H]dipyridamole to filters alone was much higher than in the presence of membranes making accurate correction for filter blanks virtually impossible.

As shown in Fig. 3.6, and in agreement with the data presented in Fig. 3.5, the rate of dissociation of [^{3}H]dipyridamole from guinea pig lung membranes in the presence of either concentration of dipyridamole was unaffected by inclusion of 20 nM NBMPR in the dissociation buffer. However, increasing the NBMPR concentration to 20 uM accelerated the rate of [^{3}H]-dipyridamole dissociation from guinea-pig lung membranes by 2.5-3.1 fold as compared with the corresponding dissociation rates of [^{3}H]-dipyridamole in the presence of either 20 nM or 20 uM non-radioactive dipyridamole alone (Table 3.4). Thus, the ability of high concentrations of NBMPR to accelerate [^{3}H]dipyridamole dissociation from its binding

sites was independent of the concentration of nonradioactive dipyridamole in the dissociation buffer.

Table 3.4 Summary of apparent Koff of dissociation of dipyridamole from guinea pig lung membranes

Conditions	Apparent Koff (min^{-1})
no addition	0.528
20 nM dipyridamole (dip) only	0.601
20 nM dip + 20 nM NBMPR	0.601
20 nM dip + 20 uM NBMPR	2.51
20 uM dip only	1.51
20 uM dip + 20 nM NBMPR	1.51
20 uM dip + 20 uM NBMPR	4.8

Apparent Koff calculated according to equation (1) described in the text. Data taken from Fig. 3.6.

3.4 DISCUSSION

The results presented in Chapter 2 establish that guinea-pig and rat lung membranes possess a high density of nucleoside transporters, as judged by assays of high-affinity [^{3}H]NBMPR binding activity. Bmax values for [^{3}H]NBMPR binding were determined to be in the region of 20 and 10 pmol/mg of protein for guinea-pig and rat lung membranes respectively, with apparent Kd values in the range 0.2-0.4 nM. In the series of experiments presented in this Chapter, I have demonstrated the existence of NBMPR-sensitive dipyridamole binding to guinea-pig lung membranes (Fig. 3.1). In marked contrast, corresponding NBMPR-sensitive dipyridamole binding sites were not detected in rat lung membranes. This result is consistent with the NBMPR-binding studies described in Chapter 2 where it was established that non-radioactive dipyridamole is a competitive inhibitor of [^{3}H]NBMPR binding with an apparent Ki of 18 nM for guinea pig lung membranes compared with a value of 8.5 uM for rat membranes, a difference of 470-fold. Therefore, it would not be expected to detect NBMPR-sensitive binding of [^{3}H]dipyridamole to rat lung nucleoside transporters, membranes from this species effectively representing a negative control for transporter-associated ligand binding.

Fig. 3.2 confirms the presence of NBMPR-sensitive dipyridamole binding in guinea-pig lung membranes only. Binding of [^{3}H]dipyridamole to lung crude membranes of

this species was of high-affinity with a Kd of 1.9 nM, comparable to the reported Kd of 3.5 nM [^{3}H]dipyridamole to guinea pig brain membranes (Marangos et al, 1985). In contrast, there was no detectable high-affinity saturable [^{3}H]dipyridamole binding to guinea pig erythrocyte membranes (Jarvis, 1986), the level of nonspecific [^{3}H]dipyridamole binding to guinea pig erythrocyte membranes being too high to make it possible to detect the low number of nucleoside transporters in erythrocyte membranes of this species (Jarvis, 1986). Mean Bmax values of 24.8 and 19.9 pmol/mg of protein for [^{3}H]dipyridamole and [^{3}H]NBMPR to guinea pig lung crude membranes, respectively (Table 3.1) suggest that dipyridamole and NBMPR bind to the transporter with the same stoichiometry.

In contrast, a study of [^{3}H]dipyridamole binding to guinea-pig brain membranes by Marangos et al (1985) reported a 3.2 fold higher Bmax for dipyridamole than for NBMPR (320 vs 100 fmol/mg protein). However, unlike the present investigation, that of Marangos et al (1985) used non-radioactive dipyridamole to correct for non-specific binding. The experiments reported in this Chapter suggest that this might give an erroneously high estimate of high-affinity binding of dipyridamole, particularly in tissues such as the central nervous system with a low density of binding sites (for guinea pig lung membranes, the Bmax for [^{3}H]dipyridamole binding is in the region of 24 pmol/mg protein compared with a Bmax of 320 fmol/mg

protein for guinea pig brain, a difference of 75 fold.

Physiological explanations for the discrepancy between dipyridamole and NBMPR binding to brain membranes include the possibility of high-affinity dipyridamole binding to NBMPR-insensitive nucleoside transporters of the type described by Belt (1983) and Belt and Noel (1985). Wu et al (1986) have reported mixed NBMPR-sensitive and NBMPR-insensitive uridine transport in primary cultures of differentiated mouse astrocytes. Additional support that dipyridamole and NBMPR bind to the NBMPR-sensitive nucleoside transporter with the same stoichiometry comes from a recent study of dipyridamole binding to human erythrocyte membranes. [^{3}H]Dipyridamole was found to bind to a single class of high affinity sites on plasma membranes from human erythrocytes (apparent Kd 0.65 nM) with a maximum number of binding sites similar to that determined for NBMPR binding (Jarvis, 1986).

Both nucleosides and other nucleoside transport inhibitors were found to block high-affinity [^{3}H]dipyridamole binding to guinea pig lung membranes. IC_{50} concentrations estimated from the data presented in Table 3.2 and Fig. 3.4 were used to determine apparent Ki values from the relationship:

$$Ki = IC_{50} / [1+([L]/Kd)]$$

where [L] is the free radioligand concentration and Kd its binding affinity. Calculated inhibitor constants were: adenosine, 0.26 mM; uridine, 1.93 mM; dilazep, 4.4 nM;

lidoflazine, 39 nM; NBMPR, 0.9 nM. Although these Ki values, based on a single [^{3}H]dipyridamole concentration, can only be regarded as approximate, they correspond well with equivalent Ki values determined for inhibition of high-affinity [^{3}H]NBMPR binding to guinea-pig lung membranes: adenosine, 0.28 mM; uridine, 2.0 mM; dilazep, 2.0 nM; lidoflazine, 110 nM (see Chapter 2, Tables 2.2 and 2.4). The apparent Ki for NBMPR inhibition of [^{3}H]dipyridamole binding (0.9 nM) also agrees well with the apparent Kd value for [^{3}H]NBMPR binding to these membranes (0.4 nM). Similarly, in human erythrocyte membranes, equilibrium dipyridamole binding in the presence of adenosine and uridine was reduced in an apparent competitive manner with apparent Ki values of 0.1 and 0.9 mM, respectively (Jarvis, 1986), inhibitor constants similar to those obtained previously for adenosine and uridine inhibition of NBMPR binding to human erythrocyte membranes (Ki values for inhibition of [^{3}H]NBMPR binding to erythrocyte membranes are 0.1 mM for adenosine (Jarvis et al, 1983) and 1.0-1.3 mM for uridine (Jarvis et al, 1982)). NBMPR and dilazep also effectively inhibited saturable [^{3}H]dipyridamole binding to human erythrocyte membranes (IC_{50} values of 1.7 nM for both inhibitors) (Jarvis, 1986). There is, therefore strong evidence to indicate that high-affinity dipyridamole binding to guinea pig lung and human erythrocyte membranes represents binding to the NBMPR-sensitive nucleoside transporter.

Figs. 3.5 and 3.6 (Table 3.4) show the kinetic pattern of [^{3}H]dipyridamole dissociation from the guinea pig lung binding-site complex in the presence of non-radioactive NBMPR. Generally, changes in the rate of dissociation may be suggestive of site to site interactions. Thus, the observed ability of 20 uM NBMPR to induce a 3.2-4.2-fold enhancement of the rate of [^{3}H]dipyridamole dissociation from guinea-pig lung membranes either in the presence of 20 nM or 20 uM dipyridamole would appear to indicate that NBMPR and dipyridamole bind to the nucleoside transporter at topographically separate sites. Support for this view comes from the finding that high concentrations of dipyridamole decrease the rate of NBMPR dissociation in human erythrocyte membranes (Jarvis et al, 1983) as well as in lung membranes as described in Chapter 2 (Section 2.3.2). The mechanism by which these two ligands interact with the nucleoside transporter is discussed further in General Discussion.

CHAPTER 4

PHOTOAFFINITY LABELLING STUDIES USING NITROBENZYLTHIOINOSINE

4.1 INTRODUCTION

The experiments described in Chapter 2 establish that NBMPR binds reversibly to high-affinity sites on both rat and guinea pig lung crude membranes and that this binding can be blocked by physiological nucleosides and by vasodilator drugs such as dipyridamole. Guinea pig membranes were more sensitive to dipyridamole inhibition than rat membranes. These sites therefore have the properties expected of NBMPR binding to nucleoside transporter polypeptides in the two species. As detailed in the General Introduction, for human erythrocyte 'ghosts', exposure of site-bound [^{3}H]NBMPR to UV light results in covalent attachment of ligand to membranes. Radiolabelling is selective for band 4.5 polypeptides, proteins that migrate as a broad band on SDS-polyacrylamide gels with an apparent Mr of 45,000-66,000 (Young et al, 1983; Wu et al, 1983). The human erythrocyte glucose transporter is also a band 4.5 polypeptide, both transporters having an apparent Mr (average) of 55,000 (Kwong et al, 1986). The pig erythrocyte nucleoside transporter migrates on SDS-polyacrylamide gels as a sharper band than the human erythrocyte nucleoside and glucose transporters and with a significantly higher apparent molecular weight (apparent Mr (average) 64,000) (Kwong et al, 1986).

The human erythrocyte glucose transporter polypeptide has been shown to be heterogenously

glycosylated. Partial or essentially complete removal of oligosaccharide following endo-β-galactosidase or endoglycosidase-F treatment of the isolated transporter results in a sharpening of its band on SDS-polyacrylamide gels and corresponding shifts to lower apparent molecular weight regions of the gel (Cairns et al, 1984; Lienhard et al, 1984). In addition, it has been established that the human and pig erythrocyte nucleoside transporters are both glycoproteins containing N-linked oligosaccharide. The oligosaccharide and polypeptide structures from the two sources are, however, different (Kwong et al, 1986).

This Chapter describes the photoaffinity labelling of guinea pig and rat lung crude membranes by [^{3}H]NBMPR. It is demonstrated that photoactivated [^{3}H]NBMPR selectively labels polypeptides in the band 4.5 region of both the rat and guinea pig lung crude membranes, with the rat radiolabelled peak migrating on SDS-polyacrylamide gels with a higher apparent molecular weight than the corresponding guinea pig protein. Covalent attachment of ligand to lung crude membranes under equilibrium binding conditions is shown to be inhibited by NBTGR, adenosine and dipyridamole. These experiments provide evidence to implicate membrane protein(s) of Mr 45,000-66,000 as components for NBMPR-sensitive nucleoside transporters in lung tissue.

Enzyme digestion experiments with endoglycosidase-F are shown to increase the electrophoretic mobility of the

radiolabelled peak of lung membranes in both species, enzyme treatment abolishing the difference in apparent Mr between the guinea pig and rat lung nucleoside transporter polypeptides. A series of experiments in which endoglycosidase-F treatment of [^{3}H]NBMPR-radiolabelled lung membranes is combined with limited trypsin digestion are also described in an attempt to further explore the nature of the molecular differences between the rat and guinea pig lung nucleoside transport proteins and to define the relationship between these transporters and those from human and pig erythrocytes.

4.2 METHODS

4.2.1 Membrane Preparation

Rat and guinea pig lung crude membranes were prepared as described in Chapter 2 (Section 2.2.1).

Haemoglobin-free erythrocyte membranes (ghosts) were prepared by osmotic lysis as described by Dodge et al (1963). Fresh blood from healthy volunteers was collected by syringe into heparin (1000 units per ml of blood). Red blood cells were washed three times with 20 volumes of a medium containing 140 mM NaCl, 5 mM KCl, 20 mM Tris-HCl (pH 7.4 at 25°C), 2 mM $MgCl_2$, 0.1 mM EDTA (disodium salt) and 5 mM glucose. The buffy coat was discarded. Approximately 1 volume of packed cells were mixed with 20 volumes of 5 mM sodium phosphate (pH 8.0 at 22°C) and left to stand for 20 min at 4°C. Ghosts were pelleted by centrifugation at 30,000g for 20 min using a Beckman L2-21 centrifuge. The majority of supernatant was removed. The loosely packed ghosts were then transferred to clean tubes, taking care to leave behind the small hard button containing the residual leukocytes and platelets not removed with the buffy coat. The membranes were washed three times with 20 volumes of phosphate buffer, made back to the original cell volume in the same buffer and stored at -70°C for up to 1 month.

4.2.2 Photoaffinity Labelling of Membranes

Rat and guinea pig lung crude membranes (final

protein concentration 0.8 mg/ml) and human erythrocyte 'ghosts' (final protein concentration 2 mg/ml) were equilibrated at room temperature for 30 min with a saturating concentration of [^{3}H]NBMPR (75 nM for erythrocyte 'ghosts' and 25 nM for lung membranes) in the presence and in the absence of 20 uM NBTGR as competing non-radioactive ligand. Samples were then cooled to 4^{o}C and supplemented with 50 mM dithiothreitol, added as a free-radical scavenger. Dithiothreitol does not interfere with [^{3}H]NBMPR binding (Jarvis et al, 1980).

Photolysis was carried out in conventional 3 ml silica spectrophotometer cuvettes (10 mm light path) with continuous stirring at 4^{o}C using a 450-watt mercury arc lamp (Conrad-Hanovia Inc., Newark, New Jersey, U.S.A.). UV exposure was at a distance of 6.5 cm from the lamp's silica cooling sleeve for a period of 45 s. Previous control experiments have shown that maximum labelling of human erythrocyte membranes occured between 30 and 120 s exposure to the mercury arc lamp (Wu et al, 1983). Samples were then diluted 10-fold with buffer containing 20 uM NBTGR and allowed to stand at room temperature for 10 min before recovery of the membrane fraction by centrifugation. The membranes were washed twice more in NBTGR-containing buffer and then extracted at room temperature with SDS-polyacrylamide gel sample buffer containing 100 mM Tris-HCl (pH 6.8), 1 mM EDTA, 10 % (w/v) SDS, 20 % (w/v) glycerol and 0.004 % (w/v) bromophenol blue. Insoluble material was

removed by centrifugation (15,000g, 5 min).

4.2.3 Enzymatic Digestion

Enzyme treatment was performed after photolysis of the membranes with [^{3}H]NBMPR as described above (Section 4.2.2).

4.2.3a Trypsin

Human erythrocyte and rat and guinea pig lung radiolabelled membranes in 50 mM Tris-HCl (pH 7.4 at 22°C) were incubated with trypsin (0.5-5 ug/mg protein) for 15 min at 1°C (Jarvis et al, 1985). Proteolysis was stopped by the addition of 20 volumes of 50 mM Tris-HCl containing 1 mM PMSF followed by centrifugation at 35,000g for 15 min. The pellets were washed once more in PMSF-containing medium and then dissolved in gel sample buffer (Section 4.2.2) or in endoglycosidase-F digestion buffer (see Section 4.2.3b).

4.2.3b Endoglycosidase-F

Treatment with endoglycosidase-F (20 units/mg protein) was carried out at 22°C for 18 hours with agitation in 100 mM sodium phosphate (pH 6.0) containing 75 mM β-mercaptoethanol, 50 mM EDTA, 0.5% (w/v) Triton X-100, 0.05% (w/v) SDS. Enzymatic digestion was terminated by addition of an equal volume of SDS-poly- acrylamide gel sample buffer containg 100 mM Tris-HCl (pH 6.8), 2 mM EDTA,

75 mM DTT, 10% (w/v)SDS, 20% (w/v) glycerol and 0.004% (w/v) Bromophenol Blue (Lienhard et al, 1984).

In some experiments, trypsin-treated membranes were further digested with endoglycosidase-F as described above.

4.2.4 SDS-polyacrylamide Gel Electrophoresis

SDS-polyacrylamide gel electrophoresis was carried out in 12% 2 mm-thick slab gels by the method of Thompson and Maddy (1982), using the Laemmli buffer system (1970). Samples dissolved in gel sample buffer were not heated before application to the gel. Radioactivity in the various regions of the gel was determined by slicing the gel into 2 mm fractions. The ^{3}H-content of these slices was measured by liquid scintillation counting in toluene containing 0.4% (w/v) Omnifluor and 3% (v/v) Protosol (New England Nuclear). Vials were allowed to stand at 37^{o}C for 36 hours before counting. The recovery of applied radioactivity from gels was typically 65-75%. Molecular weight standards from the same slab gels were stained with Coomassie Blue and scanned at 633 nm using an LKB laser densitometer.

4.2.5 Protein Determination

Protein was determined by the method of Lowry et al, (1951).

4.3 RESULTS

4.3.1 Photolysis under Equilibrium Binding conditions

[^{3}H]NBMPR photoaffinity labelling experiments under equilibrium binding conditions resulted in substantial radiolabelling of both rat and guinea pig lung membrane protein. Representative experiments, comparing the resulting radiolabelling patterns with that for human erythrocyte membranes are presented in Figs. 4.1 and 4.2. Photolysis was carried out in the presence of dithiothreitol to minimise the possibility of nonspecific labelling (Young and Jarvis, 1983; Wu et al, 1983a; 1983b). For both species, the radiolabelled protein migrated as single symmetrical peaks on SDS-polyacrylamide gels with apparent molecular weights in the same range as the human erythrocyte nucleoside transporter (Mr 45,000-66,000). The rat lung radioactive peak was broader than that in the guinea pig and had a significantly higher apparent molecular weight (apparent Mr (average) 63,000 and 55,000 , in rat and guinea pig lung crude membranes, respectively) (see also Table 4.2). Covalent incorporation of [^{3}H]NBMPR into these proteins was abolished when photolysis was carried out in the presence of NBTGR. The minor high and low molecular weight peaks observed with the erythrocyte membranes correspond to aggregates of the transporter and low molecular weight degradation products, respectively (Wu et al, 1983). A corresponding low

Figure 4.1 Photoaffinity labelling of rat lung crude membranes and human erythrocyte 'ghosts' with NBMPR

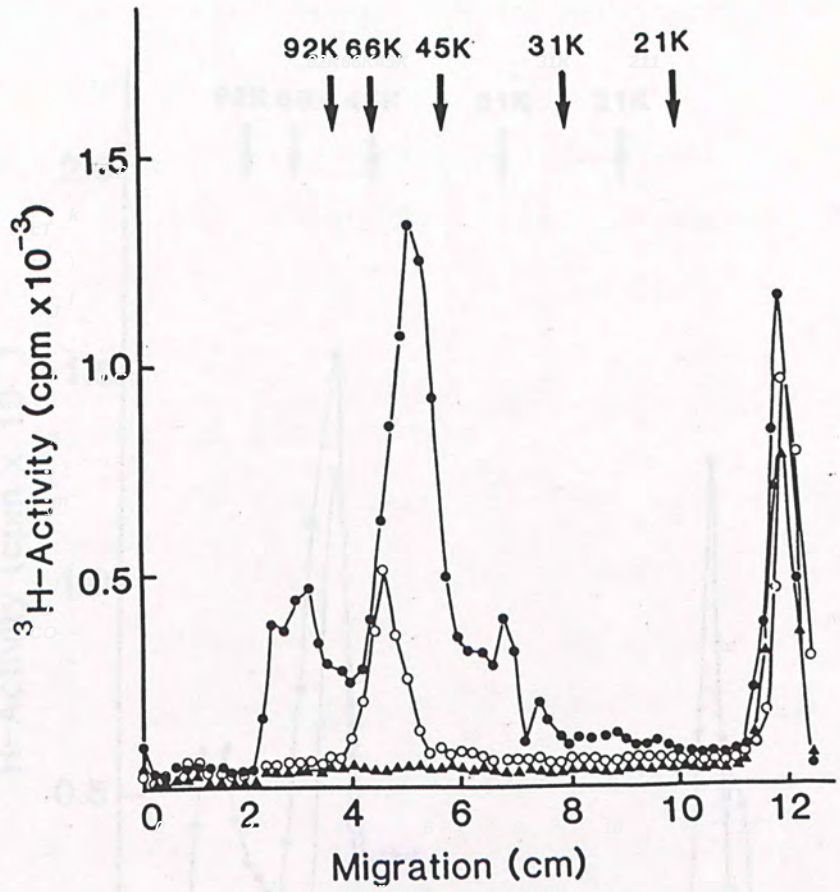

Membranes were equilibrated with saturating concentrations of [^{3}H]NBMPR in the presence and in the absence of 20 uM NBTGR and exposed to UV light for 45 s. Unreacted [^{3}H]NBMPR was removed by washing. Samples were subjected to SDS-polyacrylamide gel electrophoresis as described in the text. [^{3}H]Profiles and positions of molecular weight standards are from the same slab gel. Membranes from rat lung (○) and human erythrocytes (●). Photolysis of rat lung membranes in the presence of NBTGR (▲). Data for human erythrocyte membranes in the presence of NBTGR coplotted with the rat lung NBTGR counts (not shown).

Figure 4.2 Photoaffinity labelling of guinea pig lung crude membranes and human erythrocyte 'ghosts' with NBMPR

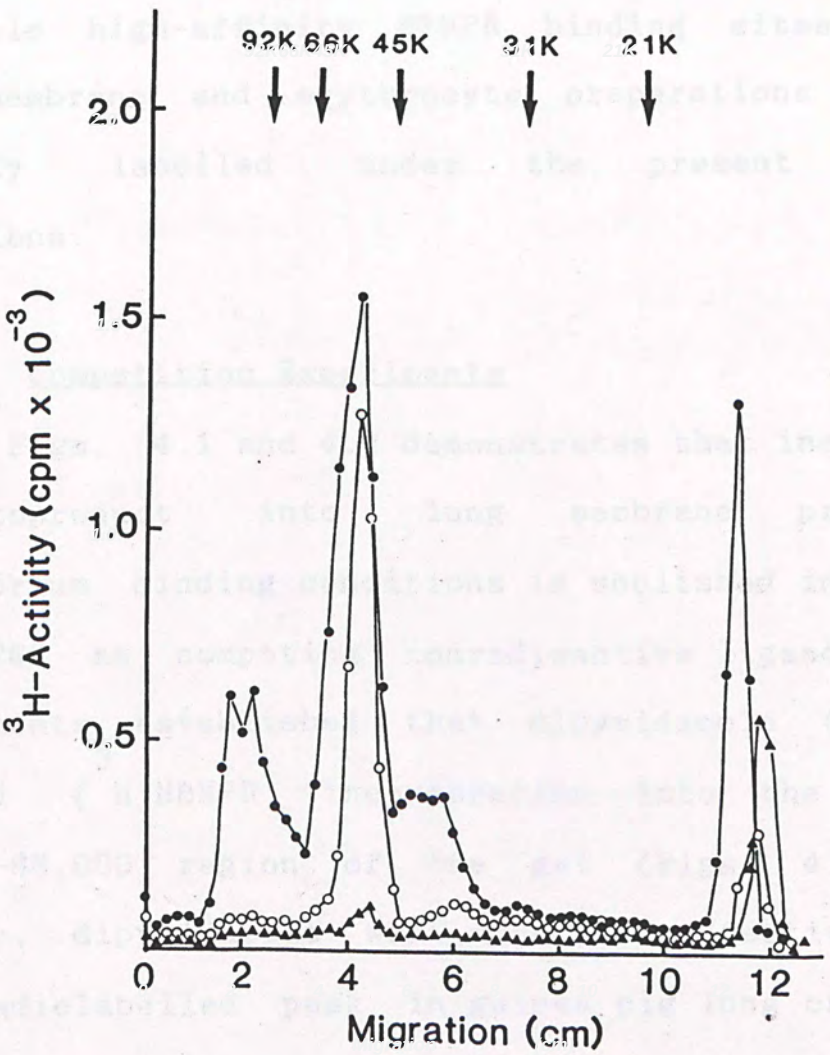

Photolysis and SDS-polyacrylamide gel electrophoresis of guinea pig lung crude membranes and human erythrocyte 'ghosts' in the presence of [^{3}H]NBMPR were carried under identical conditions to those described in the legend to fig. 4.1. Guinea pig lung membranes in the absence (○) and in the presence of NBTGR (▲). Human erythrocyte membranes in the absence of NBTGR (●).

molecular weight peak, but in smaller amount, was observed with guinea pig lung crude membranes. All preparations exhibited nonspecific labelling in the lipid region of the gel. It was calculated that approximately 10% of the available high-affinity NBMPR binding sites in both the lung membrane and erythrocyte preparations were photo-affinity labelled under the present experimental conditions.

4.3.2 Competition Experiments

Figs. 4.1 and 4.2 demonstrates that incorporation of ^{3}H-photoproduct into lung membrane protein under equilibrium binding conditions is abolished in the presence of NBTGR as competing nonradioactive ligand. Subsequent experiments established that dipyridamole (50 uM) also reduced [^{3}H]NBMPR incorporation into the apparent Mr 45,000-66,000 region of the gel (Figs. 4.3 and 4.4). However, dipyridamole was much more effective in reducing the radiolabelled peak in guinea pig lung crude membranes than in those of the rat. This correlates with the species difference in dipyridamole inhibition of reversible NBMPR binding described in Chapter Two, with the rat being less sensitive to dipyridamole inhibition. In contrast, adenosine, a physiological transported nucleoside, inhibited radiolabelling of membrane protein in the two species to a similar extent (Figs. 4.5 and 4.6). Quantitative estimates of the extents of inhibition of Mr

Figure 4.3 Effect of dipyridamole on NBMPR photoaffinity labelling of rat lung crude membranes

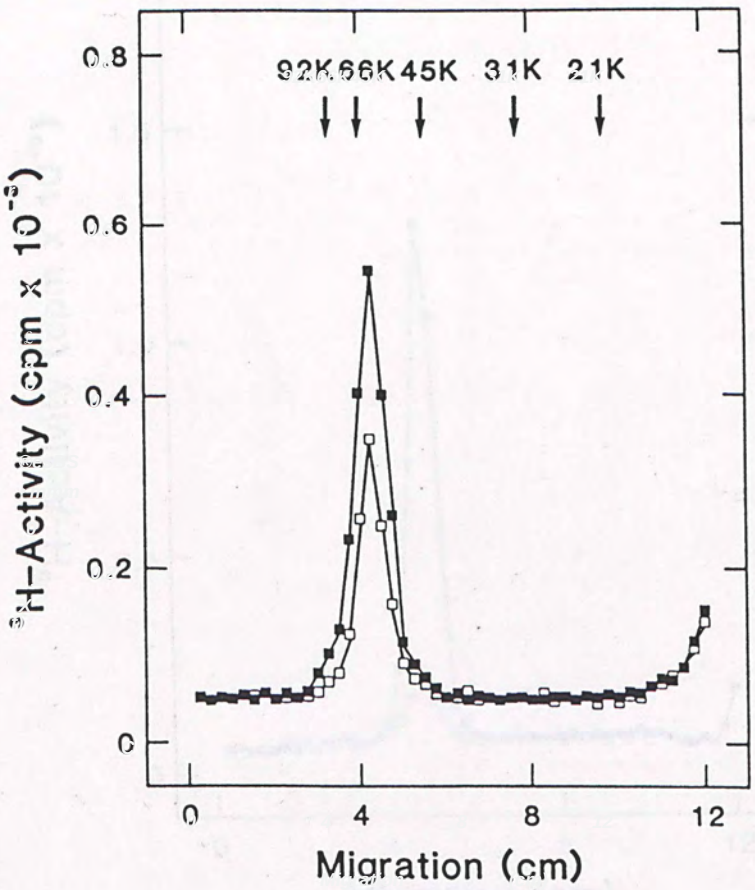

Rat lung crude membranes equilibrated with 25 nM [^{3}H]NBMPR in the presence (□) and in the absence (■) of 50 uM dipyridamole, supplemented with 50 mM DTT and exposed to high intensity UV light at 4°C for 45 s. SDS-polyacrylamide gel electrophoresis was performed as described in the text (Section 4.2.4).

Figure 4.4 Effect of dipyridamole on NBMPR photoaffinity labelling of guinea pig lung crude membranes

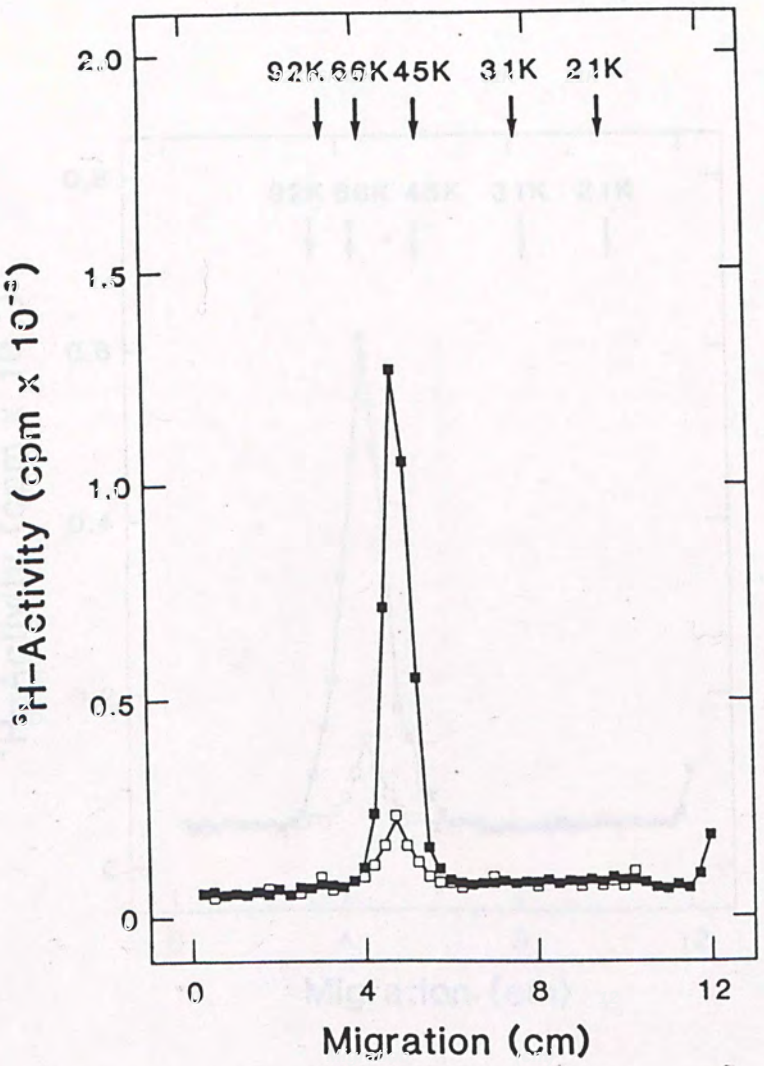

Guinea pig lung crude membranes equilibrated with 25 nM [^{3}H]NBMPR in the presence (□) and in the absence of 50 uM dipyridamole (■), supplemented with 50 mM DTT and exposed to high intensity UV light at 4°C for 45 s. SDS-polyacrylamide gel electrophoresis was performed as described in the text.

Figure 4.5 Effect of adenosine on NBMPR photoaffinity labelling of rat lung crude membranes

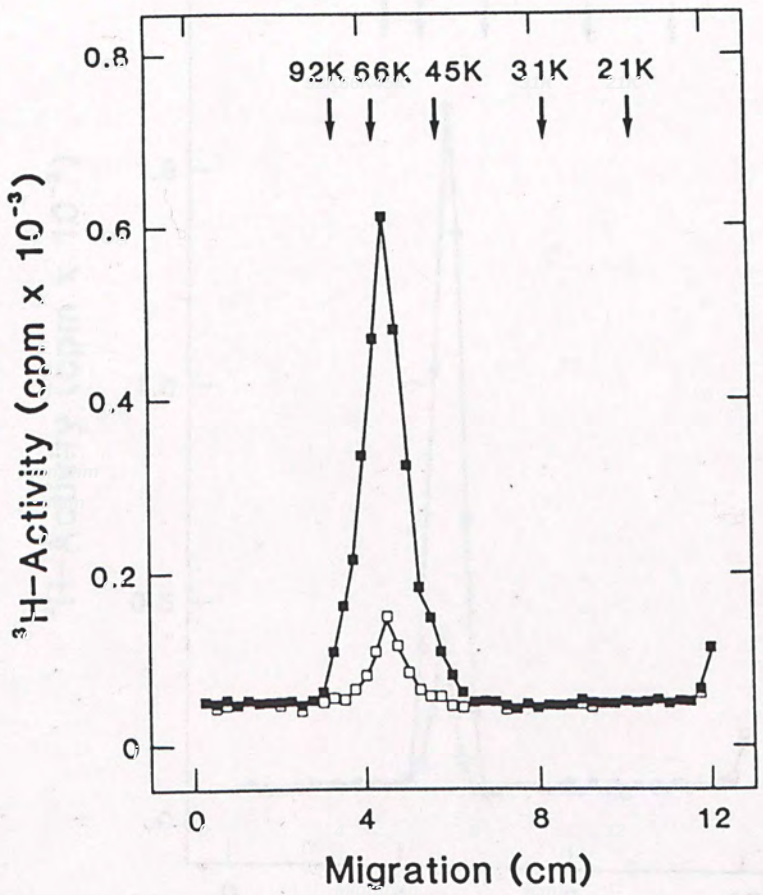

Rat lung crude membranes equilibrated with 25nM [^{3}H]NBMPR in the presence (□) and in the absence of 10 mM adenosine (■), supplemented with 50 mM DTT and exposed to high intensity UV light at 4°C for 45 s. SDS-polyacrylamide gel electrophoresis was performed as described in the text.

Figure 4.6 Effect of adenosine on NBMPR photoaffinity labelling of guinea pig lung crude membranes

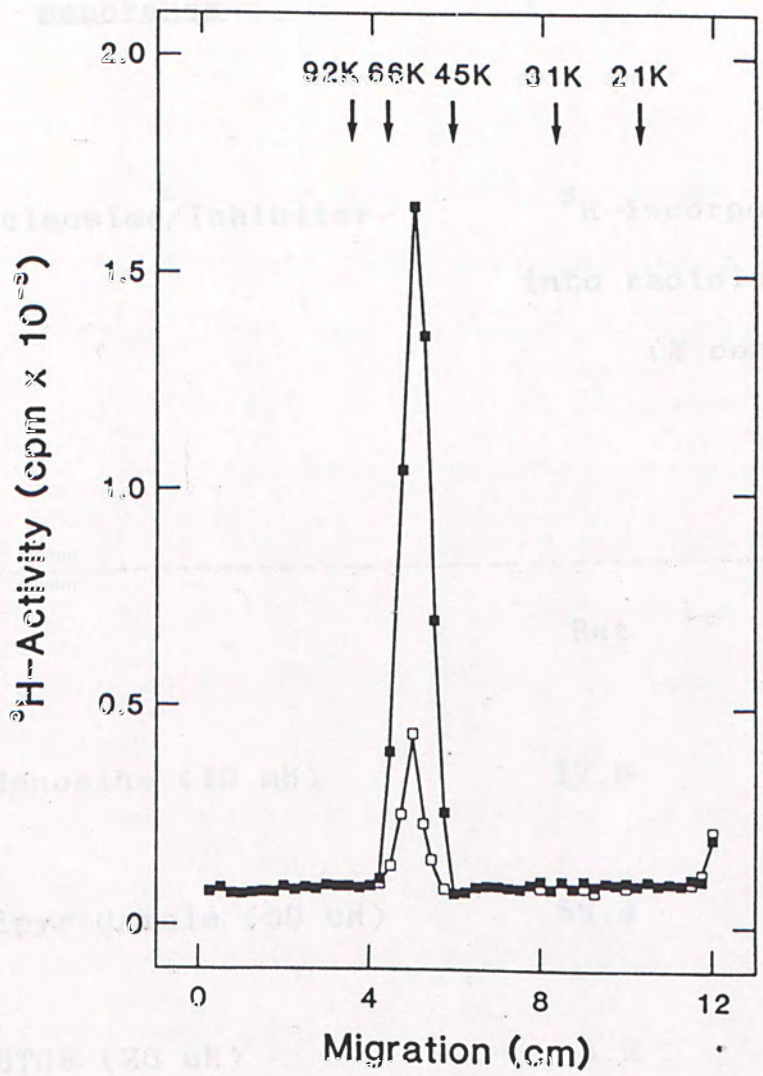

Guinea pig lung crude membranes equilibrated with 25 nM [^{3}H]NBMPR in the presence (□) and in the absence of 10 mM adenosine (■), were supplemented with 50 mM DTT and exposed to high intensity UV light at 4°C for 45 s. SDS-polyacrylamide gel electrophoresis was performed as described in Section 4.2.4.

Table 4.1 Effects of adenosine, dipyridamole and NBTGR on covalent NBMPR incorporation into protein of apparent Mr 45,000-66,000 in lung crude membranes

Nucleoside/Inhibitor	^{3}H-incorporation into radiolabelled peak (% control)	
	Rat	Guinea pig
Adenosine (10 mM)	17.6	18.3
Dipyridamole (50 uM)	56.4	17.2
NBTGR (20 uM)	3.2	2.9

Data are taken from Figs. 4.1-4.6.

45,000-66,000 radiolabelling obtained with these agents are detailed in Table 4.1.

4.3.3 Endoglycosidase-F treatment

Endoglycosidase-F cleaves the glycosidic bond of N-acetyl-glucosamine (1-4) N-acetylglucosamine linked to asparagine of the core protein of high mannose structures. Fig. 4.7 compares the SDS-polyacrylamide gel ^{3}H-profiles of radiolabelled rat and guinea pig lung crude membranes and human erythrocyte membranes incubated (18h, 22°C) in the absence and in the presence of endoglycosidase-F. In each case there was a significant sharpening of the ^{3}H-peak and a shift to a lower apparent molecular weight, an indication that the nucleoside transporter of the three species is a glycoprotein. Table 4.2 summarises the electrophoretic mobilities of the rat and guinea pig radiolabelled nucleoside transporters before and after endoglycosidase-F treatment in comparison with that of the human erythrocyte protein. Following endoglycosidase-F treatment, the rat protein showed the largest decrease in M_r such that the difference in apparent M_r between the rat and guinea pig nucleoside transporters was abolished, the deglycosylated proteins from these two sources having the same apparent M_r of 46,000 which in turn was within 1000 daltons of the deglycosylated human erythrocyte nucleoside transporter (Table 4.2). These results indicate that the molecular difference between the rat and guinea pig lung

Figure 4.7 Effects of endoglycosidase-F on the electrophoretic mobilities of the human erythrocyte and rat and guinea pig lung nucleoside transporters

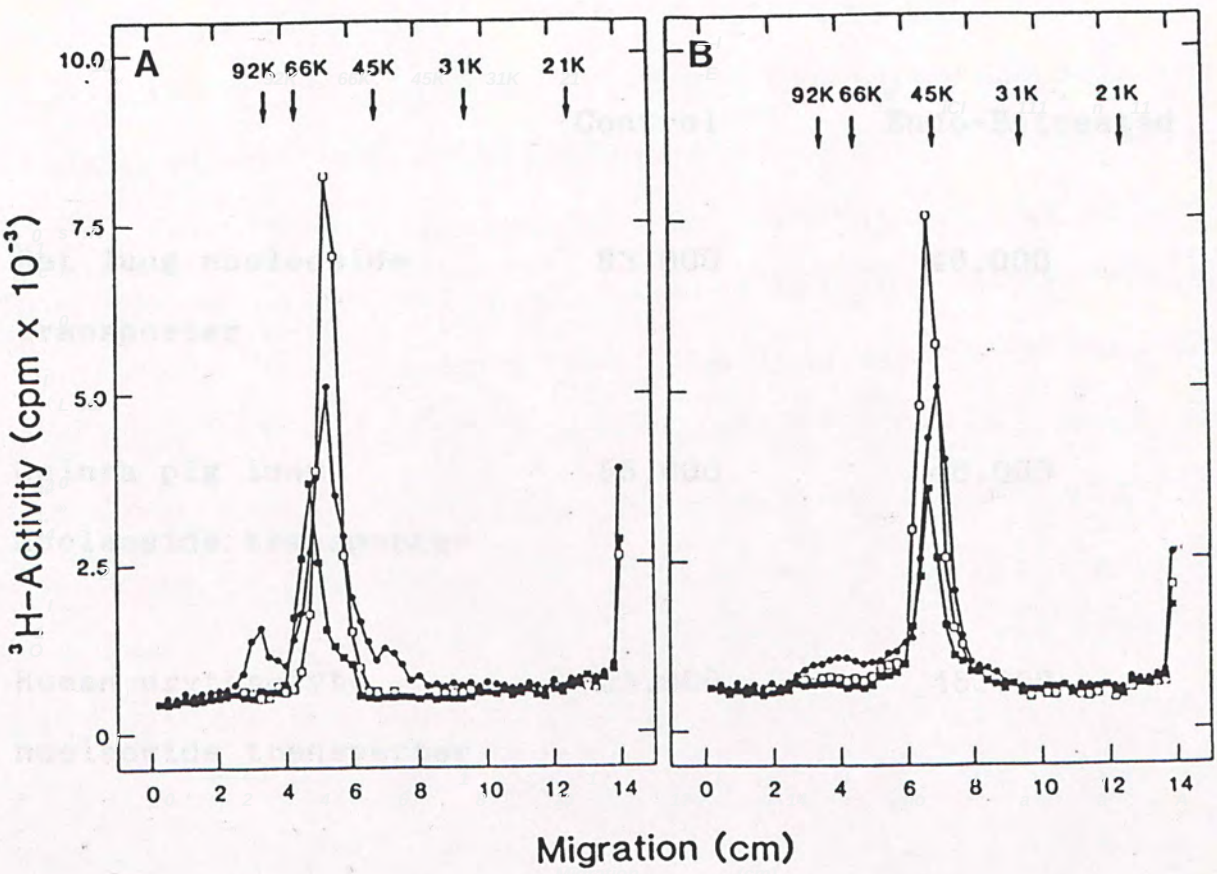

Human erythrocyte 'ghosts' and rat and guinea pig lung crude membranes radiolabelled with [^{3}H]NBMPR were incubated for 18 h at 22°C either in the absence (A) or in the presence (B) of enzyme (see Section 4.3.3) and electrophoresed as described in the text. ^{3}H-Profiles and positions of the Mr standards are from the same slab gel.

Symbols used: (●) Human ; (■) rat and (□) guinea pig.

Table 4.2 Apparent molecular weights of rat and guinea pig lung nucleoside transport polypeptides treated with endoglycosidase-F

	Control	Endo-F-treated
Rat lung nucleoside transporter	63,000	46,000
Guinea pig lung nucleoside transporter	55,000	46,000
Human erythrocyte nucleoside transporter	55,000	45,000

Data are taken from Fig. 4.7. See text for experimental details.

nucleoside transporter is due to different degrees of glycosylation.

4.3.4 Digestion with Trypsin

Digestion of human erythrocyte 'ghosts' with trypsin (0.5 ug enzyme/mg of membrane protein, 15 min at 1°C) generated a radioactive fragment with apparent molecular weight values of 39,000 (Fig. 4.8), a result in agreement with the data presented by Jarvis *et al* (1986). Preliminary experiments establishes that the NBMPR-labelled proteins in guinea pig and rat lung membranes were more resistant to trypsin cleavage than the human erythrocyte transporter. Digestion of rat and guinea pig lung membranes with trypsin (5 ug enzyme/mg protein) produced radioactive fragments similar to those from human 'ghosts', but with significantly higher apparent molecular weights (apparent Mr 44,000 and 41,000 for rat and guinea pig, respectively) (Fig. 4.8).

4.3.5 Endoglycosidase-F Digestion of Trypsinised Membranes

To further investigate molecular differences between the rat and guinea pig lung nucleoside transporters, rat and guinea pig lung membranes were subjected to sequential trypsin and endoglycosidase-F digestion. Before endoglycosidase-F treatment, the rat and guinea pig lung trypsinised nucleoside transporter fragments ran as broad bands at Mr 44,000 and 41,000, respectively (see Section

Figure 4.8 Trypsin digestion of NBMPR-labelled human erythrocyte 'ghosts' and rat and guinea pig lung crude membranes

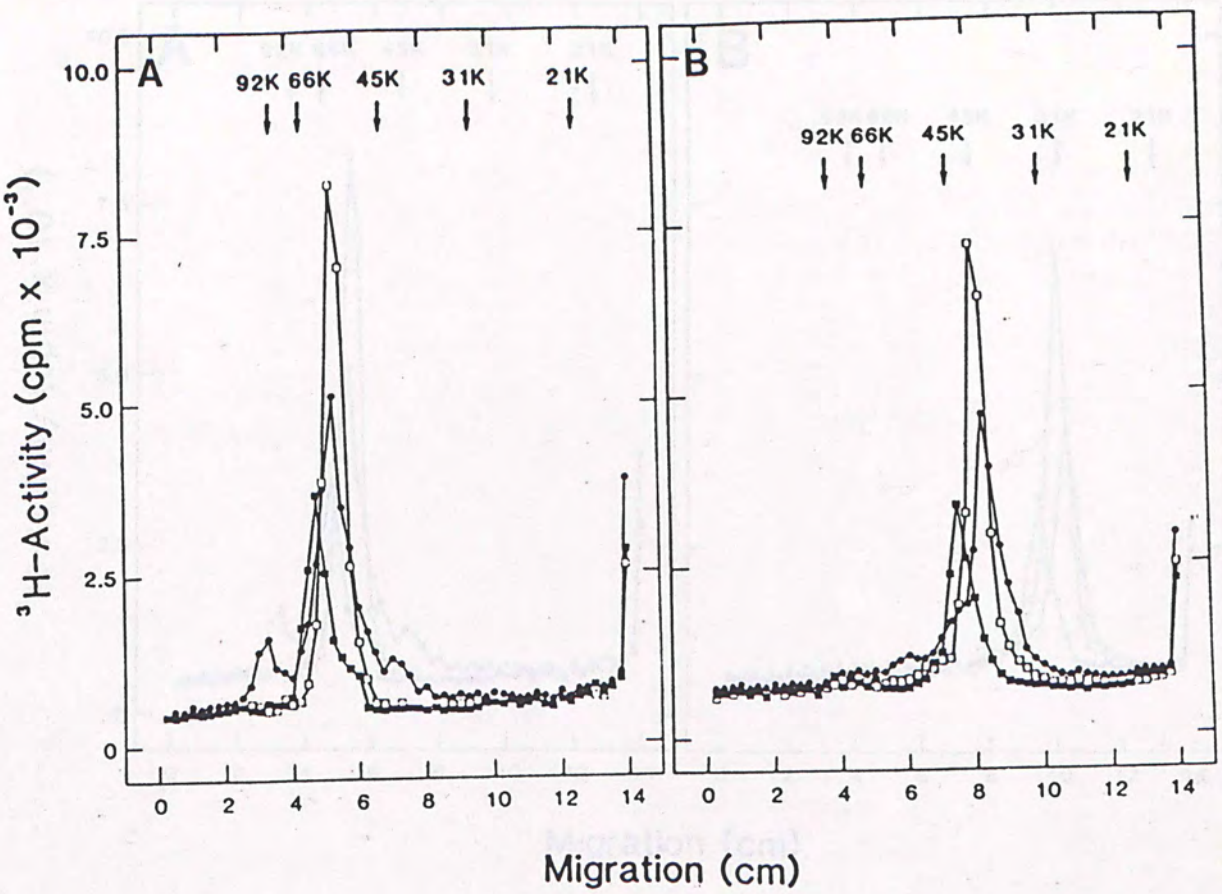

Membranes photolabelled with [^{3}H]NBMPR were incubated for 15 min at 1^{0}C (see Section 4.3.4) either in the absence (A) or in the presence (B) of trypsin and electrophoresed as described in the text. ^{3}H-Profiles and positions of the Mr standards are from the same slab gel.

Symbols used: (●), Human; (■), rat and (□) guinea pig.

Figure 4.9 Effects of trypsin and endoglycosidase-F digestion on NBMPR-labelled human erythrocyte 'ghosts' and rat and guinea-pig lung crude membranes

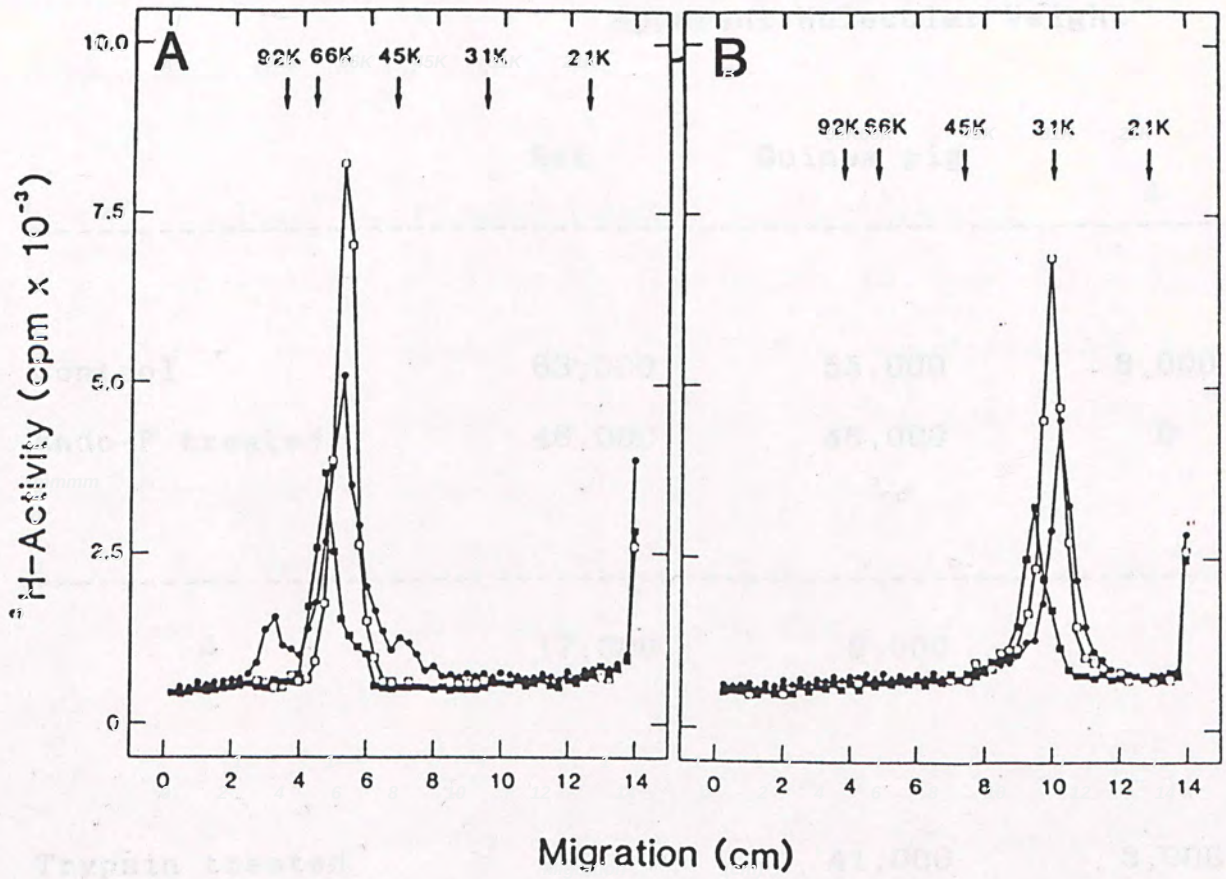

[^{3}H]NBMPR-radiolabelled membranes were first treated with trypsin and subsequently with endoglycosidase-F as described in the text (section 4.3.5). A. control, incubations in the absence of trypsin and endoglycosidase-F; B, trypsin then endoglycosidase-F.

Symbols used: (●) human; (■) rat and (□) guinea pig.

Table 4.3 Apparent molecular weight values for guinea pig and rat lung nucleoside transport polypeptides treated with endoglycosidase-F (Endo-F) and trypsin and a combination of both

	Apparent Molecular Weight		
	Rat	Guinea pig	Δ
Control	63,000	55,000	8,000
Endo-F treated	46,000	46,000	0
Δ	17,000	9,000	
Trypsin treated	44,000	41,000	3,000
Trypsin and Endo-F	33,000	31,000	2,000
Δ	11,000	10,000	

Data are taken from Figs. 4.7-4.9.

4.3.4 and Fig. 4.8). After endoglycosidase-F treatment, the apparent Mr values of these fragments decreased from 44,000 to 33,000 (rat) and 41,000 to 31,000 (guinea pig) (Fig. 4.9). Likewise, the apparent Mr of the human trypsinized fragment decreased from 39,000 to 30,000. Combined results from the enzyme digestion experiments are summarised in Table 4.3.

4.3.6 Photoaffinity Labelling with Dipyridamole

Dipyridamole absorbs strongly in the UV. It was therefore considered possible that dipyridamole might function as a photoprobe of the nucleoside transporter in a manner similar to that for NBMPR.

A procedure similar to that described for NBMPR (Section 4.2.2) was used in an attempt to photolabel lung crude membranes with [^{3}H]dipyridamole. Exposure of [^{3}H]dipyridamole (250 nM) to high-intensity UV light (450 Watt, 45 s) under equilibrium binding condition and in the presence of 50 mM DTT did not result in detectable radiolabelling of lung membranes (Fig. 4.10). In the same experiment, exposure of membranes to UV light in the presence of [^{3}H]NBMPR (50 nM) under the same conditions gave the normal radiolabelling pattern observed with this ligand (see also Fig. 4.10).

Figure 4.10 Photoaffinity labelling of guinea pig and rat lung crude membranes with dipyridamole or NBMPR

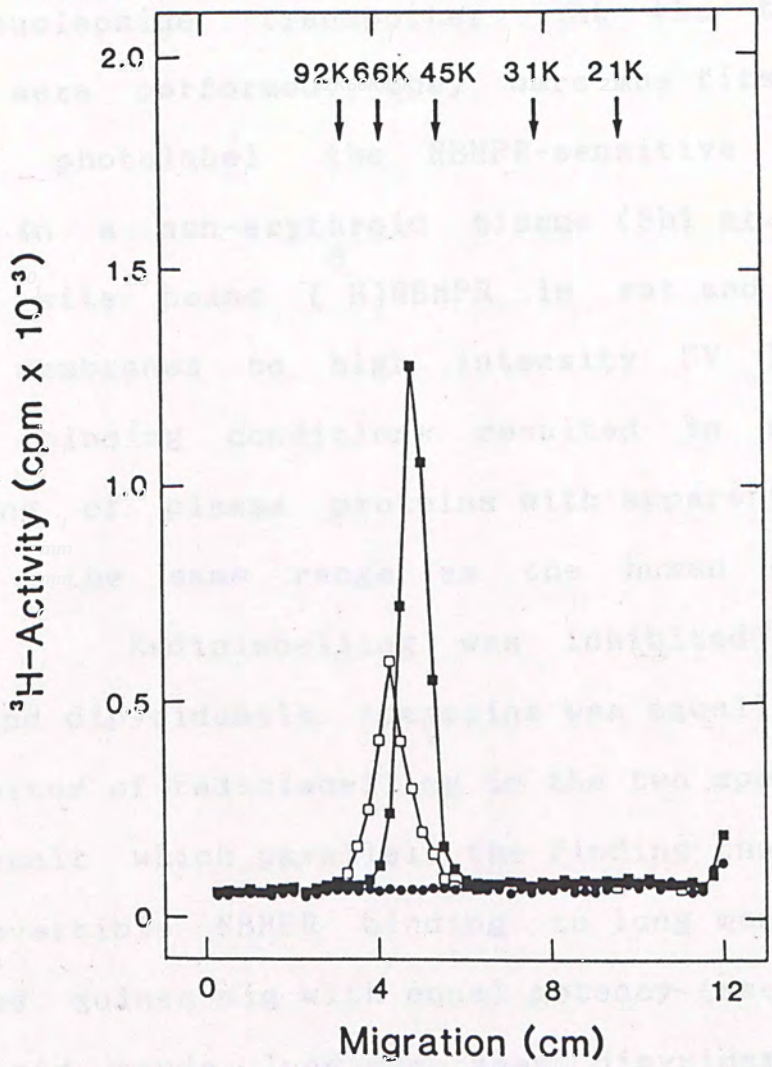

Photolysis and SDS-polyacrylamide gel electrophoresis of guinea pig and rat lung crude membranes in the presence of [^{3}H]NBMPR or [^{3}H]dipyridamole were carried under identical conditions to those described in the legend to Fig. 4.1. (see also 4.3.6). Guinea pig (■) or rat (□) lung crude membranes photolabelled with [^{3}H]NBMPR. Photolysis of membranes with [^{3}H]dipyridamole (●) co-plotted in both species. ^{3}H-Profiles and positions of Mr standards are from the same slab gel.

4.4 DISCUSSION

In this Chapter, I have sucessfully established the use of NBMPR as a photoaffinity probe of the lung NBMPR-sensitive nucleoside transporter. At the time these experiments were performed, they were the first reported attempt to photolabel the NBMPR-sensitive nucleoside transporter in a non-erythroid tissue (Shi *et al*, 1984). Exposure of site bound [^{3}H]NBMPR in rat and guinea pig lung crude membranes to high intensity UV light under equilibrium binding conditions resulted in substantial radiolabelling of plasma proteins with apparent molecular weights in the same range as the human erythrocyte transporter. Radiolabelling was inhibited by NBTGR, adenosine and dipyridamole. Adenosine was equally effective as an inhibitor of radiolabelling in the two species (Table 4.1), a result which parallels the finding that adenosine inhibits reversible NBMPR binding to lung membranes from the rat and guinea pig with equal potency (see Fig. 2.2). In guinea pig crude lung membranes, dipyridamole (50 uM) decreased ^{3}H-incorporation into the Mr 45,000-66,000 region of the gel to 17% of control, while in the rat, the same concentration of dipyridamole only reduced radiolabelling to 57% of control (Table 4.1). This difference correlates well with the Ki values established in Chapter 2 for dipyridamole as an inhibitor of reversible NBMPR binding (Ki 18 nM and 8.6 uM for guinea pig and rat, respectively). These results therefore provide strong

evidence to implicate proteins of Mr 45,000-66,000 in NBMPR-sensitive nucleoside permeation in lung tissue.

The present series of photoaffinity labelling experiments in lung were extended by Wu and Young (1984) using liver membranes. Exposure of rat and guinea pig liver membranes to high intensity UV light in the presence of [^{3}H]NBMPR again resulted in the selective NBTGR-sensitive radiolabelling of membrane proteins which migrated on SDS-polyacrylamide gels with apparent Mr values in the same range as that of the erythrocyte nucleoside transporters (45,000-66,000). A similar species differences in apparent Mr to that described in the present Chapter was also reported (apparent Mr 63,000 and 55,000 in rat and guinea pig liver nucleoside transporters, respectively).

Photolysis studies in nonerythroid cells have subsequently been extended to a variety of other tissues and cell types. Exposure of membranes from cultured mouse S49 lymphoma cells, guinea pig cardiac muscle and brain to UV light in the presence of [^{3}H]NBMPR has again been shown to result in the covalent radiolabelling of membrane proteins which migrate on SDS-polyacrylamide gels with an apparent Mr of 45,000-66,000 (Almeida *et al*, 1984; Kwan and Jarvis, 1984; Jarvis and Ng, 1985). Membrane proteins from AE^1 cells (Cohen *et al*, 1979), a nucleoside transport-deficient clone isolated from a mutagenized population of S49 cells, which lack high-affinity NBMPR

binding sites (Cass et al,1981), are not covalently labelled by [^{3}H]NBMPR (Almeida et al, 1984; Young et al, 1984). These results suggest that the NBMPR-sensitive nucleoside transport activity in different tissues and cells is catalyzed by proteins with similar molecular properties.

In this Chapter, the rat and guinea pig species difference in apparent Mr was further investigated in a series of enzyme digestion studies using endoglycosidase-F and trypsin. Endoglycosidase-F digestion demonstrated that the rat and guinea pig lung nucleoside transporters are both glycoproteins containing N-linked oligosaccharides. The observation that the difference in apparent molecular weight between the guinea pig and rat lung nucleoside transporters is abolished after endoglycosidase-F treatment strongly suggests that the Mr difference can be accounted for by differences in degree of glycosylation in the two nucleoside tranporter proteins. Additional support for this conclusion comes from subsequent studies of the rat and guinea pig liver nucleoside transporters, where the difference in apparent Mr is also abolished after endoglycosidase-F digestion, both peaks shifting to the same lower apparent Mr of 46,000 as reported in this Chapter (Wu and Young, personal communication).

The human and pig erythrocyte nucleoside transporters have also been shown to be glycoproteins containing N-linked oligosaccharide (Kwong et al, 1986). A summary of

enzyme digestion experiments on these two erythrocyte nucleoside transporters is summarised in Table 4.4. It was found that the pig nucleoside transporter was resistant to endo-ß-galactosidase digestion (endo-β-galactosidase hydrolyses internal B-galactosidase linkages of oligosaccharides belonging to the poly-N-acetyllactosamine series) and, in contrast to the present results, it was found that endoglycosidase-F treatment actually magnified the difference in apparent Mr between the human and pig erythrocyte nucleoside transporters (13,000 after enzyme digestion compared with 9,000 before). These data provide strong evidence that there are both polypeptide and carbohydrate differences between the human and pig transporters, carbohydrate differences alone only in part accounting for the different electrophoretic mobilities of the two transporter proteins on SDS-polyacrylamide gels. As seen in Fig. 4.7 (Table 4.2), the electrophoretic mobility of the human erythrocyte nucleoside transporter following endogylcosidase-F treatment coinicides (Mr difference < 1,000) with that of the deglycosylated rat and guinea pig lung nucleoside transporters when electrophoresed on the same gel, evidence that the polypeptide structure of the human erythrocyte nucleoside transporter is very similar to that of rat and guinea pig lung.

In complementary experiments with trypsin, it was established that there is at least one trypsin cleavage site present on the rat and guinea pig lung nucleoside

Table 4.4 Apparent molecular weights of erythrocyte nucleoside transport polypeptides treated with endo-β-galactosidase (endo-β) and endoglycosidase-F (endo-F)

Nucleoside Transporter	Control	Endo-β treated	Endo-F treated
Human	55,000	47,000	45,000
Pig	64,000	64,000	57,000

Data taken from Kwong et al (1986).

transporters. The trypsin digestion patterns of the lung and human erythrocyte nucleoside transporters were very similar, trypsinisation resulting in a shift of the radiolabelled peak to a lower apparent molecular weight (30, 25 and 31% decrease in apparent Mr in rat, guinea pig and human, respectively). The data presented in Table 4.3 and in Figs. 4.8 and 4.9 also establish that NBMPR and carbohydrate are attached to the same half of the guinea pig and rat transporter polypeptides. This is also the case for the human erythrocyte nucleoside transporter (Kwong et al, 1986), but contrasts with that for the human erythrocyte glucose transporter where the carbohydrate and cytochalasin-B attachment sites are located on different halves of the transporter polypeptide (Cairns et al, 1984; Daziel and Rothstein, 1984). From Table 4.3, it can be seen that the difference in apparent molecular weight between the trypsinised rat and guinea pig lung nucleoside transporters is similar before and after endoglycosidase-F treatment (Mr difference of 2,000 to 3,000). Interpretation of the these data is presented in Chapter 7, where molecular models for the rat and guinea pig nucleoside transporters are proposed.

CHAPTER 5

LUNG PURIFIED PLASMA MEMBRANES: PREPARATION AND CHARACTERIZATION

5.1 INTRODUCTION

The experiments reported in previous Chapters were performed with crude membrane preparations from guinea pig and rat lung tissue. These crude membrane preparations contain plasma membrane as well as membranes from different intracellular components such as mitochondria and endoplasmic reticulum. Crude membrane preparations from both species displayed high-affinity NBMPR binding activity (Chapter 2) and exposure of site-bound [^{3}H]NBMPR to high intensity UV light resulted in the photoaffinity labelling of lung proteins with apparent molecular weights similar to that of the human erythrocyte nucleoside transporter(Mr 45,000-65,000) (Chapter 4). It was established that there exists a marked species difference with respect to effects of various vasodilators on reversible NBMPR binding to rat and guinea pig membranes (Chapter 2, Section 2.3.1). Also, there was a significant difference in the molecular weight of the radiolabelled transporter in the two species (Chapter 4, Section 4.3.1). In Chapter 3, guinea pig lung crude membranes were used to demonstrate that NBMPR and dipyridamole bind to the NBMPR nucleoside transporter with the same stoichiometry.

Recently, Casale and coworkers (1984) reported a method of isolating purified plasma membranes from human peripheral lung tissue. The present Chapter describes a modification of that procedure which permits the preparation of a highly enriched plasma membrane

preparation from guinea pig and rat lung. The objective of these experiments was to make available more enriched lung plasma membrane preparations with a higher specific activity NBMPR binding. In Chapter 6, one application of such purified membrane preparations is described -- the reconstitution of functional lung nucleoside transporters into proteoliposomes.

The experimental section of the present Chapter is divided into two main parts. The first describes the methodology used to prepare guinea pig and rat lung purified plasma membranes and the second deals with the detailed characterisation of the two purified lung membrane preparations.

5.2 METHODS

5.2.1 Tissue and Plasma Membrane Preparation

Plasma membranes from both guinea pig and rat lung were prepared as outlined in Fig.5.1. This method is modified from that of Casale *et al*,(1984). Unless stated otherwise, all steps were performed at 0-4°C.

Dunkin Hartley guinea pigs (700-900 g) or Sprague-Dawley rats were anaesthetised with ether and the lungs perfused *in situ* with heparinised salined to remove trapped erythrocytes. Lung tissue was then removed from the animals, washed twice in ice-cold saline and homogenized in 0.25M sucrose in 10 mM Tris HCl (containing 0.5% (w/v)BSA and 0.5mM PMSF pH 7.4 at 22°C) using a Brinkman Polytron PT-10 (setting 7, 1 min). Samples were centrifuged at 30,000 g for 10 min and the pellets washed twice with 10 volumes of 0.25M sucrose-buffered medium before suspension in an equal volume of the same buffer. This crude lung homogenate (H) was filtered through double-layered guaze cloth and then centrifuged at 900 g for 10 min to remove residual tissue fragments, unbroken cells, nuclei, and large cellular debris (this fraction is designated P1). The supernatant from this initial centrifugation (S1) was sequentially centrifuged at 6000, 9000 and 20,000 g, each for 10 min (supernatants from which are designated S2, S3 and S4, respectively). $MgCl_2$ was added to the final supernatant (S4) to a 1 mM concentration in order to

enhance binding of ribosomes to smooth endoplasmic reticulum, thereby allowing their separation from plasma membranes by subsequent sucrose density gradient centrifugation (Nijjar and Ho, 1980). 8 ml of $MgCl_2$ - supplemented S4 supernatant was applied to the top of a discontinuous sucrose gradient made by layering from bottom to top with 5 ml of 50% (W/V), 10 ml of 15% (W/V) and 10 ml of 7.5% (W/V) sucrose solutions. The gradient tube was centrifuged at 35,000g for 1 h in a SW 25.1 Beckman ultracentrifuge swing-out rotor. Four distinct fractions in the sucrose gradient (Fig. 5.1) were identified and carefully removed. Each of the four fractions was subsequently diluted 1:1 with 0.1M Tris-HCl and subjected to centrifugation at 40,000g for 2 h. In initial experiments, all fractions were saved and assayed for protein, the plasma membrane marker 5′-nucleotidase assay and [^{3}H]NBMPR binding. For preparative purposes, only B1 and F2 were collected. These two fractions were pooled and diluted 1:1 with 0.1M Tris-HCl (pH 7.4) and centrifuged at 40,000g for 2 h. The supernatant was discarded and the pellet (which contained lung purified plasma membranes (PMF)) resuspended in 50mM Tris-HCl(pH 7.4 at 22^{o}C) and stored at -70^{o}C for up to 2 weeks. The purity of this PMF preparation was assessed by measurements of its 5′-nucleotidase and specific NBMPR binding activities. The protein content of fractions was determined by the method of Lowry et al, (1951) with BSA as standard.

Figure 5.1 Outline of isolation procedure for the preparation of lung plasma membranes

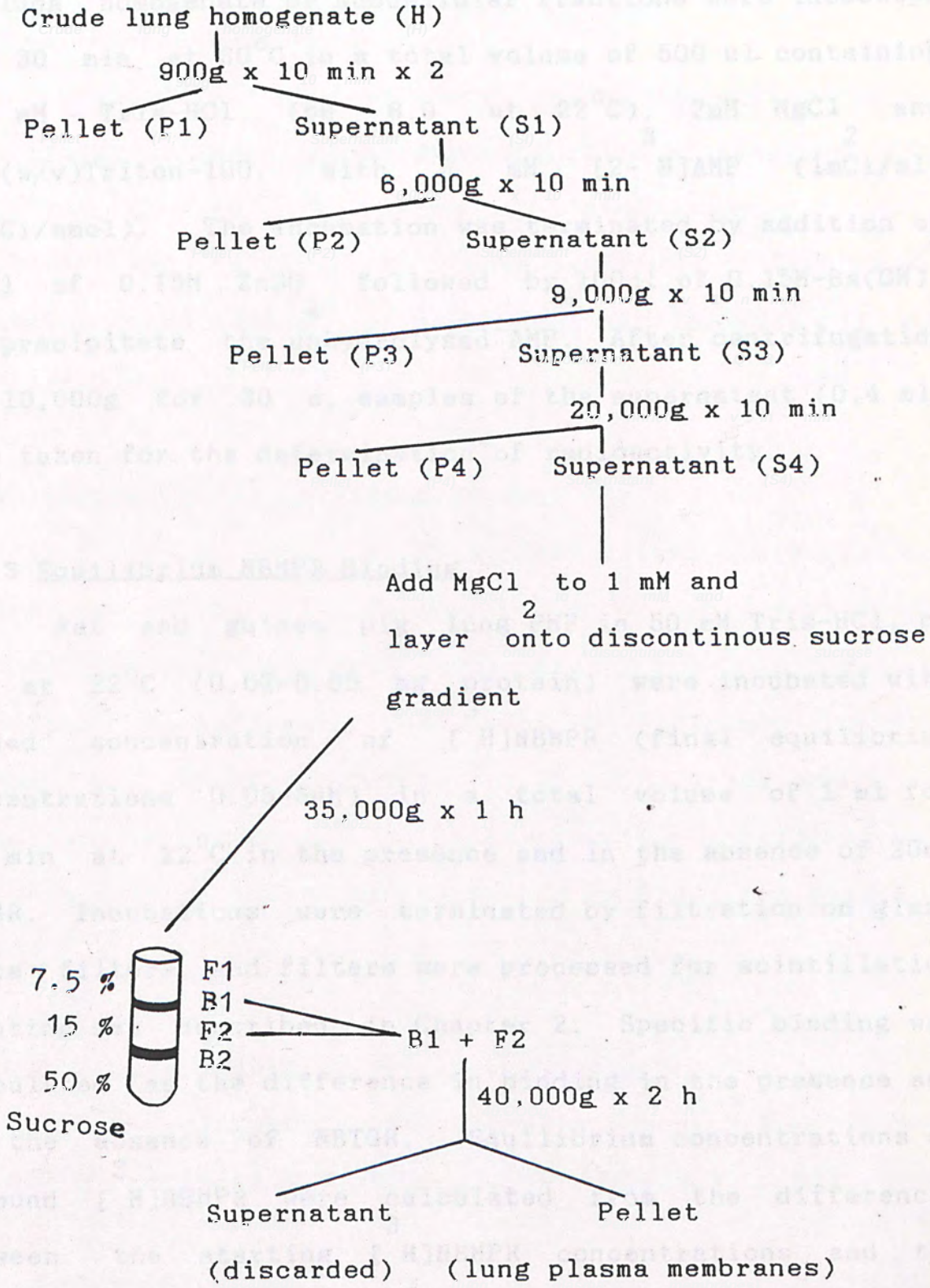

5.2.2 Plasma Membrane Enzyme Marker--5'-Nucleotidase Assay

The activity of 5'-nucleotidase (EC 3.1.3.5) was assayed as the release of [^{3}H]adenosine from [2-^{3}H]AMP as described by Belsham et al, (1980). Samples (10-20 ul) of lung homogenate or subcellular fractions were incubated for 30 min at 30^{0}C in a total volume of 500 ul containing 50 mM Tris-HCl (pH 8.0 at 22^{0}C), 2mM $MgCl_2$ and 0.1%(w/v)Triton-100, with 5 mM [2-^{3}H]AMP (1mCi/ml, 11.7Ci/mmol). The incubation was terminated by addition of 100ul of 0.15M $ZnSO_4$ followed by 100ul of 0.15M-$Ba(OH)_2$ to precipitate the unhydrolysed AMP. After centrifugation at 10,000g for 30 s, samples of the supernatant (0.4 ml) were taken for the determination of radioactivity.

5.2.3 Equilibrium NBMPR Binding

Rat and guinea pig lung PMF in 50 mM Tris-HCl, pH 7.4 at 22^{0}C (0.02-0.05 mg protein) were incubated with graded concentration of [^{3}H]NBMPR (final equilibrium concentrations 0.05-5nM) in a total volume of 1 ml for 30 min at 22^{0}C in the presence and in the absence of 20uM NBTGR. Incubations were terminated by filtration on glass fibre filters and filters were processed for scintillation counting as described in Chapter 2. Specific binding was calculated as the difference in binding in the presence and in the absence of NBTGR. Equilibrium concentrations of unbound [^{3}H]NBMPR were calculated from the differences between the starting [^{3}H]NBMPR concentrations and the

amounts of ligand bound to membranes and filters.

NBMPR binding capacities of fractions presented in Tables 5.1 and 5.2 were determined as the difference in [^{3}H]NBMPR binding at a saturating concentration (5 nM) of [^{3}H]NBMPR in the presence and in the absence of 20 uM NBTGR as described above.

In competition experiments, graded concentrations of each inhibitor were tested for inhibition of site-specific [^{3}H]NBMPR binding at 0.5nM [^{3}H]NBMPR concentration. Procedures were similar to those described in Chapter 2. Inhibitors were added to membranes at the same time as radioligand.

5.2.4 Photoaffinity Labelling of Lung PMF

Rat or guinea pig lung PMF (final concentration 0.5-1.0 mg protein/ml) in 50 mM Tris HCl (pH 7.4 at 22^{o}C) were equilibrated at room temperature for 30 min with a saturating concentration (25 nM) of [^{3}H]NBMPR in the presence and in the absence of 20 uM NBTGR as competing nonradioactive ligand. Photoaffinity labelling of membranes carried out as described in Chapter 4 (Section 4.2.2).

5.2.5 SDS-polyacrylamide gel electrophoresis

SDS-polyacrylamide gel electrophoresis was carried out in 2 mm thick 12% slab gels as described in Chapter 4 (Section 4.2.4).

5.2.6 Protein determination

Protein was determined by the method of Lowry *et al*, (1951).

5.3 RESULTS

5.3.1 Lung Purified Membrane Preparation

The protein content, 5′-nucleotidase activities and specific [^{3}H]NBMPR binding capacities of the subcellular fractions prepared from both rat and guinea pig lung by the scheme illustrated in Fig. 5.1 are listed in Tables 5.1 and 5.2. In both species, the PMF (B1P,F2P) fraction accounted for approximately 1% of the total homogenate protein and had the highest 5′-nucleotidase specific activity of all the fractions collected, the activity of this enzyme being 11.3 and 14.6 fold, respectively, greater than that in the corresponding lung homogenates (H) (Table 5.3). Similarly, the specific [^{3}H]NBMPR binding activity was 13.7 fold and 15.8 fold higher in the rat and guinea pig lung PMF fractions as compared to that in tissue homogenates from the two species (Table 5.3).

5.3.2 NBMPR Binding Parameters in Lung PMF

Fig 5.2 shows the concentration-dependence of [^{3}H]NBMPR binding to rat and guinea pig lung PMF, demonstrating the presence of both high-affinity saturable (NBTGR-sensitive) and non-saturable (NBTGR-insensitive) binding components in the two species. Specific binding saturated at about 2.5 nM [^{3}H]NBMPR. Scatchard analysis of the data revealed a single population of binding sites, with a Hill coefficient of 1.05 and 0.98 in the rat and

Table 5.1 Protein content, 5'-nucleotidase and NBMPR binding activities of rat lung fractions

Fractions	Protein		5'-nucleotidase		Specific NBMPR Binding	
	(mg/g starting lung)	Recovery (%)	Activity (unit/mg protein)	Recovery (%)	Activity (pmole/mg protein)	Recovery (%)
H	92.10±12.86	100.0	0.09±0.02	100.0	0.79±0.41	100.0
P1	19.50± 2.34	21.2	0.11±0.02	25.0	0.52±0.06	14.0
P2	8.20± 2.51	9.8	0.12±0.03	11.4	0.66±0.08	7.4
P3	8.30± 1.20	9.1	0.15±0.02	14.6	1.20±0.14	13.7
P4	9.81± 2.10	10.7	0.20±0.04	22.8	2.68±0.25	36.2
F1S	16.51± 3.25	18.0	0.08±0.01	15.4	0.31±0.02	7.0
F1P	0.33± 0.05	0.3	0.02±0.002	0.07	1.44±0.16	0.6
B1S	2.76± 0.25	3.0	0	0	0	0
F2S	2.70± 1.26	2.9	0	0	0	0
B2S	2.89± 1.51	3.1	0	0	0	0
B2P	0.67± 0.16	0.7	0.50±0.06	3.9	3.90±0.81	3.6
PMF	0.93± 0.24	1.0	1.02±0.18	11.1	10.80±2.02	13.8
Total Recovery (%)		79.8		104.3		96.3

Distribution of protein content, enzyme and NBMPR activities in subcellular fractions prepared from rat lung as described in Fig.5.1. Protein content is expressed in mg/g wet wt of starting lung tissue. 5'-Nucleotidase enzyme activity is expressed in units, where 1 unit represents the conversion of 1 umol of substrate (AMP) to products (Adenosine + phosphate) in 1 min at 30°C. Values are means (±SEM) of three separate preparations.

Table 5.2 Protein content, 5'-nucleotidase and NBMPR binding activities of guinea pig lung fractions

Fractions	Protein		5'-nucleotidase		Specific NBMPR Binding	
	(mg/g starting lung)	Recovery (%)	Activity (unit/mg protein)	Recovery (%)	Activity (pmole/mg protein)	Recovery (%)
H	86.67±11.50	100.0	0.09±0.02	100.0	3.05±0.53	100.0
P1	20.56± 3.92	23.7	0.09±0.02	22.9	6.79±1.50	52.6
P2	9.72± 3.11	11.2	0.06±0.01	7.1	1.12±0.31	4.1
P3	5.83± 2.40	6.7	0.22±0.03	15.6	3.55±0.52	7.8
P4	7.22± 1.65	8.3	0.28±0.03	24.5	2.94±0.47	8.0
F1S	23.04± 4.06	26.6	0.07±0.01	19.5	2.80±0.33	0.07
F1P	0.58± 0.06	0.6	0.41±0.08	2.9	1.58±0.32	0.35
B1S	2.88± 0.31	3.3	0.08±0.01	2.8	0	0
F2S	1.33± 0.55	1.5	0	0	0	0
B2S	0.98± 0.32	1.1	0.01±0.002	0.1	0	0
B2P	0.71± 0.13	0.8	0.58±0.08	5.0	15.60±2.24	4.2
PMF	0.62± 0.15	0.7	1.32±0.27	9.9	48.30±9.21	11.3
Total Recovery (%)		84.5		110.3		88.4

Distribution of protein content, enzyme and NBMPR binding activities in subcellular fractions prepared from guinea pig lung as described in Fig.5.1. Protein content is expressed in mg/g wet wt of starting lung tissue. 5'-Nucleotidase enzyme activity is expressed in units, where 1 unit represents the conversion of 1 umol of substrate (AMP) to products (Adenosine + phosphate) in 1 min at 30°C. Values are means (±SEM) of three separate preparations.

Table 5.3 5′-Nucleotidase and NBMPR binding activities in homogenate (H) and purified membrane fraction (PMF)

	5′-Nucleotidase Activity (unit/mg protein)		Specific NBMPR Binding (pmol/mg)	
	Rat	Guinea pig	Rat	Guinea pig
H	0.09±0.02	0.09±0.02	0.79±0.41	3.05±0.53
PMF	1.02±0.18	1.32±0.27	10.80±2.02	48.30±9.21
Ratio	11.3±3.1	14.6±4.3	13.7±7.3	15.8±3.8

Data extracted from Tables 5.1 and 5.2.

guinea pig lung PMF, respectively. PMF from the two species exhibited a similar dissociation constant (Kd) for [^{3}H]NBMPR binding but a significantly different number of binding sites (Bmax) (Table 5.4). The Kd values reported here of 0.2-0.3 nM in lung purified membranes from the two species compares favorably with their counterparts in crude membrane preparations as described in Chapter 2 (Kd of 0.22 nM and 0.38 nM in the rat and guinea pig lung crude membranes, respectively). Both species exhibited the same amount of non-specific (NBTGR-insensitive) [^{3}H]NBMPR binding to PMF (2 pmol/mg protein at 5 nM NBMPR).

5.3.3 Competition Experiments

High-affinity NBMPR binding activity in lung PMF was inhibited by mM concentrations of the physiological nucleosides, adenosine and uridine (Table 5.5). As expected, adenosine was the more effective inhibitor, consistent with the previous result obtained with lung crude membranes (see Chapter 2, Section 2.3.1).

The properties of NBMPR binding to rat and guinea pig lung PMF membranes were investigated further by studying the effects of dipyridamole and other vasodilators on high affinity binding activity in the two species. Fig. 5.4 shows representative curves for dypridamole inhibiton of NBMPR binding to lung PMF. Similar to the findings in lung crude membranes, a large difference was found to exist between the two species with respect to

Figure 5.2 Concentration dependence of NBMPR binding to rat and guinea pig lung purified membranes

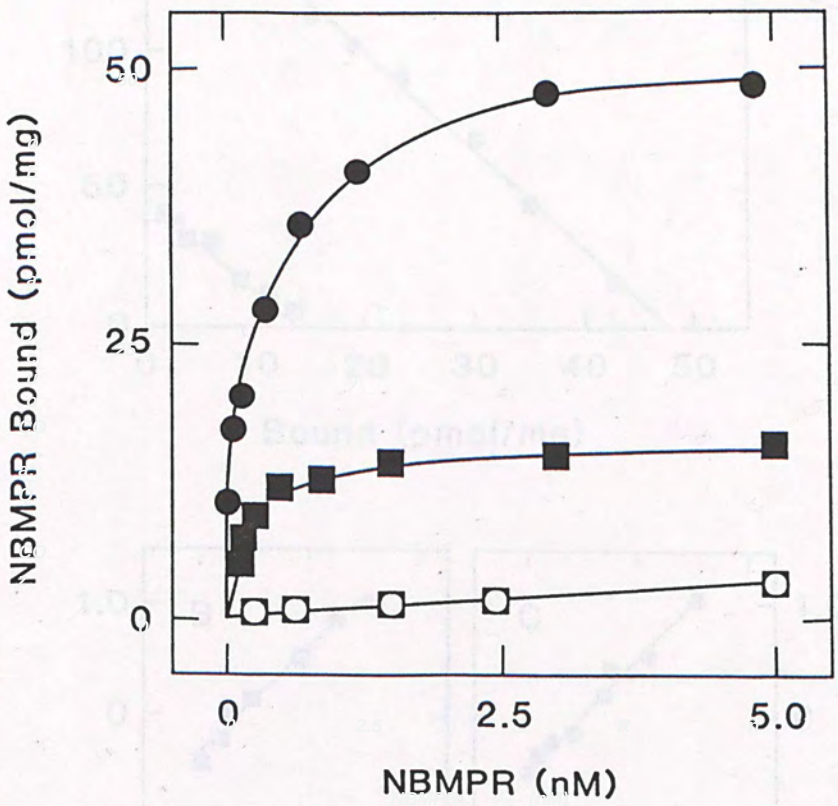

[^{3}H]NBMPR binding to rat (■ , □) and guinea pig (● , ○) lung purified membranes was measured in the absence (■ , ●) and in the presence (□ , ○) of 20 uM NBTGR as competing ligand. Values are means of duplicate estimates. Scatchard and Hill plots of these data are shown in Fig. 5.3.

Figure 5.3 Scatchard and Hill plots of site-specific NBMPR binding to rat and guinea pig lung purified membranes

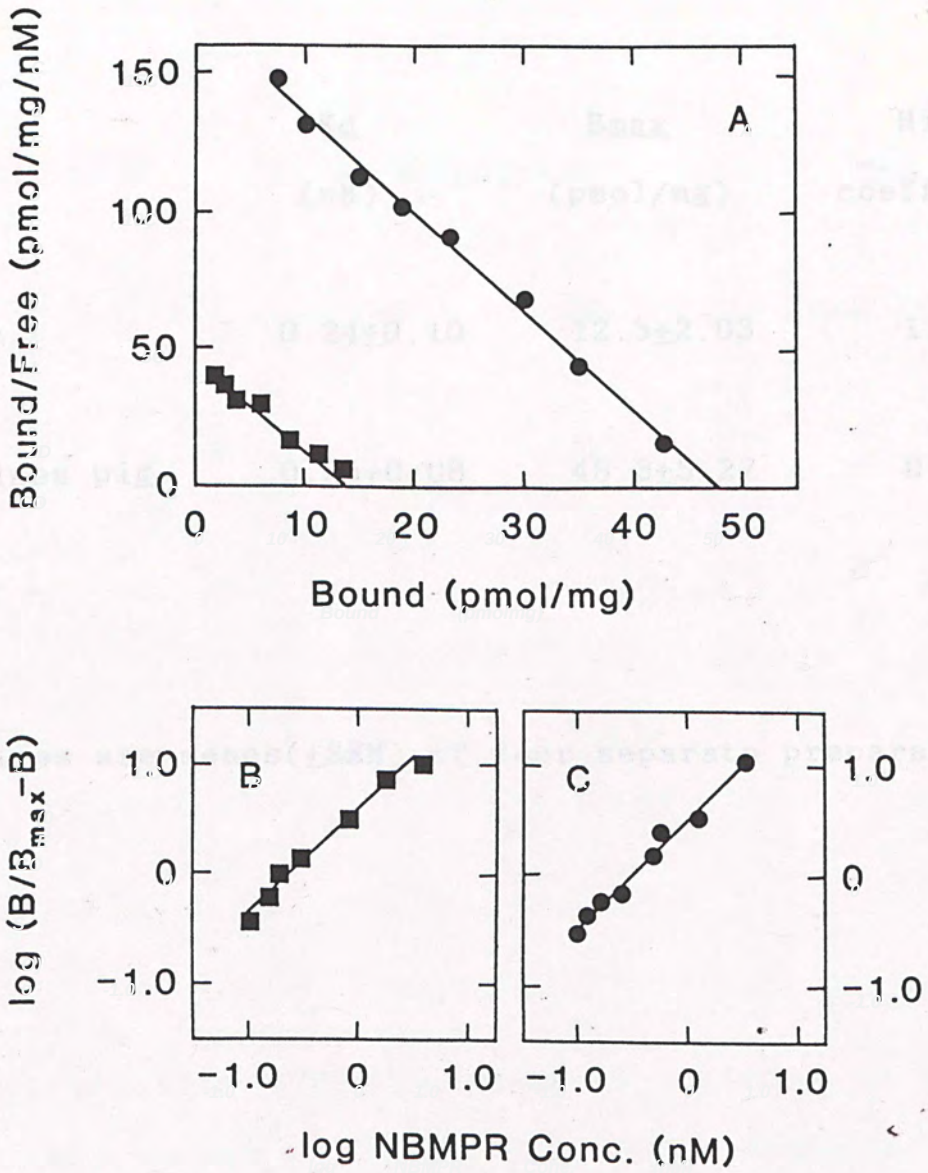

Scatchard (A) and Hill (B and C) plots of site specific binding of NBMPR to rat and guinea pig lung PMF. These plots were obtained using data for guinea pig (●) and rat (■) lung PMF presented in Fig. 5.2.

Table 5.4 Binding parameters of NBTGR-sensitive NBMPR binding to rat and guinea pig lung purified membranes (PMF)

	Kd (nM)	Bmax (pmol/mg)	Hill coefficient
Rat	0.24±0.10	12.5±2.03	1.05±0.15
Guinea pig	0.25±0.08	48.3±5.27	0.98±0.14

Values are means(±SEM) of four separate preparations.

Table 5.5 Inhibition of specific NBMPR binding to rat and guinea pig lung purified membranes by adenosine and uridine.

Inhibitor (M)		% Control	
		Rat lung PMF	guinea pig lung PMF
Adenosine	10^{-2}	10.9 ±1.7	15.3 ±2.5
	10^{-3}	51.1 ±0.6	55.8 ±4.0
	10^{-4}	83.3 ±0.5	88.5 ±0.4
Uridine	10^{-2}	53.4 ±3.5	54.2 ±1.4
	10^{-3}	82.1 ±0.1	84.9 ±2.4
	10^{-4}	87.8 ±1.2	96.2 ±2.3

Inhibition of specific NBMPR binding by adenosine and uridine was determined at 0.5nM [^{3}H]NBMPR as described in the text. Values are means(±SEM) of three experiments.

Figure 5.4 Dipyridamole inhibition of NBMPR binding to rat and guinea pig lung purified membranes

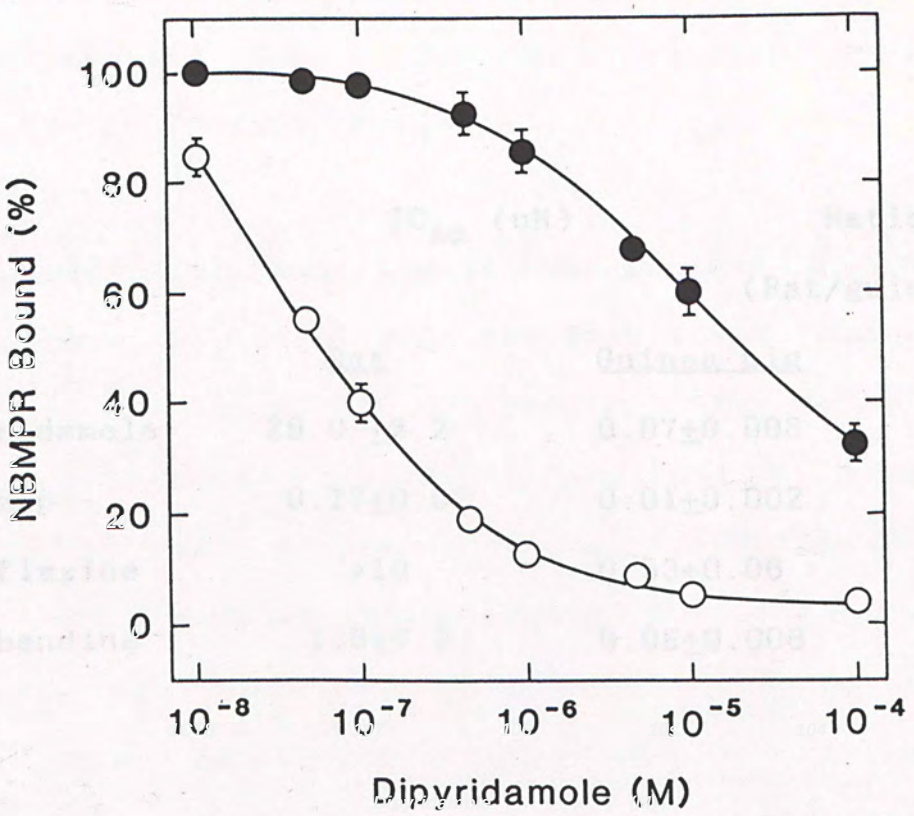

The effects of varying concentrations of dipyridamole on NBTGR-sensitive [^{3}H]NBMPR binding to guinea pig (○) and rat (●) lung purified membranes. Data are expressed as percentages of control values and are means(±SEM) of three separate experiments.

Table 5.6 IC_{50} of various vasodilators as inhibitor of NBMPR binding to rat and guinea pig lung purified membranes (PMF)

	IC_{50} (uM)		Ratio (Rat/guinea pig)
	Rat	Guinea pig	
Dipyridamole	29.0 ±3.2	0.07±0.008	414
Dilazep	0.17±0.02	0.01±0.002	17
Lidoflazine	>10	0.53±0.06	>19
Hexobendine	1.8±0.2	0.06±0.008	30

The IC_{50} for each drug was determined by testing eight to ten concentrations for inhibition of NBTGR-sensitive [^{3}H]NBMPR binding (0.5 nM). Values are means(±SEM) of three experiments.

dipyridamole sensitivity. Table 5.6 summarises the IC_{50} values of dipyridamole and the other vasodilators as inhibitors of [^{3}H]NBMPR binding to the PMF fraction in the two species. In all instances, guinea pig lung PMF was more sensitive to vasodilator inhibition than that of the rat. The largest difference was for dipyridamole, a difference of 414 fold. For the other vasodilators, the range was 17- to 30-fold (Table 5.6).

5.3.4 Photoaffinity Labelling of Lung Purified Membranes

Exposure of both rat and guinea pig lung purified membranes to UV light in the presence of [^{3}H]NBMPR under equilibrium binding conditions resulted in substantial radiolabelling of protein of Mr 45,000-66,000. In agreement with previous photoaffinity labelling experiments with lung crude membranes (Chapter 4), the radiolabelled peak of the nucleoside transporter in rat purified membranes migrated with a higher apparent molecular weight (apparent Mr 63,000) than the guinea pig nucleoside transporter (apparent Mr 55,000) (Fig. 5.5). Radiolabelling of PMF in both species was abolished when photolysis was performed in the presence of 20 uM NBTGR as competing nonradioactive ligand (Fig. 5.5).

Similar to findings reported in photoaffinity labelling experiments in lung crude membranes, dipyridamole (50 uM) reduced the radiolabelled peak much more effectively in the guinea pig lung purified membranes than

Figure 5.5 Photoaffinity labelling of rat and guinea pig lung purified membranes

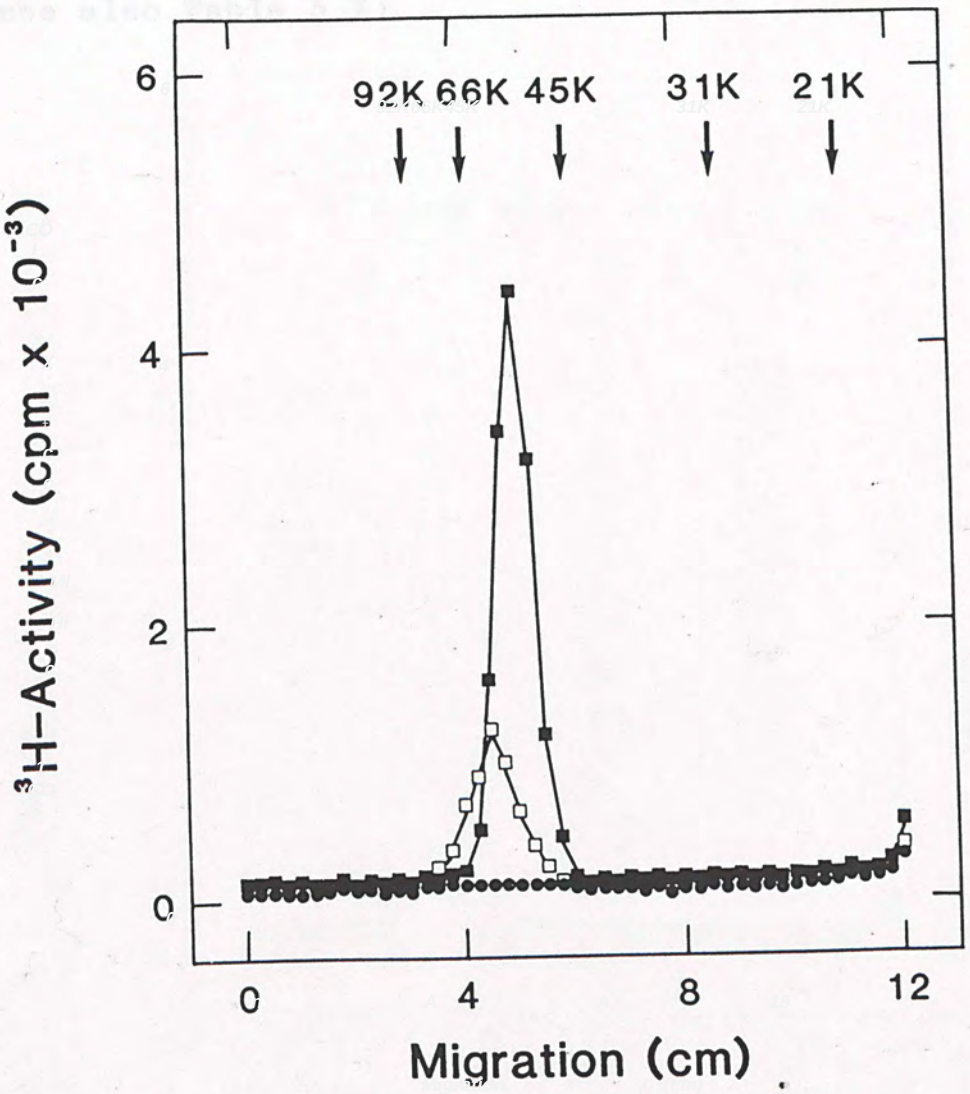

Lung purified membranes were photolabelled with [^{3}H]NBMPR and subjected to SDS-polyacrylamide gel electrophoresis as described in METHODS. ^{3}H-Profiles and positions of molecular weight standards are from the same slab gel. Lung purified membranes from rat (□) and guinea pig (■). Photolysis of membranes in the presence of 20 uM NBTGR (●) co-plotted in both species.

in the rat (Figs. 5.5 and 5.7, see also Table 5.7). Again, as expected, adenosine, inhibited radiolabelling of lung PMF in the two species to a similar extent (Figs. 5.6 and 5.7, see also Table 5.7).

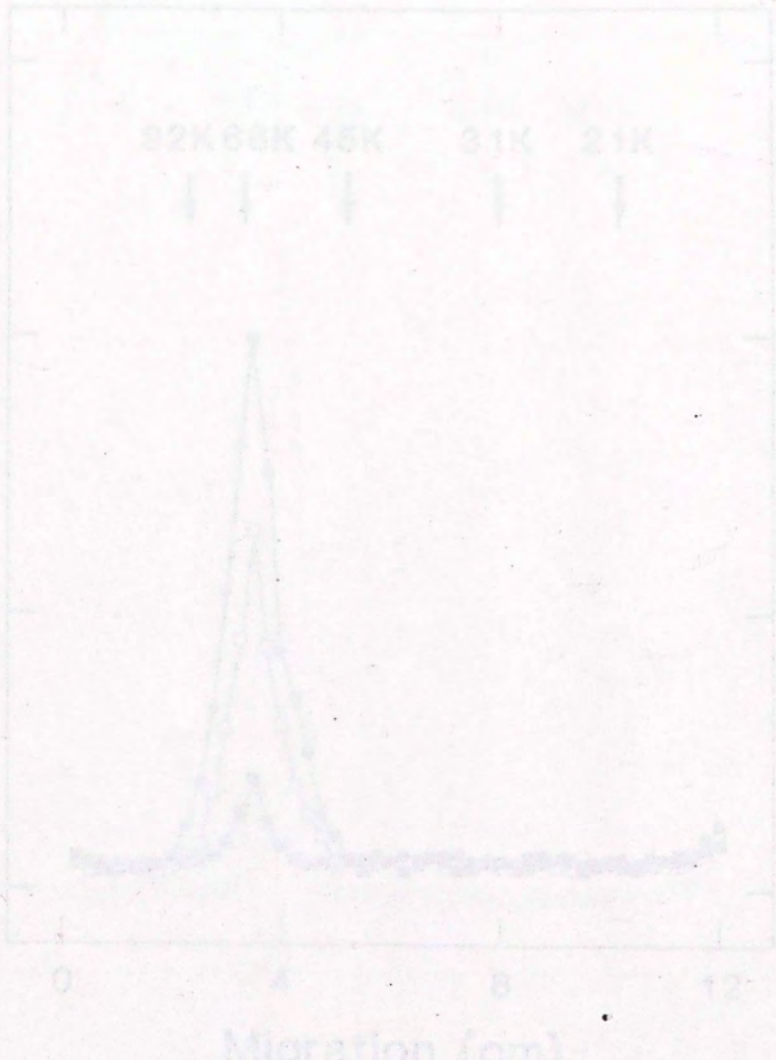

Figure 5.6 Effects of dipyridamole and adenosine on NBMPR photoaffinity labelling of rat lung purified membranes

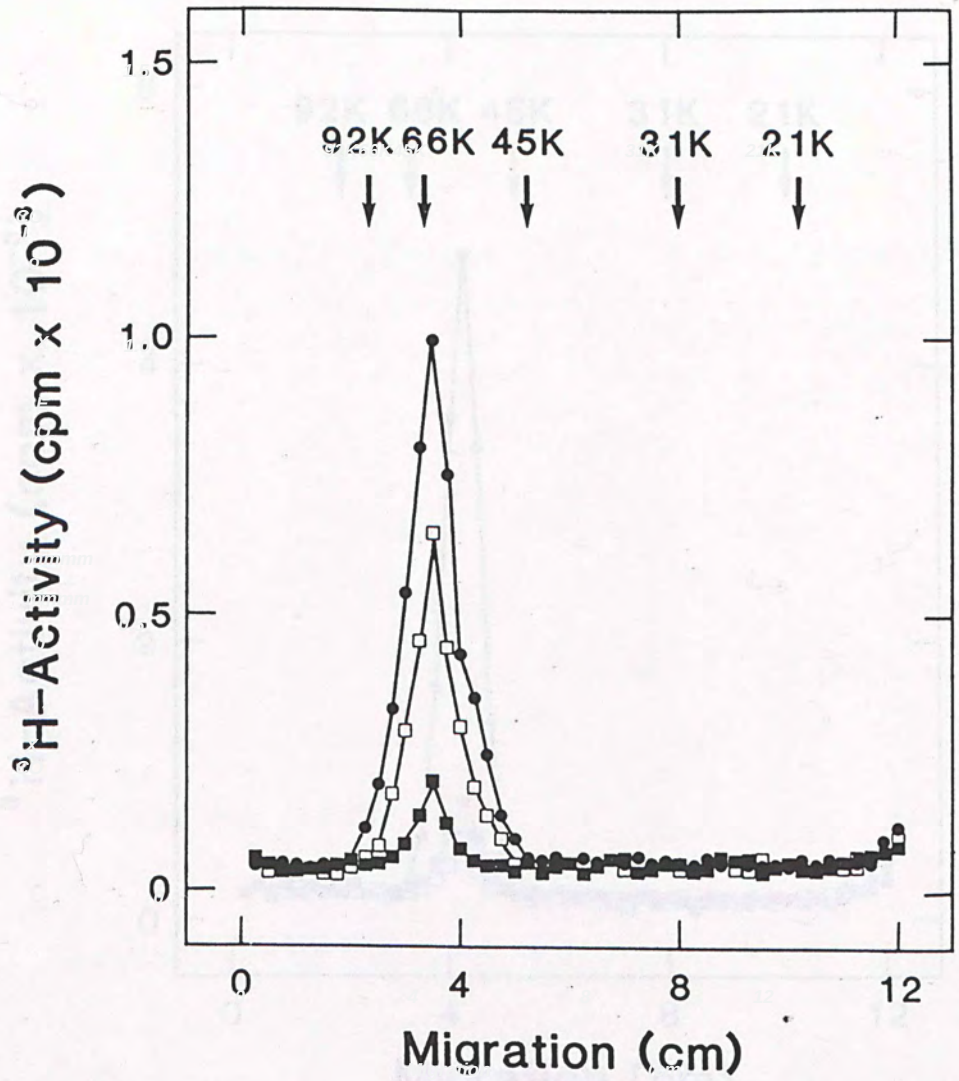

Rat lung PMF equilibrated with 25 nM [^{3}H]NBMPR in the absence (●) and in the presence of 50 uM dipyridamole (□) or 10 mM adenosine (■), were supplemented with 50 mM DTT and exposed to high intensity UV light at 4^{0}C for 45 s. SDS-polyacrylamide gel electrophoresis was performed as described in the text.

Figure 5.7 Effects of dipyridamole and adenosine on NBMPR photoaffinity labelling of guinea-pig lung purified membranes

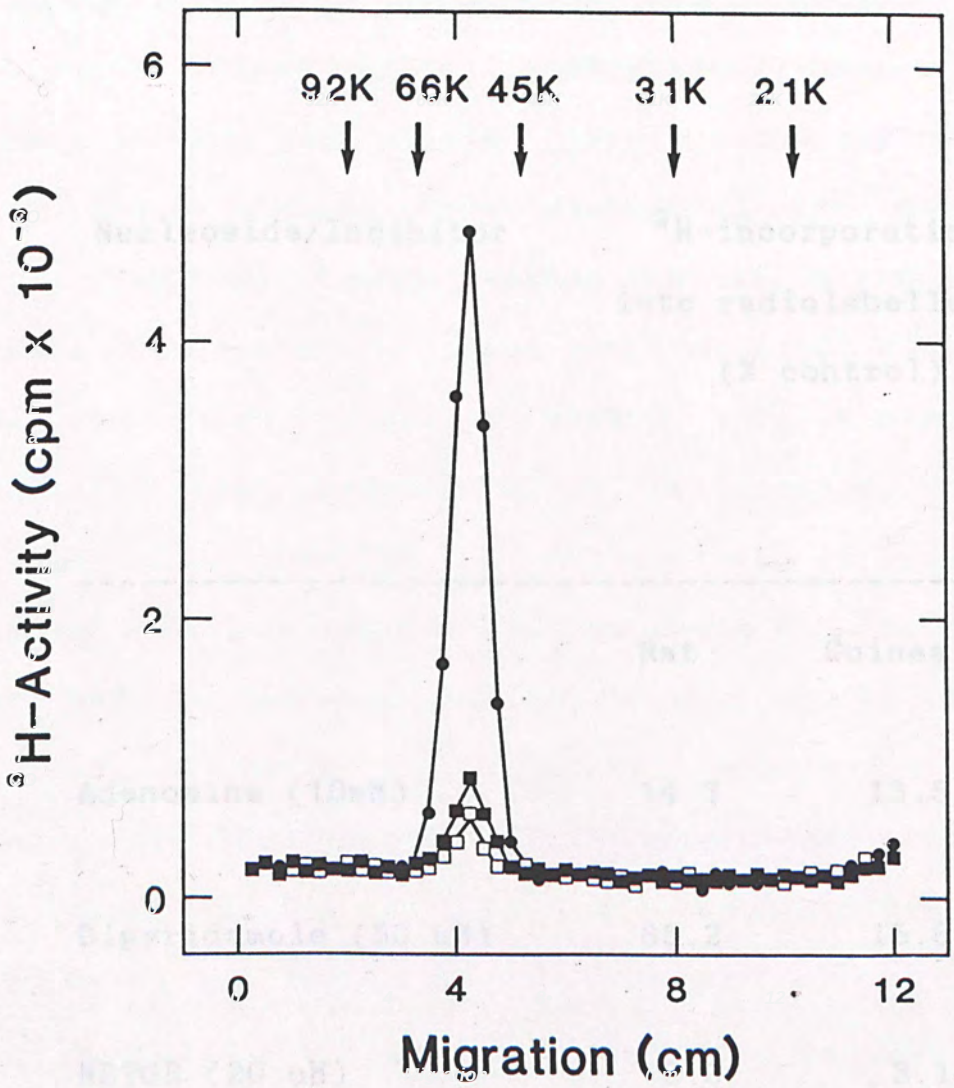

Guinea pig lung PMF equilibrated with 25 nM [^{3}H]NBMPR in the absence (●) and in the presence of 50 uM dipyridamole (□) or 10 mM adenosine (■) were photolabelled as described in the text.

Table 5.7 Effect of adenosine, dipyridamole and NBTGR on covalent NBMPR incorporation into protein of apparent Mr 45,000-66,000 in lung purified membranes (PMF)

Nucleoside/Inhibitor	^{3}H-incorporation into radiolabelled peak (% control)	
	Rat	Guinea pig
Adenosine (10mM)	14.3	13.5
Dipyridamole (50 uM)	65.2	15.8
NBTGR (20 uM)	3.0	3.1

Data are taken from Figs. 5.5-5.7.

5.4 DISCUSSION

In this Chapter, a method of isolating purified plasma membranes from rat and guinea pig lung tissue are described. Lung is composed of many cell types (e.g. smooth muscle cells, endothelial cells, epithelial cells, fibroblasts, Clara cells, macrophages, mast cells and leukocytes) and is always fibrous, thereby preventing gentle homogenization from disrupting the majority of cells. Vigorous homogenization results in the generation of small fragments of plasma membrane which will sediment at different centrifugation speeds. This may, in part, account for the presence of 5'-nucleotidase activity in fractions other than PMF. 5'-Nucleotidase is often used as a plasma membrane marker enzyme (Song and Bodansky, 1967; Nijjar and Ho, 1980; Jain, 1980). Although it is doubtful that 5'-nucleotidase is exclusively present in the plasma membrane, it is reported to be considerably enriched in plasma membrane fractions isolated from different sources (Kidwai et al, 1971).

In both species, the highest values for both 5'-nucleotidase activity and specific NBMPR binding activity were in the PMF fractions, the two activities co-purifying during the isolation procedure (5'-nucleotidase activity of 11- and 15-fold, and specific NBMPR binding activity of 14- and 16-fold higher in the rat and guinea pig lung PMF, respectively, compared to the corresponding tissue homogenates) (Table 5.3). In the

guinea pig, specific NBMPR binding in the lung PMF was only 2.5-fold higher than in the crude membrane preparation used in previous Chapters (48 and 19 pmol/mg protein in PMF and crude membranes, respectively) (Tables 5.4 and 2.1). As described in Chapter 6, this increase in specific binding activity of guinea pig lung PMF proved to be of crucial importance for the successful reconstitution of the lung nucleoside transporter into proteoliposomes. In the rat, the specific NBMPR activity of the PMF fraction was 1.5 fold better than that of the crude membrane preparation (12.5 and 8.1 pmol/mg protein in PMF and the crude membrane preparation, respectively) (Tables 5.4 and 2.1). The reasons why the isolation procedures worked better for guinea pig than rat are not clear.

Liver plasma membranes purified by Percoll density gradients (Wu and Young, 1984) also exhibited a 10-15-fold higher NBMPR-binding activity than the corresponding tissue homogenate, and the recovery of high-affinity NBMPR binding activity in the plasma-membrane fraction was broadly similar to that obtained with the plasma-membrane marker 5'-nucleotidase. These results from lung and liver are consistent with a role of NBMPR-binding proteins in cellular nucleoside transport. The fact that NBMPR binding activity co-purified with the plasma membrane marker 5'-nucleotidase activity indicates that the NBMPR binding protein is localised entirely or largely in the plasma membrane. This is in contrast to the situation for glucose

transporters in insulin-responsive cells where the intracellular membrane pool of transport protein associated with the microsomal membranes (Cushman and Wardzala, 1979). Recruitment of these inactive transporters into plasma membrane accounts for the stimulation of cellular glucose transport by insulin.

Similar to findings in lung crude membranes (Chapter 2), high-affinity NBMPR binding to lung PMF membranes was inhibited by mM concentrations of the physiological nucleosides, adenosine and uridine. As in Chapter 2, there was again a major species difference in vasodilator sensitivity with respect to inhibition of NBMPR binding.

Photoaffinity labelling patterns of lung purified membranes from the rat and guinea pig as presented in this Chapter also resemble those observed in crude membrane preparations (Chapter 4). In both rat and guinea pig lung purified membranes, substantial radiolabelling was observed in proteins of Mr 45,000-66,000 and photoaffinity labelling in both species was inhibited by adenosine and NBTGR. Dipyridamole inhibition of covalent labelling was more effective in guinea pig lung PMF than in the rat. Taken together, these observations provide additional evidence that lung NBMPR binding activity reflects a specific association of ligand with NBMPR-sensitive nucleoside transporters.

CHAPTER 6

RECONSTITUTION STUDIES OF THE NUCLEOSIDE TRANSPORTER FROM GUINEA PIG LUNG PURIFIED PLASMA MEMBRANES

6.1 INTRODUCTION

In Chapters 2 to 4, I have presented a detailed investigation of the NBMPR-sensitive nucleoside transporters present in guinea pig and rat lung plasma membranes using NBMPR as a specific ligand to probe transporter structure and (indirectly) function. It is therefore of utmost importance to establish that NBMPR binding activities demonstrated in isolated membrane preparations do indeed reflect ligand binding to elements of functional nucleoside transporters. Physiologically, lung is a major site for the removal of circulating adenosine, a potent endogenous vasodilator (Berne et al, 1983; Bakhle and Chelliah, 1983; Hellewell and Pearson, 1983). Despite its physiological and clinical importance, the transport properties of lung nucleoside transporters are poorly characterized. Transport experiments to date have been largely limited to whole tissue perfusion where detailed kinetic studies are impossible. The experiments of Hellewell and Pearson (1983) demonstrated that adenosine was efficiently taken up from the pig pulmonary vascular bed and that the process was inhibited by dipyridamole. In another approach, pig aortic endothelial cells in culture have been shown to take up adenosine very rapidly by a high-affinity process that is selectively inhibited by dipyridamole and NBMPR. These observations have led to the conclusion that the pulmonary endothelium possesses a high-affinity transport system for adenosine

removal (Pearson et al, 1978). However, the endothelial cell uptake studies can be criticised because of a failure to determine true initial rates of transport. Nucleoside uptake in these experiments therefore reflects both membrane transport and subsequent intracellular nucleoside metabolism. It is also unclear to what extent aortic endothelial cells resemble those in the lung. Direct isolation of lung endothelial cells is technically difficult (Jain, 1980).

As detailed in the General Introduction to this Thesis, NBMPR has been shown to interact specifically with functional elements of the erythrocyte nucleoside transporter and reversible ligand binding has been used as a specific quantitative assay for transporter polypeptide(s) (Jarvis and Young, 1982; Young and Jarvis, 1983). Photolysis experiments with [^{3}H]NBMPR have identified a membrane glycoprotein component of Mr 45,000-65,000 to be the nucleoside transporter in erythrocytes. Moreover, a partially purified band 4.5 preparation of human erythrocyte membranes has been shown to be capable of catalysing NBTGR-sensitive uridine transport when reconstituted into phospholipid vesicles. In these reconstitution experiments, NBMPR-binding activity co-purified with the nucleoside transport activity during preparation of the band 4.5 fraction from the initial Triton X-100 membrane extract (Tse et al, 1985). Similarly, partially purified band 4.5 polypeptides from pig

erythrocytes have been shown to demonstrate NBTGR-sensitive uridine transport activity when reconstituted into phospholipid vesicles (Kwong et al, 1987).

Given the potential problems and limitations encountered in whole organ perfusion studies and the difficulty in obtaining intact cells directly from lung, my approach towards characterizing nucleoside transport activity in lung tissue was to attempt reconstitution of the lung nucleoside transporter after detergent extraction of the purified lung plasma membrane preparation detailed in Chapter 5.

In the series of experiments described in this Chapter, n-octylglucoside was used to solubilise the nucleoside transporter from guinea pig lung plasma membranes. Guinea pig lung purified membrane preparations rather than those of the rat were used because of their higher density of NBMPR binding sites as described in Chapter 5. After removal of detergent, membrane proteins were reconstituted into proteoliposomes and the kinetic properties of carrier-mediated nucleoside transport characterised in detail. As far as I am aware, these experiments represent the first successful attempt to reconstitute a nucleoside transporter from a non-erythroid cell type or tissue.

6.2 METHODS

6.2.1 Tissue and Plasma Membrane Preparation

Purified plasma membranes from guinea-pig lung were prepared as detailed in Chapter 5 (Section 5.2.1).

6.2.2 Solubilisation of Lung Plasma Membranes

Lung plasma membranes at a final protein concentration of 1.5 mg/ml were solubilised at 4°C by suspension in 46 mM n-octylglucoside, 2 mM dithiothreitol and 50 mM Tris-HCl (pH 7.4 at 4°C) with stirring for 30 min. n-Octylglucoside was used in preference to Triton X-100 (Jarvis and Young, 1983) because it can be readily removed by dialysis. The membrane/detergent suspension was then centrifuged at 130,000g for 1 h and the supernatant retained. Detergent was removed by dialysis against four changes, each of 2 l, of 10 mM Tris-HCl, 0.2 mM DTT (pH 7.4 at 4°C) over a period of 24 h. DTT was included to maintain membrane thiol groups in the reduced state. It has previously been established that -SH groups are essential for NBMPR binding and uridine transport activity (see eg. Tse and Young, 1985). The solubilised crude lung membrane extract was stored at -70°C.

6.2.3 NBMPR Binding Measurements

6.2.3a Filtration method

High-affinity binding of NBMPR to guinea-pig lung membranes was determined by the filtration assay described in Chapter 2.

6.2.3b Centrifugal gel filtration method

High-affinity binding of NBMPR to solubilised lung membrane extract was measured by centrifugal gel filtration (Penefsky, 1977; Fry et al,1978). Briefly, columns of Sephedex G-50 (fine), which had been pre-equilibrated with 10 mM Tris-HCl (pH 7.4 at 4^{o}C), were prepared in 1 ml (tuberculin) syringes. The columns were centrifuged at 1000g for 2 min in a swinging bucket rotor of a bench centrifuge shortly before use. The prepared columns were kept on ice. Typically, solubilised lung extract in 10 mM Tris-HCl was diluted 3-fold in the same buffer and incubated at room temperature (±20 uM NBTGR) for 30 min with graded concentrations of [^{3}H]NBMPR (final equilibrium concentrations 0.25-45 nM) at a final protein concentration in the region of 0.13 mg/ml. After incubation, samples were cooled on ice for 10 min to minimise subsequent dissociation of bound ligand from the transporter. A 75 ul sample of the reaction mixture was then applied to a centrifuged column. After the sample had entered the Sephedex, the syringe column was recentrifuged as described above and the eluate collected directly into a scintillation minivial in the centrifuge bucket. Control experiments established that protein recovered in the

eluate is >85%. High-affinity NBMPR binding activity was defined as the difference in binding activity measured in the presence and in the absence of 10 uM NBTGR.

6.2.4 Reconstitution of the Solubilised Lung Membrane Extract

6.2.4a Preparation of washed asolectin

Crude asolectin (required for liposome preparation described in the next section) was washed according to Kagawa and Racker (1971). Briefly, 25 g of crude asolectin was mixed with 250 ml acetone in a brown glass bottle with a magnetic stirring bar. The contents of the bottle were bubbled vigourously with N_2 for 15 min while stirring. The bottle was then capped and stirring continued overnight. The extracted lipid was collected by centrifugation and the pellet dissolved in 100 ml anhydrous diethyl ether. This material was again centrifuged and the supernatant evaporated to dryness in a rotatory evaporator. The residue was dissolved in 100 ml chloroform : methanol (4:1) to give a concentration of 100-200 umoles phospholipid/ml. This final washed asolectin preparation was centrifuged if necessary and stored at -20^{o}C under N_2.

6.2.4b Preparation of liposomes

Acetone-washed asolectin (40 umol in

chloroform/methanol) was placed in a 13 X 10 mm pyrex tube and dried under a stream of nitrogen. The dried asolectin was re-dissolved in 0.5 ml diethyl ether and dried again under N_2 to remove traces of chloroform and methanol. After all the organic solvents had been evaporated, the pellet was suspended in 0.5 ml 10 mM Tris-HCl (pH 7.4 at 4`C). The tube was covered by parafilm and sonicated to clarity (10 min at 20-30`C) in a bath type sonicator (G112-SP1, Laboratory Supply Company Inc., Hicksville, NY) containing 0.02 % (w/v) Triton X-100 in distilled water (Kasahara and Hinkle, 1977).

6.2.4c Reconstitution of the lung nucleoside transporter

Solubilised lung extract was reconstituted into phospholipid vesicles using the method described previously by Kasahara and Hinkle (1977) for reconstitution of the human erythrocyte glucose transporter as modified by Tse et al (1985). Solubilised lung membrane extract (0.2 mg protein) was added to sonicated vesicles (10 umol, see Section 6.2.4b) in a final volume of 0.4 ml. The phospholipid:protein ratio (umol/mg) was typically kept in the range 50-80 : 1. The mixture was rapidly frozen in dry ice/ethanol, slowly thawed at room temperature and then sonicated briefly (5 s). These reconstituted proteo-liposomes were used for uridine uptake studies.

6.2.5 Transport Measurements in Reconstituted Proteo-Liposomes

Zero-*trans* influx and equilibrium exchange influx of uridine were measured at 25`C. Uptake (defined as the appearance of nucleoside in the intravesicular space) of [^{14}C]uridine by liposomes and reconstituted vesicles was measured by a centrifugal gel filtration method essentially identical to that described in Section 7.2.3b (Penefsky, 1977; Fry *et al*, 1978; Baldwin *et al*, 1981). Briefly, columns of Sephedex G-50 (fine), which had been pre-equilibrated with 20 uM NBTGR, 10 mM Tris-HCl (pH 7.4 at 22`C), were poured to the 1 ml mark in disposable 1 ml (tuberculin) syringes. The columns were centrifuged at 1000g for 2 min in the swinging bucket rotor of a bench centrifuge shortly before use. The prepared columns were kept on ice. Uptake was measured at 25`C. All other procedures were carried out at 4`C in a cold room. Zero-*trans* influx incubations were initiated by adding 45 ul of reconstituted vesicles (± 20 uM NBTGR) to 45 ul of [^{14}C] uridine (2 uCi/ml, final concentration of 50 uM) in the same 10 mM Tris-HCl buffer. Uptake at different time intervals was terminated by rapid addition of 20 ul of an ice-cold stopping solution containing 20 uM NBTGR in Tris buffer, and a 75 ul sample of the reaction mixture was immediately applied to a centrifuged column. After the sample had entered the gel, 20 ul of stopping solution was added to the syringe column which was then recentrifuged as

described above, and the eluate collected directly into a scintillation minivial in the centrifuge bucket. Radioactivity present in the eluate was measured by liquid scintillation spectrometry with appropiate quench and background correction. Blank values for uptake assays were determined by centrifugal gel column processing of samples taken immediately after mixing ice-cold NBTGR-treated vesicles and ice-cold [^{14}C] uridine. These blanks were subtracted from measurements of uridine uptake by reconstituted vesicles. Apparent initial rates of uridine uptake from graded concentrations of [^{14}C]uridine (0.05-2 mM) were measured following a 20 s incubation in the presence and in the absence of 20 uM NBTGR.

For equilibrium exchange influx, reconstituted vesicles were 'loaded' with non-radioactive uridine (0.05-15 mM) by incubation with uridine-containing Tris buffer for 2 h at 25^{o}C by which time equilibration between intravesicular and extravesicular uridine had occured (Tse et al, 1985). To initiate equilibrim exchange influx, 45 ul of 'loaded' reconstituted vesicles were mixed with an equal volume of prewarmed 10 mM Tris buffer containing the same concentration of radioactive [^{14}C]uridine (2 uCi/ml). Uptake (20 s incubation for initial rate measurements) was terminated by rapid addition of 20 ul ice-cold stopping solution containing 20 uM NBTGR in Tris buffer. A 75 ul sample of the reaction mixture was immediately applied to centrifuged Sephadex 1 ml column and

processed as described above for zero-*trans* influx.

6.2.6 Phospholipid Assay

The phospholipid content of washed asolectin was measured by phosphate analysis. The washed asolectin was diluted 10-fold with chloroform : methanol (4:1). 0.05-0.2 ml diluted asolectin was then placed in the bottom of 18 x 150 mm pyrex test tube and 0.2 ml of $Mg(NO_3)_2$ (10% (w/v) in ethanol) was added. Using a wire test tube holder, the tube was heated over a bunsen burner with rapid mixing to prevent 'bumping'. Heating was continued until brown gas was no longer released and the sample was white.

The sample was cooled and 0.5 ml 1N HCl was added. The tube was covered with a glass marble and heated in a boiling water bath for 20 min. The sample was cooled again and 10 ml of color reagent (90 ml water/10 ml ammonium molybydate solution (10% (w/v in 10 ml H_2SO_4)/5 g $FeSO_4.7H_2O$) was added. For standards, 0.2-2 umoles inorganic phosphate were added to 0.5 ml 1N HCl followed by 10 ml of color reagent. The tubes were allowed to stand for 20 min at room temperature before reading the absorbance at 660 nm.

6.2.7 Protein Determination

Protein was determined by the method of Lowry *et al*,(1951).

6.3 RESULTS

6.3.1 Solubilisation of Purified Lung Membranes

Kwong et al (1986) have established that n-octyl-glucoside is the preferred detergent compared with Triton X-100 for extraction of high-affinity NBMPR binding component(s) from human and pig erythrocyte 'ghosts'. The same detergent was used in the present study to solubilise lung membranes.

In contrast to erythrocyte membranes (Kwong et al, 1986), solubilisation of purified lung plasma membranes with n-octylglucoside did not lead to an increase in the specific activity of NBMPR binding i.e. there was no selective solubilisation of the nucleoside transporter under the condition used. Thus, extraction of lung plasma membrane protein by n-octylglucoside (46 mM) resulted in solubilisation of 70-80 % of the total plasma membrane protein and a similar percentage of NBMPR binding activity (Table 6.1). As expected, the remainder of the protein and NBMPR binding activity was recovered in the insoluble n-octylglucoside residue. The average specific activity of reversible high-affinity NBMPR binding to crude lung membrane extracts, measured after detergent removal, was 35±4 pmol/mg protein (mean of 4 experiments), a value similar to that of the starting plasma membranes. NBMPR binding was abolished in the presence of detergent but was quantitatively recovered following detergent removal by

Table 6.1 Solubilisation of NBMPR-binding activity from guinea-pig lung plasma membranes

	Total protein (mg)	Total NBMPR bound (pmol)	Specific NBMPR binding activity (pmol/mg protein)
Guinea-pig lung plasma membranes	9.11±2.02	348±45	38±4
Solubilised membrane extract	7.21±1.13	247±33	35±4
% Solubilised	79.1±13	71±10	

Lung plasma membranes were solubilised with 46 mM n-octylglucoside, 50 mM Tris-HCl (pH 7.4 at 4^{0}C) and 2 mM dithiothreitol. The 130,000g supernatant was then dialysed free of detergent and assayed for protein and high-affinity NBMPR-binding activity (at a saturating concentration of radioactive ligand, 25 nM) as described in the text. Values are means (±SEM) of four separate experiments.

dialysis (<1 and 35 pmol/mg of protein before and after detergent removal).

6.3.2. Characterization of the Solubilised Lung Membrane Extract

Fig. 6.1 shows concentration-dependence curves of [^{3}H]NBMPR binding to solubilised lung membrane extract measured at equilibrium (30 min incubation) in the presence and in the absence of 20 uM NBTGR. Binding activity is plotted against the calculated free concentrations of unbound ligand in the medium. [^{3}H]NBMPR binding to membrane extract was NBTGR-sensitive and saturable with an apparent Kd of 1.1 nM as determined by Scatchard analysis. This affinity constant compares favourably with an apparent Kd of 0.2 nM for [^{3}H]NBMPR binding to guinea-pig lung purified membranes described previously (Chapter 4, Section 4.3.2a). The Bmax value for NBTGR-sensitive [^{3}H]NBMPR binding in the experiment shown in Fig. 6.1 was 33 pmol/mg protein.

Table 6.2 demonstrates that high-affinity NBMPR binding activity in solubilised lung membrane extracts was inhibited by the physiological nucleosides adenosine and uridine. As expected, adenosine was more effective than uridine (IC_{50} 2 and 8 mM respectively, 5 nM [^{3}H]NBMPR), in agreement with their relative affinities for the nucleoside transporter in guinea lung membranes as described in Chapters 2 and 4 (IC_{50} of 0.8 and 7 mM,

Figure 6.1 Concentration dependence of NBMPR binding to solubilised extract from guinea pig lung purified plasma membranes

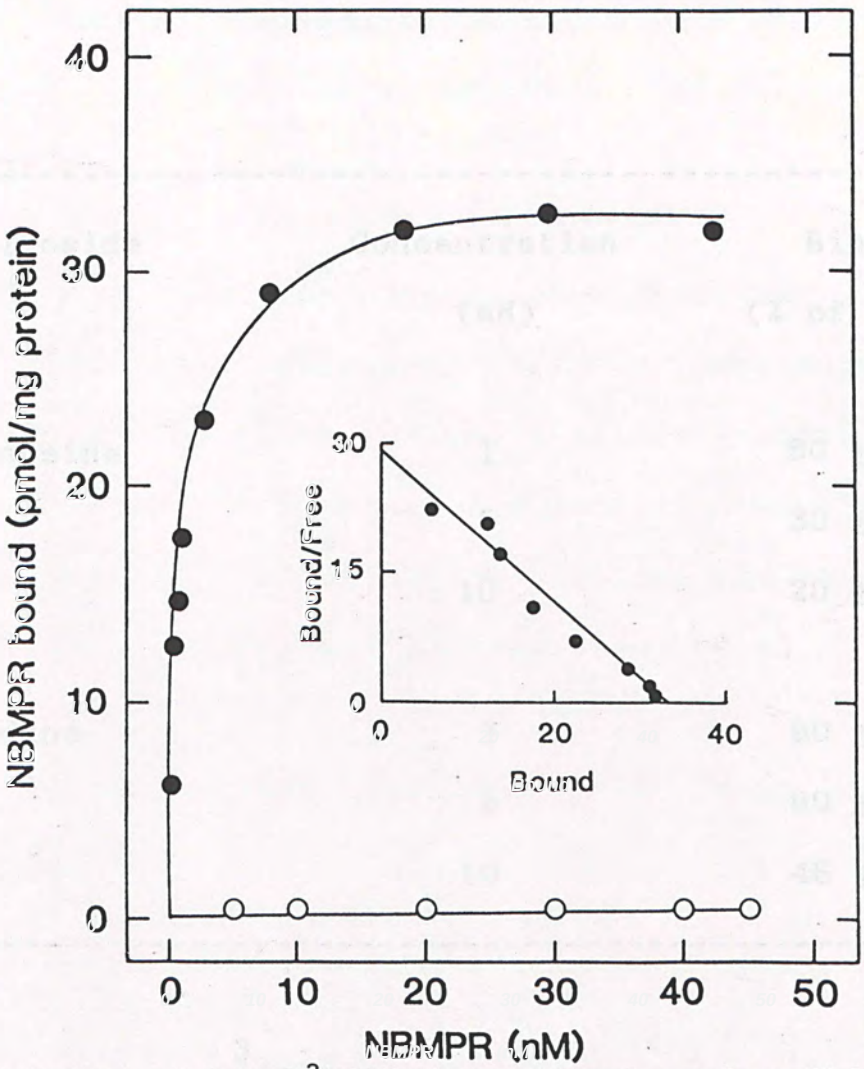

The amounts of [^{3}H]NBMPR bound reversibly to lung membrane extract were measured by centrifugal gel filtration in the presence (○) and in the absence of 20 uM NBTGR (●) and are plotted against the equilibrium concentrations of free NBMPR. The inset shows a Scatchard plot of the data (corrected for the NBTGR-insensitive component of binding). Maximum binding (33 pmol/mg protein) and apparent Kd (1.1 nM) were determined by linear regression analysis.

Table 6.2 Effects of nucleosides on high-affinity binding of NBMPR to solubilized guinea pig lung purified plasma membranes

Nucleoside	Concentration (mM)	Binding (% of Control)
Adenosine	1	60 ± 7
	5	30 ± 4
	10	20 ± 2
Uridine	1	90 ± 6
	5	60 ± 4
	10	46 ± 3

Binding of [^{3}H]NBMPR (initial concentration 5 nM) was measured at room temperature (30 min incubation) in the absence and in the presence of various concentrations of competing nucleoside (± 20 uM NBTGR to correct for non-specific binding). High-affinity binding activity in the absence of tested nucleosides was 15 pmol/mg of protein. Values are means±S.E. of triplicate estimates.

0.9 and 8.5 mM for adenosine and uridine in guinea pig lung crude and purified plasma membranes, respectively) as well as in a variety of other cell types (Young and Jarvis, 1983). The IC_{50} concentrations for lung membrane extract were used to determine apparent Ki values from the relationship

$$Ki = IC_{50} / [1 + ([L]/Kd)]$$

where [L] is the radioligand concentration and Kd its binding affinity. Calculated inhibitor constants (Ki) were 0.5 and 2 mM for adenosine and uridine, respectively. The calculated apparent Ki value for uridine compares well with its apparent Km (1.1 mM) of equilibrium exchange influx in reconstituted lung proteoliposomes (see below).

6.3.3 Reconstitution Studies of the Crude Lung Membrane Extract

6.3.3a Zero-trans Influx

Fig. 6.2 shows a representative time course of uridine uptake (50 uM, 25°C), measured in the presence and in the absence of 20 uM NBMPR. Uptake was inhibited by NBMPR. The NBMPR-sensitive component of transport exhibited a half-time for equilibration of approximately 50 s (Fig. 6.2 inset) while the NBMPR-insensitive component of uptake was linear with respect to time. Fig. 6.3 shows concentration dependence curves (± 20 uM NBMPR) for zero-trans uridine influx into vesicles reconstituted with

Figure 6.2 Time course of uridine uptake into vesicles reconstituted with n-octylglucoside solubilised guinea-pig purified lung plasma membranes

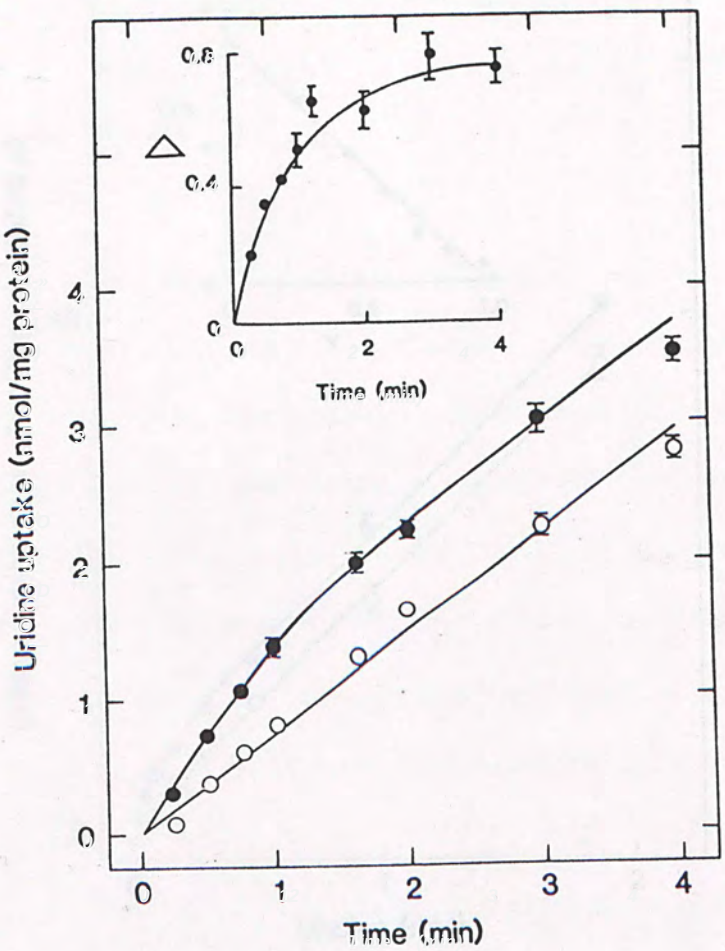

Solubilised lung membrane extract was reconstituted into phospholipid vesicles as described in the text. Uridine uptake (50 uM, 25 °C) was assayed in the absence (●) and in the presence of 20 uM NBMPR (○). The inset shows the time course of NBMPR-sensitive uridine transport (△ is the difference between uridine uptake in the absence and in the presence of NBMPR). Error bars are S.E. of triplicate estimates.

Figure 6.3 Concentration dependence of zero-trans uridine influx into vesicles reconstituted with crude membrane extract from guinea pig lung

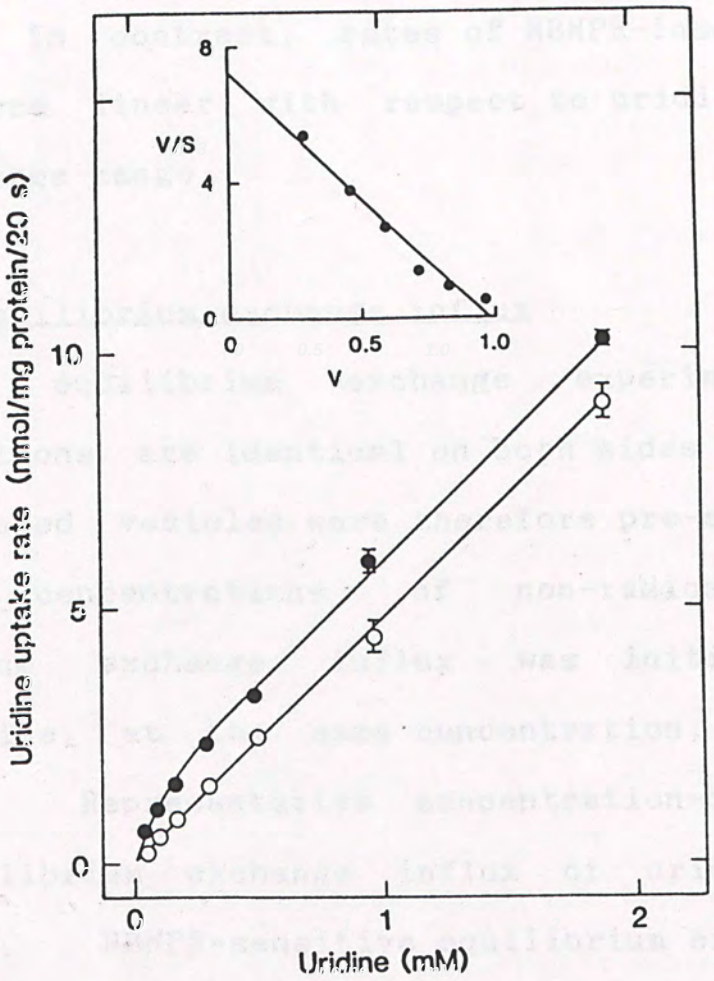

Apparent initial rates of zero-trans influx of uridine by reconstituted vesicles were measured in the presence (O) and in the absence (●) of 20 uM NBMPR as described in METHODS. The inset shows an Eadie-Hofstee plot of NBMPR-sensitive uridine transport (v/s vs v). Apparent Km and Vmax values, as estimated by linear regression analysis, were 0.14 mM and 0.97 nmol/mg in 20 s, respectively. Error bars are S.E. of triplicate estimates.

crude lung membrane extract over the concentration range of 0.05-2 mM. Rates of NBMPR-sensitive uridine transport were saturable and conformed to simple Michaelis-Menten kinetics (apparent Km 0.14 mM and Vmax 0.97 nmol/mg protein in 20 s). In contrast, rates of NBMPR-insensitive uridine uptake were linear with respect to uridine concentration over the same range.

6.3.3b Equilibrium exchange influx

In equilibrium exchange experiments, substrate concentrations are identical on both sides of the membrane. Reconstituted vesicles were therefore pre-equilibrated with varying concentrations of non-radioactive uridine. Equilibrium exchange influx was initiated by adding [^{14}C]uridine, at the same concentration, to the preloaded vesicles. Representative concentration-dependence curves for equilibrium exchange influx of uridine are shown in Fig. 6.4. NBMPR-sensitive equilibrium exchange influx of uridine was saturable and conformed to simple Michaelis-Menten kinetics. Estimated apparent Km and Vmax values were 1.1 mM and 7.1 nmol/mg of protein in 20 s, respectively, as determined from the inset v/s vs v plot (see also Table 6.3). In contrast, the NBTGR-insensitive component of uridine equilibrium exchange exhibited a linear concentration dependence. The Vmax of NBMPR-sensitive equilibrium exchange uridine influx was 7.3-fold greater than the Vmax observed for zero-trans

Figure 6.4 Concentration dependence of uridine equilibrium exchange influx by vesicles reconstituted with crude membrane extract from guinea pig lung

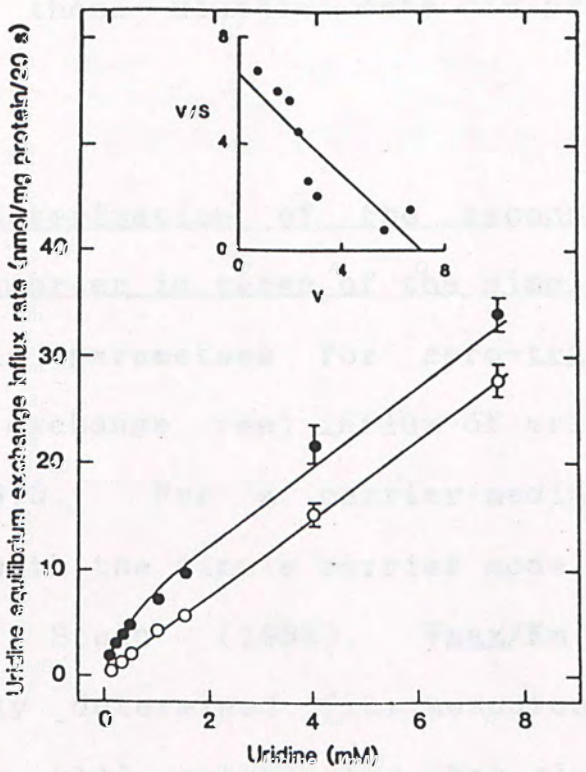

Reconstituted vesicles were pre-equilibrated with varying concentrations (0.05-15 mM) of non-radioactive uridine as described in METHODS. Apparent initial rates of uridine equilibrium exchange influx (20 s flux) were measured in the presence (○) and in the absence (●) of 20 uM NBMPR. The inset shows a v/s vs v plot of apparent initial rates of NBMPR-sensitive uridine equilibrium exchange influx. Estimated apparent Km and Vmax values were 1.1 mM and 7.1 nmol/mg of protein in 20 s, respectively. Error bars are S.E. of triplicate estimates.

influx measured at the same temperature and was paralleled by a corresponding increase in apparent Km. Thus, there was no significant difference in the Vmax/Km ratio under these two experimental conditions (Table 6.3). A full analysis of these kinetic data is presented in the next section.

6.3.3c Characterization of the reconstituted nucleoside transporter in terms of the simple carrier model

Kinetic parameters for zero-trans (zt) influx and equilibrium exchange (ee) influx of uridine are summarised in Table 6.3. For a carrier-mediated system to be compatible with the simple carrier model as defined by Lieb (1982) and Stein (1986), Vmax/Km ratios for all experimentally determined flux measurements must be equal. It has been well established that glucose and nucleoside transporters orientate randomly when reconstituted into proteoliposomes by freeze-thaw sonication (Baldwin et al, 1980; Wheeler and Hinkle, 1981; Tse and Young, 1987). On this basis, it is predicted that the reconstituted system would exhibit kinetic symmetry with respect to zero-trans influx and efflux. Therefore, assuming that V12=V21, it was possible to calculate the simple carrier resistance parameter (Roo, Ree, R12, R21; see legend to Table 6.3) for the reconstituted lung system (Table 6.3). This analysis clearly demonstrates that the loaded carrier moves at a much faster rate than the empty carrier, the mobilities

Table 6.3 Kinetic parameters for uridine equilibrium exchange and zero-trans influx in vesicles reconstituted with solubilized plasma membrane extract from guinea pig lung

Parameter measured

Condition	Vmax (nmol/mg protein in 20 s)	Km (mM)	Bmax (pmol/mg protein)	Vmax/Km (ul/mg protein in 20 s)	Turnover number /site/s
Zero-trans influx (2-1)	0.97	0.14	28	6.93	1.7
Equilibrium exchange influx	7.1	1.1	28	6.45	12.7

Simple carrier resistance parameters

	(nmol/mg protein in 20 s)$^{-1}$		(ms)
$R12=R21=(V12^{zt})^{-1}$	1.03	; nR12	588
$Ree=(V^{ee})^{-1}$	0.14	; nRee	79
Roo=R12+R21-Ree	1.92	; nRoo	1097

Independent estimates of simple carrier affinity parameter K

Estimated using	Values (uM)
$K=K21^{zt}(R21/Roo)$	75
$K=K^{ee}(Ree/Roo)$	81
Mean	78

Experimental details are described under 'METHODS'. Data from experiments illustrated in Figs. 6.2 and 6.3 are summarised in this Table. Solution 1 has been arbitrarily chosen to be the intravesicular solution. Resistance and affinity parameters according the simple carrier model were calculated according to the method of Lieb (1982). Simple carrier resistance parameters, R12 and Ree are the reciprocals of the Vmax values for zero-trans influx and equilibrium exchange, respectively. Turnover time value (nR) represents the average time it takes a single transport cycle under the appropiate experimental situation. nRoo measures the turnover time of empty carrier and nRoo=nR12+nR21-nRee while n is the total concentration of transporter. Turnover number refers to the number of substrate molecules transported per site per s.

(carrier 'mobility' implies macromolecular movement, e.g. a conformational shift, and does not denote actual translocation of the carrier) of the loaded and empty carriers differing by 14-fold (Roo/Ree=14).

Turnover numbers (i.e. the numbers of substrate molecules transported per site per s) and turnover time values (nR, i.e. the average time it takes a single transport system to complete a single transport cycle under the appropiate experimental situation, n being derived from assays of high-affinity NBMPR binding activity (Lieb, 1982; Stein, 1986)) for the reconstituted system were calculated and presented in Table 6.3. nRoo measures the turnover time of empty carrier and nRoo=nR12+nR21-nRee. Since n is a constant, the turnover time value for the empty carrier is again 14-fold greater than the equivalent value for the empty carrier. From the apparent Km values, it was possible to calculate the simple carrier affinity constant (K) for the reconstituted lung system (Table 6.3). The two independent estimates of K were similar, the mean being 78 uM.

6.3.3d Inhibitor studies of NBMPR-sensitive uridine uptake by reconstituted vesicles

A series of inhibition experiments were performed to investigate the ability of the transported nucleosides uridine, adenosine and inosine and the vasodilators, dilazep and dipyridamole to inhibit NBMPR-sensitive uridine

Table 6.4 Effects of transported nucleosides and nucleoside transport inhibitors on uridine transport into vesicles reconstituted with n-octylglucoside solubilised guinea-pig lung plasma membranes

Nucleoside		Uridine transport	Inhibitor		Uridine transport
	mM	% inhibition			% inhibition
Uridine	0.05	13±6	Dilazep	0.1 nM	25±8
	0.10	42±4		1 nM	45±7
	0.25	60±6		10 nM	50±6
	0.50	71±11		100 nM	58±7
Inosine	0.05	15±7	Dipyri-	0.1 nM	5±3
	0.10	50±7	damole	1 nM	10±2
	0.25	67±5		10 nM	42±7
	0.50	80±5		100 nM	60±8
Adenosine	0.05	35±5	NBTGR	20 uM	100±3
	0.10	68±2			
	0.25	85±3			
	0.50	90±11			

Rates of NBMPR-sensitive uridine transport (50 uM) by vesicles (20 s flux, 25°C) were measured as described in the text. Inhibitors were pre-incubated with reconstituted vesicles for 15 min at 25°C before addition of permeant. Values are means(±SEM) of three separate determinations.

uptake by the reconstituted vesicles. Results presented in Table 6.4 confirmed that NBMPR-sensitive uridine uptake by the reconstituted vesicles was inhibited by the nucleoside permeants inosine and adenosine. Adenosine was a more effective inhibitor of the reconstituted transporter than inosine (IC_{50} 0.07 and 0.10 mM respectively, 50 uM [^{14}C] uridine), in agreement with their relative affinities for the nucleoside transporter in other cell types. As expected from the concentration-dependence experiments reported in Sections 6.3.3, cold uridine acted as an apparent inhibitor of tracer uridine influx. NBMPR-sensitive uridine transport in the reconstitited vesicles was also inhibited by dilazep, dipyridamole and NBTGR. IC_{50} values were 10 and 15 nM for dilazep and dipyridamole respectively. These values correspond well with IC_{50} values determined for inhibition of high-affinity NBMPR binding to guinea-pig lung purified membranes (10 and 70 nM for dilazep and dipyridamole, respectively) (Chapter 4, Section 4.3.2b). The above results therefore suggest that high-affinity binding of NBMPR to lung membranes represents a specific interaction with element(s) of the NBMPR-sensitive nucleoside transporter, a conclusion consistent with previous reports in erythrocytes (Young and Jarvis, 1983).

6.3.3e Control experiments

Control experiments were performed to establish

Table 6.5 Reconstitution of nucleoside transport activity with n-octylglucoside solubilised guinea-pig lung membranes

	Uridine uptake		
	-NBMPR	+NBMPR	
	(pmol/20-s assay)		
Reconstituted vesicles	8.7±0.1	3.9±0.2	4.8±0.22
Lipid only	3.8±0.2	3.9±0.2	0
Protein only	0	0	0

Uridine uptake by vesicles (50 uM, 20 s flux at 25°C) was measured as described in the text. In the preparation of 'reconstituted vesicles', crude n-octylglucoside extract was reconstituted with added soybean phospholipids. For the 'lipid only' and 'protein only' controls, reconstitution was performed in the absence of added protein and lipid, respectively. Each transport assay contained 15.3 ug of protein and 0.77 umol of lipid (reconstituted vesicles) or 15.3 ug of protein (protein only) or 0.77 umol of phospholipids (lipid only).

whether added phospholipid was essential for reconstitution of nucleoside transport activity. Table 6.5 demonstrates that the NBMPR-sensitive uridine transport activity of the crude lung membrane preparation was totally dependent upon the presence of added phospholipid, membrane extract alone having no detectable NBMPR-sensitive uridine uptake activity. Liposomes alone only exhibited NBMPR-insensitive uptake of nucleoside, reflecting simple diffusion of isotopic permeant across the lipid bilayer (see also Section 6.3.4).

6.3.4 Nucleoside Uptake into Liposomes

Uridine was used as the permeant for the reconstitution experiments described in this Chapter. Uridine was selected in preference to other nucleosides because its kinetics of transport into intact erythrocytes have been extensively studied. The kinetic parameters obtained in the lung reconstituted system could therefore be compared directly with published values for the reconstituted erythrocyte nucleoside transporter. In the present series of experiments, I have compared the uptake of inosine, adenosine and uridine into liposmes. Fig. 6.5 compares the time courses of uridine, inosine and adenosine uptake measured in vesicles prepared in the absence of protein. The estimated initial rates of nucleoside permeation into protein-free liposomes were 3.7, 10.1 and 52.3 pmol/umol phospholipid per min for inosine, uridine

and adenosine, respectively, giving ratios of 1: 2.7 : 14.0 with respect to inosine. This uptake of nucleosides into protein-free liposomes represents simple diffusion across the vesicle membrane and correlates well with their respective octanol/water partition coefficients (adenosine 0.10; uridine 0.037; inosine 0.0087) (Jarvis and Young, 1982).

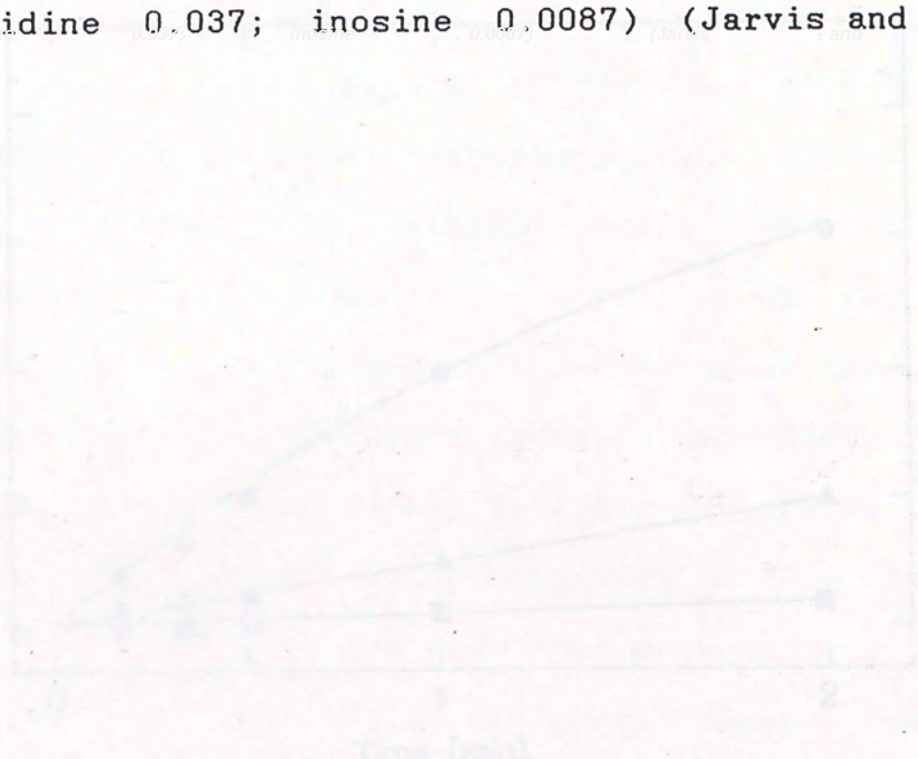

Figure 6.5 Time courses of inosine, uridine and adenosine uptake into liposomes

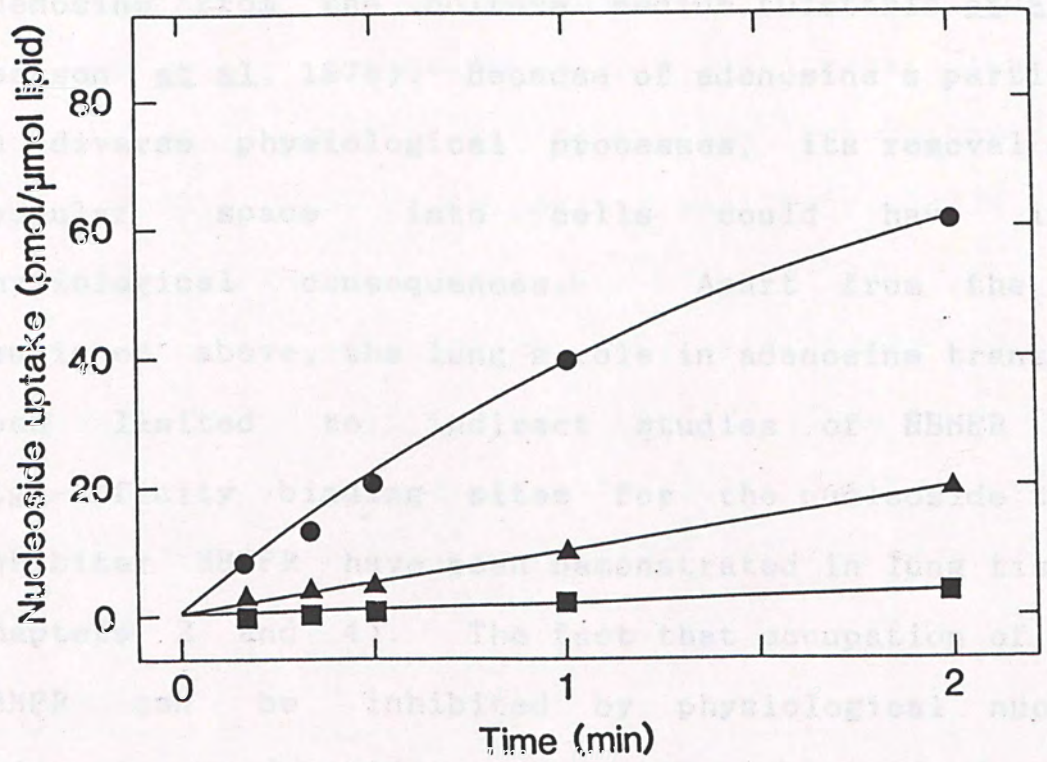

Inosine (■), uridine (▲) and adenosine (●) uptake (50 uM) were measured at 25°C by the centrifugal gel filtration method as described in 'METHODS'. Liposomes were prepared in the absence of protein by the standard reconstitution procedure. Each assay contained 0.52 umol lipid. Values are means of duplicate estimates.

6.4 DISCUSSION

Adenosine is removed on passage through the pulmonary circulation of guinea-pig and rat *in vivo* (see Chapter 1) and it has also been demonstrated that vascular endothelium (and smooth muscle cells) in culture take up adenosine from the culture medium (Dieterle *et al*, 1978; Pearson *et al*, 1978). Because of adenosine's participation in diverse physiological processes, its removal from the vascular space into cells could have important physiological consequences. Apart from the studies mentioned above, the lung's role in adenosine transport has been limited to indirect studies of NBMPR binding. High-affinity binding sites for the nucleoside transport inhibitor NBMPR have been demonstrated in lung tissue (see Chapters 2 and 4). The fact that occupation of sites by NBMPR can be inhibited by physiological nucleosides (adenosine and uridine) and other recognized nucleoside transporter inhibitors such as dipyridamole provides only indirect evidence that NBMPR is binding to functional elements of lung nucleoside transporter.

In the present series of experiments, I have been able to demonstrate using the freeze-thaw-sonication procedure of Kasahara and Hinkle (1977) and Tse *et al* (1985) that crude n-octylglucoside extract of guinea-pig purified plasma membranes is capable of catalysing NBMPR-sensitive uridine transport when reconstituted into phospholipid vesicles. This reconstituted membrane system

also exhibited high-affinity NBMPR binding activity. The choice of using n-octylglucoside as detergent rather than Triton X-100 was because n-octylglucoside can be completely removed by dialysis, in contrast to Triton X-100 which has a low critical micelle concentration (Yu et al, 1973) and has therefore to be removed by adsorption onto polystyrene beads (Biobeads SM 2). Detergent removal by this method is associated with significant absorption of protein onto the beads (Jarvis and Young, 1981). Purified plasma membranes from guinea pig lung was used in preference to rat lung because of a higher specific NBMPR binding activity i.e. more binding sites (see Chapter 5). Attempts to reconstitute the nucleoside transporters from crude lung membranes from either species were unsuccessful because of the lower density of NBMPR binding site (data not shown).

The solubilised crude membrane extract exhibited a mean high-affinity NBMPR binding activity of 35 ± 4 pmol/mg protein (Fig. 6.1 and Table 6.1) and an apparent Kd of 1.1 nM. This binding was inhibited by adenosine and uridine. When this preparation was reconstituted into proteoliposomes, NBMPR-sensitive uridine transport was demonstrated (Fig. 6.2). This transport was inhibited by adenosine and inosine, confirming that the transporter exhibits broad specificity for both purine and pyrimidine nucleosides. Specific (NBMPR-sensitive) uridine transport in the reconstituted vesicles was also inhibited by dilazep

and dipyridamole, both being potent inhibitors of nucleoside transport in many other cell types. IC_{50} values for inhibition of NBMPR-sensitive transport by these vasodilators in reconstituted lung membrane vesicles correlates with their apparent Ki values as inhibitors of high-affinity NBMPR binding to intact lung membranes (Chapter 3, Section 2.3.1 and Chapter 5, Section 5.3.3). For uridine, Ki values for inhibition of NBMPR binding (Chapter 2, Section 2.3.1) correlates well with the apparent Km of NBMPR-sensitive equilibrium exchange influx of uridine (1.1 mM, see Section 6.3.3b). These results therefore provide strong evidence that the lung NBMPR binding protein is identical to the lung NBMPR-sensitive nucleoside transport protein.

Liposomes exhibit a 5-fold greater diffusion permeability to adenosine than to uridine, this being a consequence of adenosine's higher lipid solubility (Section 6.3.4). Physiologically, this means that cells are significantly permeable to adenosine, even in the absence of a nucleoside carrier. Experimentally, the large magnitiude of NBTGR-insensitive adenosine uptake into liposomes makes this nucleoside unsuitable as a permeant for reconsititution studies. As might therefore be expected, attempts to directly demonstrate carrier-mediated adenosine transport by the reconstituted guinea pig lung nucleoside transporter were unsuccessful (data not shown).

In permeation studies with vesicles, it is important to differentiate between transport and binding of permeant, particularly since binding might also be blocked by inhibitors of transport. The uridine uptake processes described in reconstituted lung vesicles evidently represent transport since uridine uptake by the vesicles was time-dependent, and uptake rates saturated as uridine concentrations were increased (Figs. 6.2 and 6.3). Furthermore, the numbers of uridine molecules taken up in vesicles that had incorporated the lung nucleoside transporter greatly exceeded the number of available NBMPR-binding sites in the preparation. The number of uridine molecules taken up per s in reconstituted vesicles assayed under equilibrium exchange influx conditions is 13 times the number of available high-affinity NBMPR binding sites (Table 6.3), calculated assuming that each transporter binds one molecule of NBMPR. Therefore, NBTGR-sensitive uridine transport as measured in the present experiments reflects carrier-mediated nucleoside permeation into the reconsitituted vesicles rather than binding. In addition, reconstitution of nucleoside transport activity from lung plasma membranes extract also exhibited an absolute requirement for added phospholipid (Table 6.5), further strong evidence for carrier-mediated nucleoside permeation into the reconstituted vesicles rather than binding.

The kinetic studies presented in this Chapter

demonstrate that the simple carrier model of Lieb (1982) and Stein (1986) can be applied to uridine transport in the reconstituted lung system, Vmax/Km ratios of uridine uptake under zero-*trans* influx and equilibrium exchange influx conditions being the same (Lieb, 1982; Stein, 1986). The relative magnitudes of the two resistance parameters demonstrates that the loaded and empty carriers exhibit a 14-fold difference in mobility (*i.e.* Roo/Ree=14, Table 6.3). This compares favourably with a difference of 21-fold for reconstituted human erythrocyte band 4.5 polypeptides measured at 15^{o}C (Tse and Young, 1987) and implies that the movement of the empty carrier is the rate determining step of uridine transport in reconstituted vesicles. However, unlike erythrocytes, the mobilities of substrate-loaded and empty carriers are equal in intact cultured cells (see Chapter 1). Variation in membrane lipid composition between erythrocytes and other cell types may offer a potential explanation for these cell-type differences in kinetic behaviour (Tse and Young, 1987a, b).

The estimated mean K value of 78 uM measured at 25'C for the reconstituted lung transporter is slightly higher than the K value of 120 uM obtained for reconstituted human erythrocyte band 4.5 polypeptides measured at 15^{o}C (Tse and Young, 1987). The lung value would be expected to be numerically even smaller at lower temperature (Plagemann and Wohlhueter, 1984b). K is not a direct measure of carrier affinity, but is a composite of both mobility and

affinity rate constants. Therefore, the difference in K between the reconstituted guinea pig lung and human erythrocyte transporters might reflect differences in either carrier mobility, affinity or both.

In conclusion, n-octylglucoside can be used to solubilise the nucleoside transporter from guinea pig lung membranes. It was established that the lung transporter could be reconstituted into liposomes and that the resulting proteoliposomes exhibited NBMPR-sensitive uridine transport.

6.5 ACKNOWLEDGEMENT

The experiments described in this Chapter were conducted in collaboration with Dr. C.M. Tse.

CHAPTER 7

GENERAL DISCUSSION

7.1 INTRODUCTION

The preceding Chapters describe ligand binding and photoaffinity labelling studies of the rat and guinea pig lung nucleoside transporters as well as detailed kinetic analyses of the reconstituted nucleoside transporter solubilised from guinea-pig lung plasma membranes. This final Chapter attempts to draw these investigations together and also presents a discussion of the molecular similarities and differences between erythrocyte nucleoside transporters and those from rat and guinea pig lung.

7.2 FUNCTIONAL PROPERTIES OF LUNG NUCLEOSIDE TRANSPORTERS

7.2.1 Ligand Binding Studies

As described in Chapters 2 and 5, I have been able to demonstrate the presence of saturable, high-affinity binding sites from NBMPR in crude and purified membrane preparations from both rat and guinea-pig lung. Kd for NBMPR binding to these sites in both species (0.2-0.4 nM) was very similar to the corresponding binding of inhibitor to erythrocytes and other cell types (apparent Kd 0.1-1 nM) (Jarvis and Young, 1980; Cass *et al*, 1981). Similar to findings in erythrocytes, NBMPR binding to lung membranes was inhibited by transported nucleosides and by dipyridamole and other vasoactive compounds. The observation that guinea pig lung membranes possess a 2-fold higher density of NBMPR binding sites than the rat (approximately 19 *vs* 8 pmol/mg protein (Table 2.1) is consistent with previous *in vivo* perfusion studies by Kolassa *et al* (1971) which found that guinea pig lung was able to remove 50% more adenosine than rat lung. Thus, the higher density of NBMPR binding sites in guinea pig reflects a larger nucleoside transport capacity in removing adenosine during passage through the pulmonary circulation.

There was also a large species difference in dipyridamole sensitivity with respect to inhibition of NBMPR binding to rat and guinea pig lung crude membranes,

with apparent Ki values in the two differing by 280-fold (Table 2.4 and Fig. 2.3). Again, this correlates with previous reports that adenosine uptake by intact rat lung is approximately 100 times less sensitive to dipyridamole inhibition than guinea pig lung (Kolassa et al, 1971; Bakhle and Chelliah, 1983). My finding that high-affinity, saturable [^{3}H]dipyridamole binding sites are absent from rat lung membranes is also consistent with the intact lung studies. Lung NBMPR and dipyridamole binding sites therefore have the properties expected of nucleoside transporter proteins in this tissue. Also, pharmacokinetic experiments in mice have shown that accumulation of the cytotoxic nucleoside tubercidin in lung tissue is inhibited by preadminstration of NBMPR-phosphate, a prodrug form of NBMPR (Kolassa et al, 1982). There is therefore good evidence that high-affinity NBMPR and dipyridamole binding to guinea pig and rat lung membranes reflects a specific association with functional nucleoside transporters. High-affinity binding of [^{3}H]dipyridamole to guinea pig lung membranes was inhibited by NBMPR, transported nucleosides and lidoflazine. As discussed in detail in Chapters 2 and 3, there was a good correlation between (a) inhibition constants for inhibition of [^{3}H]NBMPR and [^{3}H]dipyridamole binding and (b) between inhibition constant for inhibition of ligand binding to lung membranes and inhibition of NBMPR-sensitive nucleoside transport in other cell types.

7.2.2 Reconstitution Studies

Kinetic and inhibitor studies suggest that NBMPR binds to the permeation site of the erythrocyte nucleoside transporter (see e.g. Jarvis and Young, 1987). In lung, the demonstration that solubilised guinea pig lung membrane extract exhibits both NBMPR binding activity as well as NBMPR-sensitive uridine transport activity when reconstituted into proteoliposomes (Chapter 6) provides additional support for the view that reversible NBMPR binding studies on lung membranes do indeed reflect properties of NBMPR-sensitive nucleoside transporters in this preparation.

The estimated turnover number of 1.7 molecules of uridine transported/site/s under zero-trans influx conditions for the reconstituted lung systerm (Chapter 3, Table 6.3) was 2.5-fold lower than the corresponding turnover number for the reconstituted human erythrocyte nucleoside transporter (4.4 molecules of uridine transported/site/s) (Tse and Young, 1987a). However, this difference is rather small compared with published data for intact erythrocytes vs other cell types (Table 1.1). Thus, in erythrocytes, the turnover number for uridine transport at 25^{o}C varies from 140-180 molecules/site/s in erythrocytes from various species compared to 8-30 molecules/site/s in cultured non-erythroid cell, a difference of 4.5-23 fold. Thus, low turnover numbers are not an intrinsic property of NBMPR-sensitive nucleoside

transporter from non-erythroid cells and tissues. The turnover number of the guinea pig lung nucleoside transporter *in situ* remains to be determined. As for differences in the relative mobilities of loaded *vs* unloaded carrier (Chapter 6, Section 6.3.3c), differences in turnover number between different cell types might possibly reflect variations in membrane lipid composition (Tse and Young, 1987a). Recently, Tefft *et al* (1986) have demonstrated that the transport activity of the reconstituted glucose transporter can be modulated by altering the composition of the lipid bilayer.

The reconstituted guinea pig lung nucleoside transporter exhibited broadly similar kinetic properties to the human erythrocyte protein. Therefore, the present results suggest that these two transporters are functionally similar. Moreover, the two transporters also exhibit similar apparent molecular weights on SDS-polyacrylamide gels (see Chapter 4). It is therefore anticipated that the lung and erythrocyte transporters from these two species exhibit extensive structural homology. In this context, it should be noted that the amino acid sequences of the human liver and erythrocyte glucose transporters have recently been shown to be highly homologous, and perhaps identical (Mueckler *et al*, 1985).

7.2.3 Physiological and Pharmacological Aspects

The lung processes the entire blood volume every 20 seconds or so in man, and because it has a relatively large capillary surface area, it has a unique opportunity to exert a control function over the contents of arterial blood. The other cell type in a position to modulate the contents of arterial blood are erythrocytes. The relative abilities of lung endothelium and erythrocyte to remove adenosine from plasma will depend on their relative nucleoside transport capacities. For example, rat and guinea pig lung purified membranes possess a much higher density of NBMPR binding sites than that found in erythrocyte 'ghosts' from these species (48 and 13 pmol/mg protein in guinea pig and rat lung purified membranes, respectively, compared with 0.1 and 1 pmol/mg protein in guinea pig and rat erythrocyte membranes, respectively). These considerable differences in transporter density between lung and erythrocytes are consistent with a physiological role of guinea pig and rat lung in the removal of circulating adenosine. In contrast, *in vivo* and *in vitro* studies of the removal of adenosine from the rabbit pulmonary circulation indicate that rabbit lung does not contribute to the uptake of adenosine *in vivo*, blood cells being primarily responsible for adenosine removal during single passage through the rabbit pulmonary circulation (Catravas, 1984). Rabbit erythrocytes have a high density of NBMPR binding sites (approximately 9,500

sites per cell, compared with 300 for rat and 27 for guinea pig) (Clanachan et al, 1983; Jarvis et al, 1982). In man, where there is also a high density of NBMPR binding sites in erythrocytes (approximately 10^4 sites per cell) (Jarvis et al, 1982), the relative contributions of lung endothelial cells and erythrocytes to the removal of adenosine during passage through the pulmonary circulation has not been determined, but would, on the basis of the present investigation, be expected to be dominated by erythrocytes.

7.3 DO DIPYRIDAMOLE AND NBMPR BIND TO THE SAME SITE ?

Although the inhibitory effect of dipyridamole on nucleoside transport was first observed more than 20 years ago, the mechanism by which this clinically available drug achieves this effect is largely unknown and in dispute (see Chapter 1). Kinetic experiments and inhibitor studies of [^{3}H]NBMPR and [^{3}H]dipyridamole binding described in this Thesis (Chapters 2 and 3) were carried out to clarify the mechanism of dipyridamole interaction with the NBMPR-sensitive lung nucleoside transporter.

Dipyridamole was found to be a competitive inhibitor of NBMPR binding to lung membranes of both the guinea pig and rat, and nucleosides and NBMPR were found to block high-affinity [^{3}H]dipyridamole binding to guinea pig lung membranes. These observations are consistent with the view that dipyridamole competes directly with nucleosides (and NBMPR) for the permeation site of the transport system. In support of this conclusion is the finding that dipyridamole was found to be a potent competitive inhibitor of uridine equilibrium exchange influx into guinea pig erythrocytes (Jarvis, 1986) with an apparent K_i value of 1 nM (*c.f.* an apparent K_d of 0.7 nM for high-affinity dipyridamole binding to human erythrocyte membranes) (Jarvis, 1986). Dipyridamole binding to human erythrocyte membranes is also blocked by nucleosides and nucleoside transport inhibitors. Furthermore, inhibition of dipyridamole binding by uridine and adenosine were apparently competitive with inhibition

constants similar to previous estimates of apparent Km values for equilibrium exchange transport of these nucleosides (Plagemann et al, 1982; Jarvis et al, 1983). Also, previous studies have shown that dipyridamole competitively interacts with NBMPR for the NBMPR-binding site on human erythrocytes (Hammond et al, 1981). Finally, although the chemical structures of dipyridamole and NBMPR appear to have little in common (Figs. 1.2 and 1.4), X-ray diffraction studies point to similarities in the three-dimensional crystal structures of the two molecules (Jarvis, 1986). There are therefore strong grounds to consider that NBMPR and dipyridamole bind to the same site on the nucleoside transporter. Although NBMPR is a competitive inhibitor of nucleoside zero-trans influx and equilibrium-exchange influx, it is a non-competitive inhibitor of zero-trans nucleoside efflux (Jarvis et al, 1983a), indicating that the ligand binds preferentially to the outward facing conformation of the transporter (Jarvis et al, 1983a; see also Fig. 1.3). Similarly, dipyridamole is a non-competitive inhibitor of zero-trans uridine efflux from guinea pig erythrocytes (Jarvis, 1986).

The kinetic and inhibitor binding studies of NBMPR and dipyridamole binding presented in this Thesis (Chapters 2 and 3) and also the other studies detailed above would also be consistent with a more complex model of nucleoside transport in which dipyridamole binding at one site induces a conformational change in the transporter,

thereby allosterically altering the affinity of permeant and NBMPR at their binding site. Support for this view comes from the finding that high micromolar concentrations of dipyridamole decrease the rate of NBMPR dissociation from both rat and guinea pig lung membranes (Section 2.3.2a) and also that micromolar concentrations of NBMPR dramatically increased the rate of dipyridamole dissociation. Generally, changes in the rate of dissociation are indicative of site to site interactions. Hence, these dissociation data are inconsistent with a simple single site model for NBMPR and dipyridamole binding to the nucleoside transporter. Instead, they provide compelling evidence for the existence of topographically separate allosteric sites. Independent studies with other systems have confirmed that high concentrations of dipyridamole decrease the rate of NBMPR dissociation from the transporter (Jarvis et al, 1983; Hammond and Clanachan, 1985). This effect has been argued by some investigators to simply reflect nonspecific interactions with the transporter or other membrane components following partition of the lipophilic inhibitor into the membrane. In this context, it has been pointed out that dipyridamole is not a specific inhibitor of nucleoside transport (see Chapter 1, Section 1.3.2c). However, the effect of NBMPR on dipyridamole dissociation is more difficult to dismiss in this way.

A model of the guinea pig lung nucleoside

transporter consistent with the experimental data presented in this Thesis and that in the literature are presented in Fig. 7.1. The major features of the guinea pig nucleoside transporter model are as follows: (a) NBMPR binds to the outward-facing conformation of the nucleoside permeation site, binding of NBMPR allosterically reducing the affinity of dipyridamole for binding to its site. (b) the dipyridamole binding site is also located on the external membrane surface in view of the finding that dipyridamole inhibition of nucleoside transport in guinea pig erythrocytes is competitive with respect to zero-*trans* influx of nucleoside, but non-competitive with respect to nucleoside efflux. (c) binding of dipyridamole to its binding site allosterically decreases the affinity of the permeation site for both nucleoside permeants and NBMPR. This model of the guinea pig lung nucleoside transporter is considered to also be applicable to NBMPR-sensitive nucleoside transporters in other cell types and tissues. With respect to the rat lung nucleoside transporter, it is proposed that the dipyridamole binding site is in its low affinity state, even when the permeation site is unoccupied by NBMPR.

Figure 7.1 A proposed molecular model for the guinea-pig lung transporter

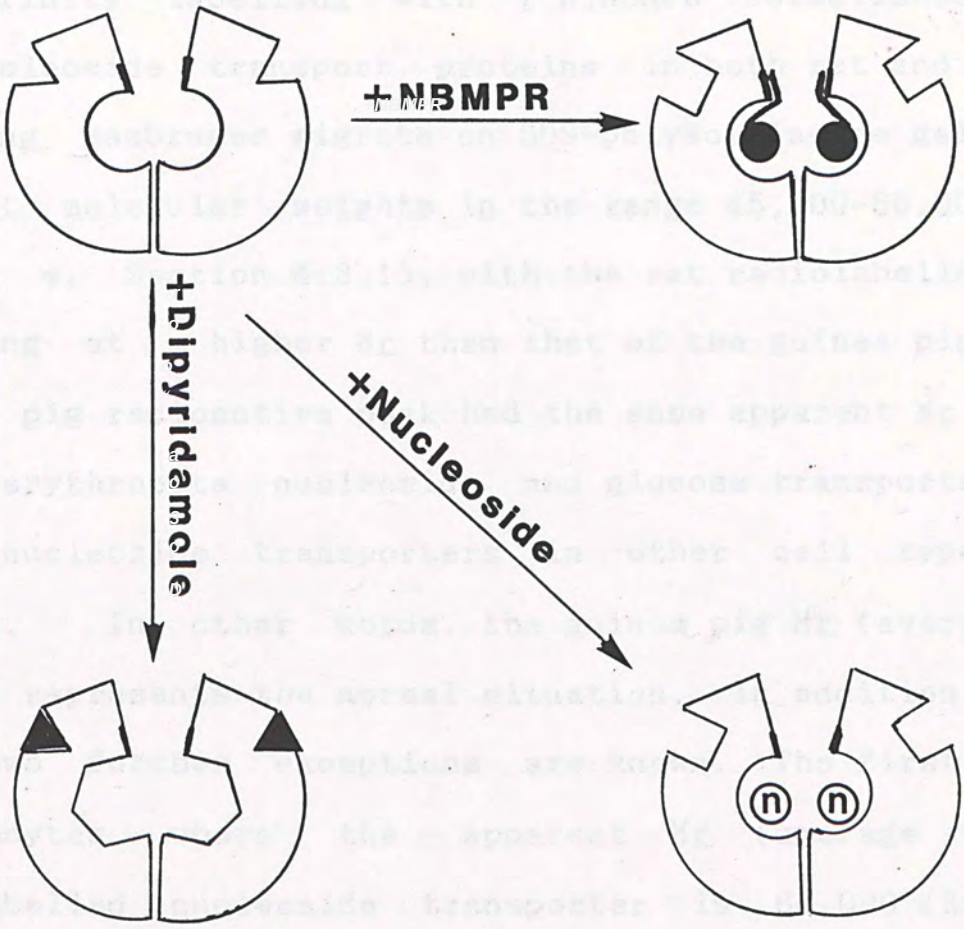

The nucleoside transporter is drawn as a dimer in its outward-facing conformation. Each monomer represents a Mr of 55,000 dalton polypeptide containing one nucleoside permeation site and one dipyridamole-binding site to be consistent with the 1:1 stoichiometry for NBMPR/dipyridamole binding reported in Chapter 3, Section 3.3.2.

dipyridamole-binding site (high-affinity)

dipyridamole-binding site (low-affinity)

NBMPR binding site / permeation site (high-affinity)

NBMPR binding site / permeation site (low-affinity)

▲, dipyridamole; ⓝ, nucleoside; ●, NBMPR.

7.4 MOLECULAR PROPERTIES AND TRANSMEMBRANE TOPOLOGY OF NUCLEOSIDE TRANSPORT PROTEINS

As detailed in Chapter 4, the technique of photoaffinity labelling with [^{3}H]NBMPR established that the nucleoside transport proteins in both rat and guinea pig lung membranes migrate on SDS-polyacrylamide gels with apparent molecular weights in the range 45,000-66,000 (see Chapter 4, Section 4.3.1), with the rat radiolabelled peak migrating at a higher Mr than that of the guinea pig. The guinea pig radioactive peak had the same apparent Mr as the human erythrocyte nucleoside and glucose transporters and also nucleoside transporters in other cell types and species. In other words, the guinea pig Mr (average) of 55,000 represents the normal situation. In addition to the rat, two further exceptions are known. The first is pig erythrocytes where the apparent Mr (average of the radiolabelled nucleoside transporter is 64,000 (Kwong *et al*, 1986). The second exception concerns a Novikoff hepatoma variant (Novikoff-UA cells) where nucleoside transport is not inhibited by nanomolar concentrations of NBMPR (Gati *et al*, 1986). Surprisingly, these cells possess NBMPR binding sites which upon photoaffinity labelling with [^{3}H]NBMPR have an apparent Mr in the range 72,000-80,000 (Gati *et al*, 1986). The functional significance of NBMPR binding sites in this cell line is, at present, unclear.

The finding that photolabelled nucleoside

transporters present in rat liver and lung have the same apparent Mr of 63,000 (Wu and Young, 1984; Chapter 4, Section 4.3.3), while those of guinea pig lung and liver have a common apparent Mr of 55,000 (Wu and Young, 1984; Chapter 4, Section 4.3.3) suggests a degree of structural homology between nucleoside transporters present in different tissues of the same species. Recent studies with rat erythrocytes also demonstrate that the rat radioactive peak in the band 4.5 region has a higher apparent molecular weight than that of the human erythrocyte transporter (Jarvis and Young, 1986). As reported in Chapter 4, Section 4.4, the apparent Mr difference between rat and human and guinea pig nucleoside transporters can be accounted for by more extensive glycosylation of the rat protein. Thus, endoglycosidase-F reduces the apparent Mr of the human and guinea pig transporters from Mr 55,000 to 46,000 (guinea pig lung) and 45,000 (human erythrocyte), while in the rat, the Mr for the lung nucleoside transporter reduces from Mr 63,000 to 46,000.

As detailed in the General Introduction, the human erythrocyte nucleoside and glucose transporter proteins have indistinguishable electrophoretic mobilities on SDS-polyacrylamide gels. More significantly, the deglycosylated polypeptides exhibit almost identical apparent molecular weights of 44,000 and 45,000, respectively (Kwong et al, 1986). It has been suggested that these similarities reflect some degree of structural

homology between the two proteins (Kwong et al, 1986;). Exploration of the transmembrane topology of the nucleoside and glucose transporters shows additional evidence of molecular similarities between the two carrier proteins.

Current information on the transmembrane arrangement of the human erythrocyte glucose transporter is derived from proteolytic studies of the erythrocyte transporter (Cairns et al, 1984; Deziel and Rothstein, 1984; Shanahan and D'Artel-Ellis, 1984; Janmohamed et al, 1985) and hydropathy plots of the polypeptide amino acid sequence determined by gene cloning experiments of the equivalent transporter in HepG2 cells (Mueckler et al, 1985). The polypeptide is believed to go through the membrane 12 times (Mueckler et al, 1985), schematically represented by four membrane spanning domains in Fig. 7.2. The N- and C-terminals are exposed to the cytoplasm, with the site of carbohydrate attachment close to the N-terminal on the outside of the membrane. Cytochalasin-B, a competitive inhibitor of glucose transport can, like NBMPR, be used to photolabel the transporter (Baldwin et al, 1981; Kasahara and Hinkle, 1977). The cytochalasin-B binding site is located on the inside of the membrane on the C-terminal half of the transporter (Deziel and Rothstein, 1984; Janmohamed et al, 1985). An important feature of the model is the presence of a large central cytoplasmic loop which contains two trypsin cleavage sites differing in position by the equivalent of approximately 800 daltons. With

regard to possible sites of glycosylation, the recently determined amino acid sequence of the human HepG2 hepatoma glucose transporter contains two asparagine residues, one of which (Asn411) is located within a postulated membrane-spanning domain of the transporter (Muekler et al, 1985), and its location is consistent with the site of glycosylation of the erythrocyte glucose transporter determined by enzyme and chemical cleavage studies (Cairns et al, 1984).

In contrast to the glucose transporter, the NBMPR attachment site to the human erythrocyte nucleoside transporter is located on the outer surface of the transporter relatively near the site of carbohydrate attachment, with a trypsin cleavage site located on a cytoplasmic domain of the transporter (Kwong et al, 1985). As detailed in Chapter 4, the human and pig erythrocyte nucleoside transporters are both glycoproteins but with different carbohydrate structures. The polypeptide structures of the two transporters also differ, the deglycosylated pig protein migrating on SDS-polyacrylamide gels with an apparent molecular weight of 57,000 compared with 44,000 for the deglycosylated human transporter (Kwong et al, 1986). Proteolytic digestion experiments suggest that the human and pig nucleoside transporters are similar with respect to their arrangement in the erythrocyte membrane, the loci of enzyme cleavage sites also being similar. Simplified models of the transmembrane topology

of the human and pig erythrocyte nucleoside transporters, based on that of the human erythrocyte glucose transporter are presented in Fig. 7.2. (Kwong et al, 1986, 1987). The postulated polypeptide difference between the human and pig nucleoside transporters is that the pig protein has a larger cytoplasmic loop (Kwong et al, 1987).

Trypsin treatment of the radiolabelled guinea pig lung nucleoside transporter yielded a glycosylated transporter fragment of similar Mr as the corresponding human erythrocyte cleavage product. Trypsin treatment reduced, but did not abolish the Mr differences between the rat and the guinea pig and human nucleoside transporter (3,000 vs 8,000, see also Table 4.3). This Mr difference was still apparent after endoglycosidase-F treatment (Table 4.3). On the basis of these data, it is concluded that the rat has 2 sites of glycosylation and that in addition, there is a 2,000-3,000 dalton difference in the site of trypsin cleavage in the rat compared with human and guinea pig, the rat cleavage site being nearer to the C-terminal. It is interesting that the rat trypsin cleavage site correspond in position to the second trypsin cleavage site on the glucose transporter. It remains to be established whether trypsin also cleaves the human and guinea pig nucleoside transporters at this site.

Figure 7.2 Schematic representation of the transmembrane arrangement of the human erythrocyte glucose (A) and nucleoside (B) transporters and pig erythrocyte nucleoside transporter (C) and guinea-pig lung nucleoside (D) and rat lung nucleoside transporter (E)

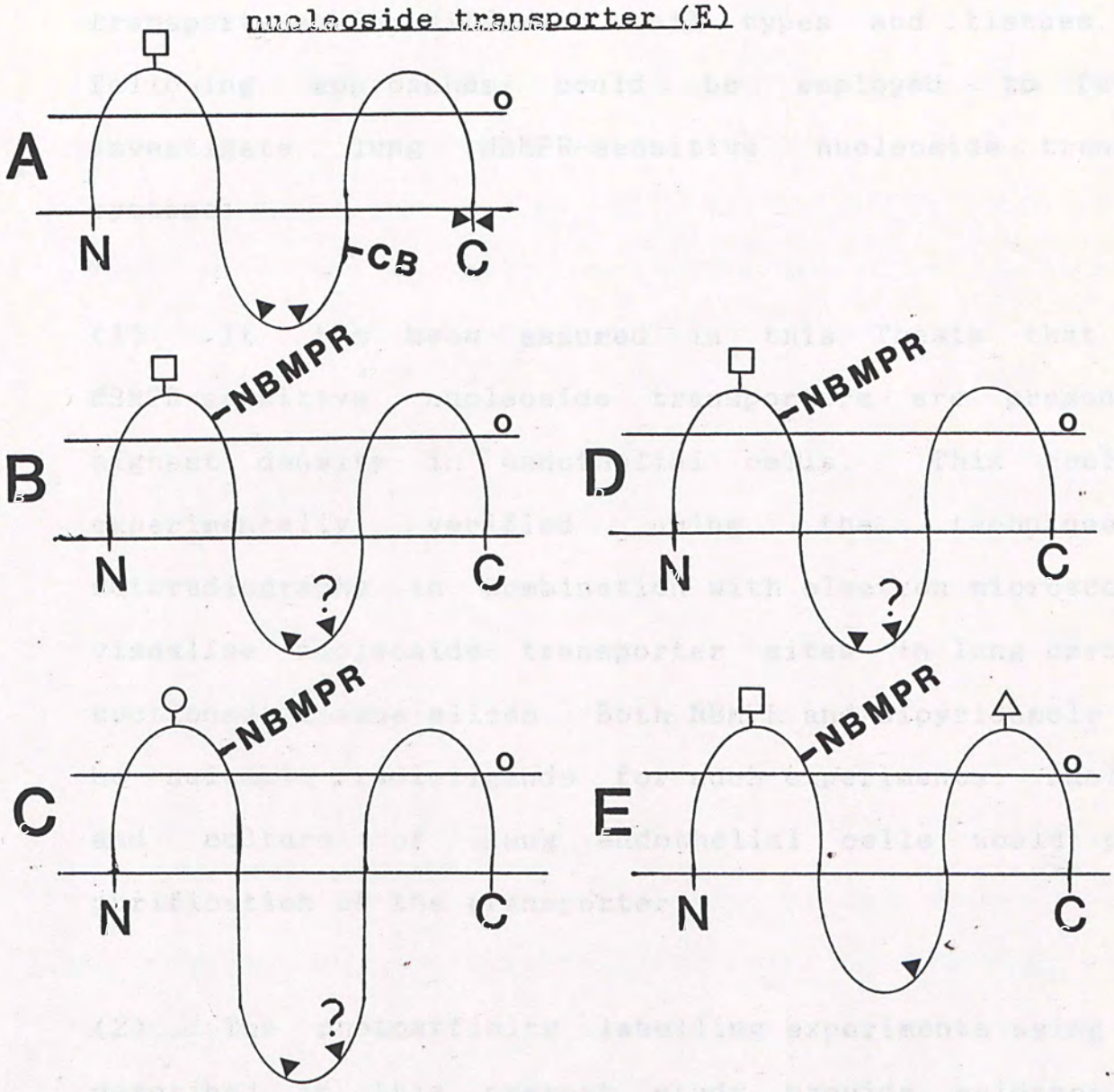

□, ○, △, carbohydrate moieties; -CB, cytochalasin-B labelling site; -NBMPR, NBMPR labelling site; ▲, trypsin cleavage site; N, N-terminal; C, C-terminal; o, outside of membrane.

7.5 FUTURE EXPERIMENTS

The ligand binding and molecular studies described in this Thesis on nucleoside transport proteins in rat and guinea pig lung membranes should serve as useful starting points for future in depth comparisons of nucleoside transporters in different cell types and tissues. The following approaches could be employed to further investigate lung NBMPR-sensitive nucleoside transport systems:

(1) It has been assumed in this Thesis that lung NBMPR-sensitive nucleoside transporters are present in highest density in endothelial cells. This could be experimentally verified using the technique of autoradiography in combination with electron microscopy to visualise nucleoside transporter sites in lung cryostat-sectioned tissue slices. Both NBMPR and dipyridamole would be suitable radioligands for such experiments. Isolation and culture of lung endothelial cells would permit purification of the transporter.

(2) The photoaffinity labelling experiments using NBMPR described in this present study provide evidence that NBMPR-sensitive nucleoside transporters from different sources have broadly similar molecular weights to that of the human erythrocyte system. It is envisaged that this technique will continue to prove useful in the molecular

characterization of NBMPR-sensitive nucleoside transporters from different cell types and tissues. Unfortunately, however, NBMPR cannot be used as a photoprobe for NBMPR-insensitive nucleoside transporters. Development of appropiate photolabile substrate analogue probes would be useful for this purpose and could also be applied to molecular studies of sodium-dependent nucleoside transport proteins. Such substrate probes would also finally resolve the controversial problem of whether NBMPR binds to the permeation site on the NBMPR-sensitive nucleoside transporter or to a separate modifier site.

(3) Reversible [^{3}H]dipyridamole binding studies should be further undertaken to characterise further the relationship between the NBMPR and dipyridamole binding sites. [^{3}H]Dipyridamole may also have use in the study of NBMPR-insensitive nucleoside transporters.

(4) The reconstitution methodology described in this Thesis should be used further to explore functional and pharmacological characterization of lung NBMPR-sensitive nucleoside transporters. Reconstitution studies along with transport experiments in intact cells should be undertaken to explore the possible existence of NBMPR-insensitive and sodium-dependent nucleoside transporters in lung tissue.

(5) The purified guinea pig and rat lung nucleoside

transporter should be subjected to controlled proteolysis (e.g. trypsin digestion) and the resulting polypeptides separated and analysed for N-, C-terminals, amino acid composition and sequence. Lung nucleoside transporter amino acid sequences would, of course, be compared closely with corresponding sequences derived from the erythrocyte nucleoside and glucose transporters, thus establishing the extent of structural homology between erythroid and non-erythroid systems and providing considerable additional information concerning structure-function relationships between nucleoside and glucose transporters and between dipyridamole-sensitive (guinea-pig, human) and dipyridamole-insensitive nucleoside transporters (rat).

(6) In addition to its use as a means of exploring the structure of the NBMPR-sensitive nucleoside transporter, [^{3}H]NBMPR photolabelling has also been exploited in screening tests for monoclonal antibodies directed against the carrier protein (Jarvis et al, 1985b; Good et al, 1987). Another way to explore molecular similarities between lung and erythrocyte NBMPR nucleoside transporters will be to test monoclonal antibodies directed against the erythrocyte protein for cross-reactivity with the lung systems.

APPENDIX

APPENDIX

A 1 MATERIALS

A 1.1 Radioisotopes

[G-^{3}H]NBMPR (specific radioactivity, 17-37 Ci/mmol and >98% radiochemically pure) and [^{3}H]Dipyridamole (specific radioactivity, 110 Ci/mmol and > 96% radiochemically pure) were purchased from Moravek Biochemicals, Brea, CA. [2-^{14}C]Uridine (specific radioactivity, 53 mCi/mmol and >98% radiochemically pure), [2-^{3}H]AMP (1mCi/ml, 11.7Ci/mmol) and calibrated n-[^{3}H]Hexadecane standard were purchased from the Radiochemical Centre, Amersham, Buckinghamshire, United Kingdom.

A 1.2 Chemicals

NBTGR was a generous gift from Professor A.R.P. Paterson, University of Alberta Cancer Research Group. Dipyridamole (2,2',2'',2'''-(4,8-dipiperedinopyrimido [5,4-d]pyrimidine-2,6-diyldinitrilo) tetraethanol) (Persantin injection) was provided by Boehringer Ingelheim, Bracknell, Berkshire, United Kingdom. NBMPR purchased from Sigma Chemical Co., Kingston-upon-Thames, Surrey, U.K. Dilazep, Lidoflazine and Hexobendine were generously given by Roche Pharmaceuticals, Switzerland. Molecular weight standards for SDS-polyacrylamide gel electrophoresis, ammonium

persulphate and TEMED, acrylamide (>99.9% pure) were from Bio-Rad Laboratories, Richmond, California, USA. Sodium dodecyl sulphate (lauryl) (sequanal grade) was from Pierce Chemical Company, Rockford, Illinois, USA. Dithiothreitol, n-Octylglucoside, PMSF, POPOP, PPO, Sephadex G-50 (fine), inosine, trypsin (type XIII), Triton X-100, were from Sigma, St. Louis, MO, USA. Endoglycosidase-F, Protosol and Omnifluor were from New England Nuclear, Boston, MA, USA. Soybean phospholipid (asolectin) was obtained from Associated Concentrates, Woodside, NY, USA. All other reagents were of analytical grade.

REFERENCES

Almeida, A.F., Jarvis, S.M., Young, J.D. and Paterson, A.R.P. (1984). Photoaffinity labelling of the nucleoside transporter of cultured mouse lymphoma cells. FEBS Lett., 176:444-448.

Aronow, B., Allen, K., Patrick, J. and Ullman, B. (1985). Altered nucleoside transporters in mammalian cells selected for resistance to the physiological effects of inhibitors of nucleoside transport. J. Biol. Chem., 260:6226-6233.

Aronow, B., Toll, D., Patrick, J., McCarter, K. and Ullman, B. (1986). Dipyridamole-insensitive nucleoside transport in mutant murine T lymphoma cells. J. Biol. Chem., 261:14467-14473.

Bakhle, Y.S. and Vane, J.R. (1974). Pharmokinetic function of the pulmonary circulation. Physiol. Rev., 54: 1007-1045.

Bakhle, Y.S. and Vane, J.R. (1977). Metabolic functions of the lung. Marcel Dekker Inc., New York.

Bakhle, Y.S. and Chelliah, R. (1983). Metabolism and uptake of adenosine in rat isolated lung and its inhibition. Br. J. Pharmac., 79:509-515.

Baldwin, J.M., Lienhard, G.E. and Baldwin, S.A. (1980). The monosaccharide transport system of the human erythrocyte. Orientation upon reconstitution. Biochim. Biophys. Acta, 599:699-714.

Baldwin, J.M., Gorga, J.C. and Lienhard, G.E. (1981). The monosaccharide transporter of the human erythrocyte:

transport activity upon reconstitution. J. Biol. Chem., 256:3685-3689.

Barberis, C., Minn, A. and Gayet, J. (1981). Adenosine transport into guinea-pig synaptosomes. J. Neurochem., 35:347-354.

Barker, P.H. and Clanachan, A.S. (1982). Inhibition of adenosine accumulation into guinea -pig ventricle by benzodiazepines. Eur. J. Pharmac., 78:241-244.

Belsham, G.J., Denton, R.M. and Tanner, M.J. (1980). Use of a novel rapid preparation of fat-cell plasma membranes employing Percoll to investigate the effects of insulin and adrenaline on membrane protein phosphorylation within intact fat-cells. Biochem. J., 192:457-467.

Belt, J.A. (1983a). Heterogeneity of nucleoside transport in mammalian cells. Two types of transport activity in L1210 and other cultured neoplastic cells. Mol. Pharmacol., 24:479-484.

Belt, J.A. (1983b). Nitrobenzylthioinosine-insensitive uridine transport in human lymphoblastoid and murine leukemia cells. Biochem. Biophys. Res. Comm., 110:417-423.

Belt, J.A. and Noel, L.D. (1985). Nucleoside transport in Walker 256 rat carcinosarcoma and S49 mouse lymphoma cells. Differences in sensitivity in nitrobenzylthioinosine and thiol reagents. Biochem. J., 232:681-688.

Belt, J.A. and Noel, L.D. (1986). Isolation of L1210 mutants altered in both NBMPR-sensitive and -insensitive nucleoside transport. Proc. Annu. Meet. Am. Assoc. Cancer Res. 27:23.

Bender, A.S., Wu, P.H. and Phillis, J.W. (1980). The characterisation of [^{3}H]adenosine uptake into rat cerebral cortical synaptosomes. J. Neurochem., 35:629-640.

Berne, R.M. (1980). The role of adenosine in the regulation of coronary blood flow. Circ. Res., 47:807-813.

Berne, R.M., Rall, T.W. and Rubio, R. (1983). Regulatory Function of Adenosine. Martinus Nijhoff, Boston.

Binet, L. and Burnstein, M. (1950). Poumon et action vasculaire de l'adenosine-triphosphate. Presse. Med., 58:1201-1203.

Cabantchik, Z.I. and Ginsburg, H. (1977). Transport of uridine in human red blood cells Demonstration of a simple carrier-mediated process. J. Gen. Physiol., 69:75-96.

Cairns, M.T., Elliot, D.A. Scudder, P.R., and Baldwin, S.A. (1984). Proteolytic and chemical dissection of the human erythrocyte glucose transporter. Biochem. J., 221:179-188.

Casale, T.B., Friedman, M., Parada, N., Plekes, J. and Kaliner, M. (1983). Preparation of a human lung purified plasma membrane fraction: confirmation by enzyme markers, electron microscopy, and histamine

H receptor binding. J. Membr.Biol. 79:33-39.
1

Cass, C.E. and Paterson, A.R.P. (1976). Nitrobenzylthioinosine binding sites in the erythrocyte membrane. Biochim. Biophys. Acta, 419:285-294.

Cass, C.E., Gaudette, L.A., and Paterson, A.R.P. (1974). Mediated transport of nucleosides in human erythrocytes. Specific binding of the inhibitor nitrobenzylthioinosine to nucleoside transport sites in the erythrocyte membrane. Biochim. Biophys. Acta, 345:1-10.

Cass, C.E., Kolassa, N. Uehara, Y., Dahlig-Harley, E., Harley, E.R. and Paterson, A.R.P. (1981). Absence of binding sites for the transport inhibitor nitrobenzylthioinosine on transport-deficient mouse lymphoma cells. Biochim. Biophys. Acta, 649:769-777.

Catravas, J.D. (1984). Removal of adenosine from the rabbit pulmonary circulation, in vivo and in vitro. Circ. Res., 54:603-611.

Clanachan, A.S., Paterson, A.R.P., Hammond, J.R. and Jarvis, S.M. (1983). Species differences in nucleoside transport by mammalian erythrocytes. In Regulatory Function of Adenosine, edited by Berne, R.M., Rall, T.W and Rubio, R. Boston, Martinus Nijhoff Publishers, pp505.

Cohen, A., Leung, C. and Thompson, E. (1985). Characterisation of mouse lymphoma cells with altered nucleoside transport. J. Cell Physiol.,

123:431-434.

Coleman, R.A. (1976). Effects of some purine derivatives on the guinea pig trachea and their interaction with drugs that block adenosine uptake. Br. J. Pharmac., 57:51-57.

Cushman, S.W. and Wardzala, L.J. (1980). Potential mechanism of insulin action on glucose transport in the isolated rat adipose cell. Apparent translocation of intracellular transport systems to the plasma membrane. J. Biol. Chem., 255:4758-4762.

Dahlig-Harley, E., Eilam, Y., Paterson, A.R.P. and Cass, C.E. (1981). Binding of nitrobenzylthioinosine to high-affinity sites on the nucleoside-transport mechanism of HeLa cells. Biochem. J., 200:295-305.

Daly, J.W. (1982). Adenosine receptors:Targets for future drugs. J. Med. Chem., 25:197-207.

Davies, L.P., Baird-Lambert, J. and Jamieson, D.D. (1982). Potentiation of pharmacological responses to adenosine, in vitro and in vivo. Gen. Pharmac., 13:27-33.

De Clercq, E., Descampis, J., Veshalst, G., Walker, R.T., Jones, A.S., Torrence, P.F. and Shugar, D.J. (1980). Comparative efficacy of antiherpes drugs against different strains of herpes simplex virus. J. Inf. Dis. 141:563-574.

De Clercq, E. (1984). Biochemical aspects of selective antiherpes activity of nucleoside analogues.

Biochem. Pharmacol. 33:2159-2169.

Deziel, M.R. and Rothstein, A. (1984). Proteolytic cleavages of cytochalasin B binding components of band 4.5 proteins of the human red blood cell membrane. Biochim. Biophys. Acta, 776:10-20.

Dodge, J.T., Michell, C., and Hanahan, D. (1963). The preparation and chemical characteristics of haemoglobin-free ghosts of human erythrocytes. Arch. Biochem. Biophys., 100:119-130.

Duhm, J. (1974). Inosine permeability in erythrocytes of various mammalian species. Biochim. Biophys. Acta, 343:213-237.

Eilam, Y. and Cabantchik, Z.I. (1977). Nucleoside transport in mammalian cell membranes: a specific inhibitory mechanism of high affinity probes. J. Cell Physiol. 92:185-202.

el Kouni, M.H., Diop, D. and Cha, S. (1983). Combination therapy of schistomiasis by tubercidin and nitrobenzylthioinosine 5′-monophosphate. Proc. Natl. Acad. Sci. USA, 30:6667-6670.

Feldman, R.L., Nichols, W.W., Pepine, C.J. and Conti, C.R. (1981). Acute effects of intravenous dipyridamole on regional coronary hemodynamics and metabolism. Circ., 64:333-344.

Fishman, A.P. and Pietra, G.G. (1974). Handling of bioactive material by the lung. N. Engl. J. Med., 290:884-890, 953-959.

Fox, I.H. and Kelly, W.N. (1978). The role of adenosine and 2'-deoxyadenosine in mammalian cells. Ann. Rev. Biochem., 47:655-686.

Fry, D.W., White, J.C. and Goldman, I.D. (1978). Rapid separation of low molecular weight solutes from liposomes without dilution. Anal. Biochem., 90:809-815.

Fujii, M., Kikuchi, Y. Koyanagi, S., Okamatsu, S., Tomoike, H, and Nakamura, M. (1981). Effects of dilazep on regional myocardial blood flow during selective coronary hypotension. Arzneim.-Forsch./Drug Res., 31:2067-2071.

Gati, W.P., Belt, J.A. Jakcobs, E.S., Young, J.D., Jarvis, S.M. and Paterson, A.R.P. (1986). Photoaffinity labelling of a nitrobenzylthioinosine-binding polypeptide from cultured Novikoff hepatoma cells. Biochem. J., 236:665-670.

Gauri, K.K. (1981). Antiviral Chemotherapy: Design of Inhibitors of Viral Functions. Academic Press, London.

Gillis, C.N. and Roth, R.A. (1976). Pulmonary disposition of circulating vasoactive hormones. Biochem. Pharmacol., 25:2547-2553.

Good, A.E., Craik, J.D., Jarvis, S.M., Kwong, F.Y.P., Young, J.D., Paterson, A.R.P. and Cass, C.E. (1987). Characterisation of monoclonal antibodies that recognise band 4.5 polypeptides associated with

nucleoside transport in pig erythrocytes. Biochem. J., 244:749-755.

Hammond, J.R. and Clanachan, A.S. (1985). Species differences in the binding of [^{3}H]nitorbenzylthioinosine to the nucleoside transport system in mammalian central nervous system membranes: evidence for interconvertible conformations of the binding site/transporter complex. J. Neurochem., 45:527-535.

Hammond, J.R., Paterson, A.R.P. and Clanachan, A.S. (1981). Benzodiazepine inhibition of site-specific binding of nitrobenzylthioinosine, an inhibitor of adenosine transport. Life Sciences, 29:2207-2214.

Harley, E.R., Paterson, A.R.P. and Cass, C.E. (1982). Initial rate of transport of adenosine and tubercidine in cultured cells. Cancer Res., 42:1289-1295.

Harmon, R.E., Robins, R.K. and Townsend, L.R. (1978). Chemistry and Biology of Nucleosides and Nucleotides. Academis, Press, London and New York.

Hellewell, P.G. and Pearson, J.D. (1983). Metabolism of circulating adenosine by the porcine isolated perfused lung. Cir. Res., 53:1-7.

Hess, C.E. and Zirkle, J.W. (1980). Cytosine arabinoside (CA) in adult acute non-lymphocytic leukemia (ANLL). A ten year experience. Clin. Res., 28:313A.

Hopkins, S.V. (1973). The potentiation of the action of

adenosine on the guinea pig heart. Biochem Pharmac., 22:341-348.

Hopkins, S.V. and Goldie, R.G. (1971). A species difference in the uptake of adenosine by heart. Biochem. Pharmac., 20:3359-3365.

Huang and Drummond, G.I. (1976). Effect of adenosine on cyclic AMP accumulation in ventricular myocardium. Biochem. Pharmac., 25:2713-2719.

Jain, M.K. (1980). Membrane components: Isolation, composition and metabolism. In: Introduction to Biological Membranes. M.K. Jain and R.C. Wagner, editors, pp.25-52. John Wiley and Sons, New York.

Jakcobs, E.S. and Paterson, A.R.P. (1986). Sodium-dependent concentrative nucleoside transport in cultured intestinal epithelial cells. Biochem. Biophys. Res. Commun., 140:1028-1035.

Janmohamed, N.S., Young, J.D. and Jarvis, S.M. (1985). Proteolytic cleavage of [^{3}H]nitorbenzylthioinosine labelled nucleoside transporter in human erythrocytes. Biochem. J., 230:777-784.

Jarvis, S.M. (1986a). Nitrobenzylthioinosine-sensitive nucleoside transport system: mechanism of inhibition by dipyridamole. Mol. Pharmacol., 30:659-665.

Jarvis, S.M. (1986b). Trans-stimulation and trans-inhibition of uridine efflux from human erythrocyte by permeant nucleosides. Biochem. J., 233:295-297.

Jarvis, S.M. (1986c). Inhibition of nucleoside transport by

dipyridamole. Can. J. Phusiol. Pharmacol., 64:AXIV.

Jarvis, S.M. and Martin, B.W. (1986). Effects of temperature on the transport of nucleosides in guinea pig erythrocytes. Can. J. Physiol. Pharmacol. 64:193-198.

Jarvis, S.M. and Young, J.D. (1980). Nucleoside transport in human and sheep erythrocytes: evidence that nitrobenzylthioinosine binds specifically to functional nucleoside transport sites. Biochem. J., 190:377-383.

Jarvis, S.M. and Young, J.D. (1981). Extraction and partial purification of the nucleoside transport system from human erythrocytes based on the assay of nitrobenzylthioinosine binding activity. Biochem. J., 194:331-339.

Jarvis, S.M. and Young, J.D. (1982). Nucleoside translocation in sheep reticulocytes and in erythrocytes from newborn lambs. A proposed molecular model for the nucleoside transporter. J. Physiol., 324:47-66.

Jarvis, S.M. and Young, J.D. (1986a). Nucleoside transport in rat erythrocytes: two components with differences in sensitivity to inhibition by nitrobenzylthioinosine and p-cholromercuriphenyl sulphonate. J. Membr. Biol., 43:1-10.

Jarvis, S.M., Young, J.D. (1987). Photoaffinity labelling of nucleoside transporter polypeptides. Pharmacol.

Therapeut., 32:339-359.

Jarvis, S.M., Young, J.D., Ansay, M., Archibald, A.L., Harkness, R.A. and Simmonds, R.J. (1980a). Is inosine the physiological energy source of pig erythrocytes. Biochim. Biophys. Acta, 597:183-188.

Jarvis, S.M., Ellory, J.C. and Young, J.D. (1980b). Nucleoside transport in human erythrocytes: apparent molecular weight of the nitrobenzylthioinosine binding complex estimated by radiation inactivation analysis. Biochem. J., 190:373-376.

Jarvis, S.M., McBride, D. and Young, J.D. (1982a). Erythrocyte nucleoside transport: asymmetrical binding of nitrobenzylthioinosine to nucleoside permeation sites J. Physiol., 324:31-46.

Jarvis, S.M., Hammond, J.R., Paterson, A.R.P. and Clanachan, A.S. (1982b). A study of uridine transport and nitrobenzylthioinosine binding by mammalian erythrocytes. Biochem. J., 208:83-88.

Jarvis, S.M., Hammond, J.R., Paterson, A.R.P. and Clanachan, A.S. (1983a). Nucleoside transport in human erythrocytes. A simple carrier with directional symmetry in fresh cells, but with directional asymmetry in cells from outdated blood. Biochem. J. 210:457-561.

Jarvis, S.M., Janmohamed, S.N. and Young, J.D. (1983b). Kinetics of nitrobenzylthioinosine binding to the human erythrocyte nucleoside transporter. Biochem.

J., 216:661-667.

Jarvis, S.M., Fincham, D.A., Ellory, J.C., Paterson, A.R.P. and Young, J.D. (1984). Nucleoside transport in human erythrocytes. Nitrobenzylthioinosine binding and uridine transport activites have similar radiation target sizes. Biochim. Biophys. Acta, 772:227-300.

Jarvis, S.M., Martin, B.W. and Ng, A.S. (1985). 2-Chloroadenosine, a permeant for the nucleoside transporter. Biochem. Pharmacol., 34:3237-3241.

Jarvis, S.M., Young, J.D., Wu, J.S.R., Belt, J.A. and Paterson, A.R.P. (1986a). Photoaffinity labelling of the human erythrocyte glucose transporter with 8-azidoadenosine. J. Biol. Chem., 261:11077-11085.

Jarvis, S.M., Ellory, J.C. and Young, J.D. (1986b). Radiation inactivation of the human erythrocyte nucleoside and glucose transporters. Biochim. Biophys. Acta, 855:312-312.

Johnstone, R.M., Larrick, J., Turbide, C. and Adam, M. (1985). The sheep reticulocyte sheds membrane protein during maturation in the erythrocyte. 13th Int. Congress Biochem. abstract MO-428.

Kagawa, Y. and Racker, E. (1971). Partial resolution of the enzymes catalyzing oxidative phosphorylation. XXV. Reconstitution of vesicles catalyzing ^{32}P-adenosine triphospate exchange. J. Biol. Chem., 246:5477-5487.

Kasahara, M. and Hinkle, P.C. (1977). Reconstitution and purification of the D-glucose transporter from human erythrocytes. J. Biol. Chem., 252:7384-7390.

Kidwai, A.M., Radcliffe, M.A. and Daniel, E.E. (1971). Studies on smooth muscle plasma membrane: 1. Isolation and characterization of plasma membrane from rat myometrium. Biochim. Biophys. Acta, 233:538-275.

Kim, H.D. and McManus, T.J. (1971). Studies on the energy metabolism of pig red cells.I. The limiting role of membrane permeability in glycolysis. Biochim. Biophys. Acta, 230:1-11.

Kim, H.D., Watts, R.P., Luthra, M.G., Schwalbe, C.R., Conner, R.T. and Brendel, K. (1980). A symbiotic relationship of energy metabolism between a 'non-glycolytic' mammalian red cell and the liver. Biochim. Biophys. Acta, 589:256-263.

Kinsella, D., Troup, W. and McGregor, M. (1962). Studies with a new coronary vasodilator drug: Persantin. Am. Heart J., 63:146-151.

Kolassa, N. and Pfleger, K. (1975). Adenosine uptake by erythrocytes of man, rat and guinea-pig and its inhibition by hexobendine and dipyridamole. Biochem. Pharmacol., 24:154-156.

Kolassa, N., Pfleger, K. and Rummel, W. (1970). Specificity of adenosine uptake into the heart and inhibition by dipyridamole. Eur. J. Pharmac., 9:265-268.

Kolassa, N., Plank, B. and Tram, M. (1971). Species differences in action and elimination of adenosine after dipyridamole and hexobendine. Eur. J. Pharmac., 13:320-325.

Kolassa, N., Stengg, R. R. and Turnheim, K. (1978). Influence of hexobendine, dipyridamole, dilazep, lidoflazine, inosine and purine riboside on adenosine uptake by the isolated epithelium of guinea jejunum. Pharmacology, 16:54-60.

Koren, R., Shohami, E., Bibi, O. and Stein, W.D. (1978). Uridine transport properties of mammalian cell membranes are not directly involved with growth control or oncogenesis. FEBS Lett., 86:71-75.

Koren, R., Cass, C.E. and Paterson, A.R.P. (1983). The kinetics of dissociation of the inhibitor of nucleoside transport, nitrobenzylthioinosine, from high-affinity binding sites of cultured namster cells. Biochem. J., 216:299-308.

Kwan, K.J. and Jarvis, S.M. (1984). Photoaffinity labelling of adenosine transporter in cardiac membranes with nitrobenzylthioinosine. Am. J. Physiol., 246:H710-H715.

Kwong, F.Y.P. (1987) In 'Erythrocyte nucleoside transporters: photoaffinity labelling, isolation and molecular studies' (thesis).

Kwong, F.Y.P., Choy, Y.M., Jarvis, S.M. and Young, J.D. (1985). Molecular differences between human and pig

erythrocyte nucleoside transporters. Biochem. Soc. Trans., 13:238-239.

Kwong, F.Y.P., Baldwin, S.A., Scudder, P.R., Jarvis, S.M., Choy, Y.M. and Young, J.D. (1986). Erythrocyte nucleoside and sugar transport. Endo- galactosidase and endoglycosidase-F digestion of partially-purified human and pig transporter proteins. Biochem. J., 240:349-356.

Kwong, F.Y.P., Tse, C.M., Jarvis, S.M., Choy, M.Y.M. and Young, J.D. (1987). Purification and reconstitution studies of the pig erythrocyte nucleoside transporter. Biochim. Biophys. Acta (submitted).

Laemmli, U.K. (1970). Cleavage of structural proteins during the assembly of the head of bacteriophage T4. Nature (Lond.), 227:680-685.

Le Hir, M. and Dubach, U.C. (1984). Sodium gradient-energised concentrative transport of adenosine in renal brush border vesicles. Pflug. Arch., 401:58-63.

Le Hir, M. and Dubach, U.C. (1985). Uphill transport of pyrimidine nucleosides in renal brush border vesicles. Pflg. Arch., 404:238-243.

Lieb, W.R. (1982). A kinetic approach to transport studies. In 'Red Cell Membranes. A Methodological Approach' pp.135-164, Ed. by Ellory, J.C. and Young, J.D., Academic Press, London.

Lienhard, G.E., Crabb, J.H. and Ransome, K.J. (1984).

Endoglycosidase-F cleaves the oligosaccharides from the glucose transporter of the human erythrocyte. Biochim. Biophys. Acta, 769:404-410.

Lowry, O.H., Rosebrough, N.J., Farr, A.L. and Randall, R.J. (1951). Protein measurement with the Folin phenol reagent. J. Biol. Chem., 193:265-275.

Lynch, T.P., Jakobs, E.S., Paran, J.H. and Paterson, A.R.P. (1981a) Treatment of mouse neoplasms with high doses of tubercidin. Cancer Res., 41:3200-3206.

Lynch, T.P., Paran, J.H. and Paterson, A.R.P. (1981b). Therapy of mouse leukemia L1210 with combination of nebularine and nitrobenzylthioinosine 5′-monophosphate. Cancer Res., 41:560-565.

Maiden, M.C.J., Davis, E.O., Baldwin, S.A., Moore, D.C.M. and Henderson, P.J.F. (1987). Mammalian and bacterial sugar transport proteins are homologous. Nature 325:641-643.

Marangos, P.J., Clark-Rosenberg, R. and Patel, J. (1982a). [^{3}H]Nitrobenzylthioinosine is a photoaffinity probe for adenosine uptake sites in brain. Eur. J. Pharmac., 85:359-360.

Marangos, P.J., Patel, J., Clark-Rosenberg, R. and Martino, A.M. (1982). [^{3}H]Nitrobenzylthioinosine binding as a probe for the study of adenosine uptake sites in brain. J. Neurochem., 39:184-191.

Marangos, P.J., Finkel, M.S., Verma, A., Matuuuri, M.F., Patel, J. and Patterson, R.E. (1984). Adenosine

uptake sites in dog heart and brain: interaction with calcium antagonists. Life Sci. 35:1109-1116.

Marangos, P.J., Houston, M. and Montgomery, P. (1985). [^{3}H]Dipyridamole: A new ligand probe for brain adenosine uptake sites. Eur. J. Pharmacol., 117:393-394.

Mueckler, M., Caruso, C., Baldwin, S.A., Panice, M., Blench, I., Morries, H.R., Allard, W.J., Lienhard, G.E. and Lodish, H.F. (1985). Sequence and structure of a human glucose transporter. Science, 229:941-945.

Mustafa, S.J. (1980). Cellular and molecular mechinism(s) of coronary flow regulation by adenosine. Mol. Cell. Biochem. 31:67-87.

Newby, A.C. (1984). Adenosine and the concept of 'retaliatory metabolites'. TIBS, 98:42-44.

Nijjar, M.S. and Ho, J.C. (1980). Isolation of plasma membranes from rat lungs: Effect of age on the subcellular distribution of adenylate cyclase activity. Biochim. Biophys. Acta, 600:238-243.

Nimit, Y., Skolnick, P. and Daly, J.W. (1981). Adenosine and cyclic AMP in rat cerebral cortical slices: Effects of adenosine uptake inhibitors and adenosine deaminase inhibitors. J. Neurochem., 36:908-912.

Oliver, J.M. and Paterson, A.R.P. (1971). Nucleoside transport.I. A mediated process in human erythrocytes. Can. J. Biochem., 49:262-270.

Paterson, A.R.P. and Oliver, J.M. (1971). Nucleoside transport. II. Inhibition by p-nitrobenzylthioguanosine and related compounds. Can. J. Biochem., 49:270-274.

Paterson, A.R.P., Kolassa, N. and Cass, C.E. (1981). Transport of nucleoside drugs in animal cells. Pharmacol. Therap., 12:515-536.

Paterson, A.R.P., Lau, E.Y., Dahlig, E. and Cass, C.E. (1980). A common basis for inhibition of nucleoside transport by dipyridamole and nitrobinzylthioinosine? Mol. Pharmacol., 18:40-44.

Paterson, A.R.P., Jakcobs, E.S., Harley, E.R., Cass, C.E. and Robins, M.J. (1983). Inhibitors of nucleoside transport as probes and drugs. In 'Develoment of Target-Oriented Cancer Drugs'. pp. 41-56. Ed. by Cheng, Y.C., Goz, B. and Minkoff, M. Raven Press, New York.

Pazdur, J., Kryzystyniak, K. and Kopec, M. (1980). Effects of dipyridamole on human blood lymphocytes. Biochem. Pharmac., 29:2515-2517.

Phillis, J.W., Edstrom, J.P., Kostopoulos, G.K. and Kirkpatrick, F.R. (1979). Effects of adenosine and adenine nucleotides on synaptic transmission in the cerebral cortex. Can. J. Physiol. Pharmac., 57:1289-1312.

Plagemann, P.G.W. and Richey, D.P. (1974). Transport of nucleosides, nucleic acid bases, choline and glucose

by animal cells in culture. Biochim. Biophys. Acta, 344:263-305.

Plagemann, P.G.W. and Wohlhueter, R.M. (1980). Permeation of nucleosides and nucleic acid bases and nucleotides in animal cells. Curr. Top. Membr. Transp., 14:225-230.

Plagemann, P.G.W. and Wohlhueter, R.M. (1982). The hypoxanthine transporter of Novikoff rat hepatoma cells exhibits directional symmetry and equal mobility when empty or substrate-loaded. Biochim. Biophys. Acta, 688:505-514.

Plagemann, P.G.W. and Wohlhueter, R.M. (1984a). Kinetics of nucleoside transport in human erythrocytes. Alterations during blood preservation. Biochim. Biophys. Acta, 778:176-184.

Plagemann, P.G.W. and Wohlhueter, R.M. (1984b). Nucleoside transport in cultured mammalian cells. Multiple forms with different sensitivity to inhibition by nitrobenzylthioinosine or hypoxanthine. Biochim. Biophys. Acta, 773:39-52.

Plagemann, P.G.W. and Wohlhueter, R.M. (1984c). Effect of temperature on kinetics and differential mobility of empty and loaded nucleoside transporter of human erythrocytes. J. Biol. Chem. 259:9024-9027.

Plagemann, P.G.W. and Wohlhueter, R.M. (1984d). Effect of sulfhydryl reagents on nucleoside transport in cultured mammalian cells. Arch. Biochem. Biophys.

223:489-500.

Plagemann, P.G.W. and Wohlhueter, R.M. (1985). Nitrobenzylthioinosine-sensitive and -resistant nucleoside transport in normal and transformed rat cells. Biochim. Biophys. Acta, 816:387-395.

Plagemann, P.G.W., Wohlhueter, R.M. and Kraupp, M. (1985). Adenosine uptake, transport and metabolism in human erythrocytes. J. Cell Physiol., 125:330-336.

Rogler-Brown, T. and Parks, R.E. jr. (1980). Tight binding inhibitors. VIII. Studies of the interactions of 2'-deoxycoformycin and transport inhibitors with the erythrocytic nucleoside transport system. Biochem. Pharmac., 29:2491-2497.

Roos, H. and Pfleger, K. (1972). Kinetics of adensoine uptake by erythrocytes and the influence of dipyridamole. Molec. Pharmac., 8:117-125.

Rosenblit, P.D. and Levy, D. (1980). Photoaffinity labelling of the adenosine transport system in adipocyte plasma membranes. Arch. Biochem. Biophys., 204:331-339.

Rozengurt, E., Mierzejewski, K. and Wigglesworth, N.M. (1978). Uridine transport and phosphorylation in mouse cells in culture: effect of growth-promoting factors, cell cycle transit and oncogenic transformation. J. Cell Physiol. 97:241-251.

Sakai, K., Aono, J. and Haruta, K. (1981). Species differences in renal vascular effects of

dipyridamole and in the potentiation of adenosine action by dipyridamole. J. Cardiovasc. Pharmac., 3:420-430.

Sano, N. (1974). Enhancement of coronary vasodilating action of adensoine by dilazep and dipyridamole in the dog. Jap. J. Pharmac., 24:471-478.

Schwenk, M., Hegazy, E. and Lopez del Pino, V. (1984). Uridine uptake by isolated intestinal epithelial cells of guinea-pig. Biochim. Biophys. Acta, 805:370-374.

Shanahan, M.F. and D'Artel-Ellis, J. (1984) Orientation of the glucose transporter in the human erythrocyte. J. Biol. Chem., 259:13878-13884.

Slaughter, R.S., Fenwick, R.G. and Barnes, E.M. (1981). Hypoxanthine and thymidine compete for transport in Chinese hamster fibroblasts. Arch. Biochem. Biophys., 211:494-499.

Song, C.S. and Bodansky, O. (1967). Subcellular localizationand properties of 5'-nucleotidase in the rat liver. J.Biol. Chem., 242:694-699.

Steck, T.L. (1974) The organization of proteins in the human red cell membranes. J. Cell Biol., 62:1-19.

Stein, W.D. (1986). Transport and Diffusion Across Cell Membranes. Academic Press.

Stone, T.W. (1981). Physiological roles for adenosine and adenosine 5'-triphosphate in the nervous system. Neurosci., 6: 523-555.

Tattersall, M.H.N. and Fox, R.M. (1981). Nucleosides and Cancer Treatment. Academic Press, Sydney.

Tefft, R. E., Carruthers, A. and Melchior, D.L. (1986). Reconstituted human erythrocyte sugar transporter activity is determined by bilayer lipid head groups. Biochemistry 25:3709-3718.

Thompson, S. and Maddy, A.H. (1982). Gel electrophoresis of erythrocyte membrane proteins. 'In Red Cell Membranes. A Methodological Approach', pp.67-94. Ed. by Ellory, J.C. and Young, J.D., Academic Press, London.

Tse, C.M. and Young, J.D. (1987a). Kinetic and orientation studies of the human erythrocyte nucleoside carrier. J. Biol. Chem. (submitted).

Tse, C.M. and Young, J.D. (1987b). Choice of permeant for nucleoside transporter reconstitution studies. Biochim. Biophys. Acta. (submitted).

Tse, C.M., Wu, J.S.R. and Young, J.D. (1985a). Evidence for the asymmetrical binding of p-chloromercuriphenyl-sulphonate to the human erythrocyte nucleoside transporter. Biochim. Biophys. Acta, 818:316-324.

Tse, C.M., Belt, J.A., Jarvis, S.M., Paterson, A.R.P., Wu, J.S.R. and Young, J.D. (1985b). Reconstitution studies of the human erythrocyte nucleoside transporter. J. Biol. Chem., 260:3506-3511.

Turnheim, K., Plank, B. and Kolassa, N. (1978). Inhibition of adenosine uptake in human erythrocytes by

adenosine-5′-carboxamides, xylosyladenine, dipyridamole, hexobendine and p-nitrobenzyl-thioguanosine. Biochem. Pharmacol., 27:2191-2197.

Valentine, W.N., Paglia, D.E. and Gilsanz, F. (1977). Hereditary haemolytic anaemia with increased red cell adenosine deaminase (45- to 70-fold) and decrease adenosine triphosphate. Science, 195:783-786.

Van Belle, H. (1970). The disappearance of adenosine in blood: Effect of lidoflazine and other drugs. Eur. J. Pharmac., 11:241-248.

Walker, R.T., De Clercq, E. and Eckstein, F. (1979). Nucleoside analogues:Chemistry, Biology and Medical Applications. Plenum Press, London and New York.

Wheeler, T.J. and Hinkle, P.C. (1981). Kinetic properties of the reconstituted glucose transporter from human erythrocytes. J. Biol. Chem., 256:8907-8914.

Wheeler, T.J. and Hinkle, P.C. (1985). The glucose transporter of mammalian cells. Ann. Rev. Physiol., 47:503-517.

Wiemik, P.H. (1980). In Cancer Chemotherapy, Annual 2, pp. 176-207 (Pinedo, M.H. ed.). Elsevier, New York.

Wiley, J.S., Jones, S.P. and Sawyer, W.H. (1983). Cytosine arabinoside transport by human leukemic cells. Eur. J. Cancer Clin. Oncol., 19:1067-1074.

Wiley, J.S., Taupin, J., Jamieson, G.P., Snook, M., Sawyer, W.H. and Finch, L.R. (1985). Cytosine arabinoside

transport and metabolism in acute leukemias and T cell lymphoblastic lymphoma. J. Clin. Invest. 75:632-642.

Williams, E.F., Barker, P.H. and Clanachan, A.S. (1984). Nucleoside transport in heart: species differences in nitrobenzylthioinosine binding, adenosine accumulation, and drug-induced potentiation of adenosine action.

Wohlhueter, R.M. and Plagemann, P.G.W. (1982). On the functional symmetry of nucleoside transport in mammalian cells. Biochim. Biophys. Acta, 689:249-260.

Wohlhueter, R.M., Marz, R. and Plagemann, P.G.W. (1978). Properties of the thymidine transport system of Chinese hamster ovary cells as probed by nitrobenzylthioinosine. J. Membr. Biol., 42:247-264.

Wohlhueter, R.M., Marz, R. and Plagemann, P.G.W. (1979a). Thymidine transport in cultured mammalian cells. Kinetic analysis, temperature dependence and specificity of the transport system. Biochim. Biophys. Acta, 553:261-268.

Wohlhueter, R.M., Plagemann, P.G.W. and Sheppard, J.R. (1979b). Endogenous cyclic AMP does not modulate transport of hexoses, nucleosides, or nucleobase in Chinese hamster ovary cells. J. Supramol. Struct., 11:51-60.

Wohlhueter, R.M., Brown, W.E. and Plagemann, P.G.W. (1983). Kinetic and thermodynamic studies on nitrobenzylthioinosine binding to the nucleoside transporter of Chinese hamster ovary cells. Biochem. Biophys. Acta, 731:168-176.

Wu, P.H. and Phillis, J.w. (1982). Nucleoside transport in rat cerebral cortical synaptosomal membrane: A high affinity probe study. Int. J. Biochem., 14:1101-1105.

Wu, J.S.R. and Young, J.D. (1984). Photoaffinity labelling of nucleoside-transport proteins in plasma membranes isolated from rat and guinea-pig liver. Biochem. J., 220:499-506.

Wu, J.S.R., Kwong, F.Y.P., Jarvis, S.M. and Young, J.D. (1983a). Identification of the erythrocyte nucleoside transporter as a band 4.5 polypeptide. photoaffinity labelling studies using nitrobenzylthioinosine. J. Biol. Chem., 258:13745-13751.

Wu, J.S.R., Jarvis, S.M. and Young, J.D. (1983b). The human erythrocyte nucleoside and glucose transporters are both band 4.5 membrane polypeptides. Biochem. J., 214:995-997.

Wu, J.S.R., Teoh, R., Vallance-Owen, J. and Young, J.D. (1986). Nucleoside transport in primary cultures of differentiated mouse astrocytes. Neurosci. Lett. (Suppl.) 25:S49

Young, J.D. (1976) Nucleoside transport variation in sheep erythrocytes. J. Physiol. (Lond.), 259:57-58.

Young, J.D. (1978). Nucleoside transport in sheep erythrocytes: genetically controlled transport variation and its influence on erythrocyte ATP concentrations. J. Physiol., 227:325-399.

Young, J.D. and Jarvis, S.M. (1983). Nucleoside transport in animal cells. Review. Bioscience Reports, 3:309-322.

Young, J.D., Jarvis, S.M., Robins, M.J. and Paterson, A.R.P. (1983). Photoaffinity labelling of the human erythrocyte transporter by N^6-(p-azidobenzyl)-adenosine and nitrobenzylthioinosine. Evidence that the transporter is a band 4.5 polypeptide. J. Biol. Chem., 258:2202-2208.

Young, J.D., Jarvis, S.M., Belt, J.A., Gati, W.P. and Paterson, A.R.P. (1984). Identification of the nucleoside transporter in cultured mouse lymphoma cells. Photoaffinity labelling of plasma enriched fractions from nucleoside transport competent (S49) and nucleoside transport-deficient (AE1)cells with [^{3}H]nitrobenzylthioinosine. J. Biol. Chem., 259:8363-8365.

Young, J.D., Paterson, A.R.P. and Henderson, J.F. (1985). Nucleoside transport and metabolism in erythrocytes from the Yucatan minature pig. Evidence that inosine functions as an *in vivo* energy substrate. Biochim.

Biophys. Acta, 842:214-224.

Young, J.D., Jarvis, S.M., Clanachan, A.S., Henderson, J.F. and Paterson, A.R.P. (1986). Nitrobenzylthioinosine- an *in vivo* inhibitor of pig erythrocyte energy metabolism. Am.J. Physiol., 251:C90-C94.

Zeidler, R.B., Metzler, M.H.,Moran, J.B. and Kim, H.D. (1985). The liver is an organ site for the release of inosine metabolised by non-glycolytic pig red cells. Biochim. Biophys. Acta, 838:321-328.